



Seconda Università degli studi di Napoli

Facoltà di Ingegneria

Corso di laurea in Ingegneria Aerospaziale

Tesi di Laurea

EUROPA JUPITER SYSTEM MISSION : orbital analysis of Jupiter Ganymede Orbiter

Relatore

Ch. Prof. Ing. **Marco D'Errico**
Dipartimento di Ingegneria Aerospaziale e Meccanica

Candidato

Armando Marotta
Matr. 831/20

Correlatore

Dott.ssa **M. Rosaria Santovito**
Consorzio di Ricerca su Sistemi di Telesensori Avanzati
Co.Ri.S.T.A.- Napoli

TABLE OF CONTENTS

Introduction	6
Chapter 1: Europa Jupiter System Mission	8
1.1 Mission Introduction	8
1.2 Ganymede	11
1.2.1 Orbit and rotation	14
1.2.2 Composition	15
1.2.3 Magnetosphere	16
1.3 Mission Analysis	19
1.3.1 Mission Phases	19
1.3.2 End of mission options	24
1.4 Spacecraft subsystem	24
1.4.1 Structure and configuration	25
1.4.2 Power subsystem	28
1.4.3 Thermal control	30
1.4.4 Propulsion	30
1.4.5 Attitude and Orbit Control Subsystem	31
1.4.6 Mechanism	32
1.4.7 Telecommunication	32
1.4.8 Data Handling	33
1.5 Laser Altimetry and Radar Sounder performance	34
1.5.1 Laser Altimetry	35
1.5.1.1 Science goals related to Laser Altimetry	35
1.5.1.2 Sun radiation effects for LA	37
1.5.2 Radar Sounder	37
1.5.2.1 Science goals related to Radar Sounder	39
1.5.2.2 Jupiter radiation effects for RS	40

Chapter 2: JGO orbital propagator	41
2.1 Planetary Data System, NAIF and SPICE	41
2.1.1 SPICE kernels	42
2.1.2 SPICE Toolkit	43
2.1.3 Temporal reference	46
2.1.4 Spatial reference frames	48
2.1.5 SPICE routines if interest	50
2.2 Orbital propagator structure	53
2.2.1 Spacecraft ephemeris	56
2.2.2 Jupiter and Sun eclipse	60
Chapter 3: Validation and results	70
3.1 Validation graphs	70
3.1.1 Validation graphs for one spacecraft orbital period	70
3.1.2 Validation graphs for one ganymedian revolution period	80
3.1.3 Sun useful plots	90
3.2 Graph results for Jupiter eclipse	92
3.2.1 Graph result for 180 terrestrial days of propagation	92
3.2.2 Graph result for one ganymedian revolution period	95
3.3 Graph result for Sun eclipse	98
3.3.1 Graph result for 180 terrestrial days of propagation	98
3.3.2 Graph results for one ganymedian revolution period	101
3.4 Useful graphs	103
Annex	105
Conclusions	110
Acronyms	112
Bibliography	115
Acknowledgements	121

TABLE OF IMAGES

Chapter 1

1.1	Hypothetical salt water under crust of Europa surface	8
1.2	Interaction between Ganymede and Jupiter magnetic field	8
1.3	Image of Ganymede	10
1.4	Orbital and physic characteristics of Ganymede	12
1.5	Resonance of Galilean moons	13
1.6	Interior of Ganymede	14
1.7	Magnetic field of Ganymede	16
1.8	Resume for JGO orbital tour	18
1.9	Space vector <i>Ariane 5</i>	19
1.10	Transfer from earth to Jupiter	20
1.11	Part of the science phase around Callisto	21
1.12	Elliptical orbit for magneospheric studies	22
1.13	Near-polar 200 Km altitude orbit	23
1.14	Central cylinder of spacecraft	25
1.15	Solar panel for JGO spacecraft	26
1.16	Fully deployed spacecraft	26
1.17	Instrument accommodation	27
1.18	Available solar array power during mission	28
1.19	EAM main engine details	30
1.20	Scheme of data handling system	33
1.21	Main instrument requirement	37
1.22	Off-nadir clutter phenomenon	38

Chapter 2

2.1	Solar System Geometry	41
2.2	SPICE kernels architecture	43

2.3	Orbital parameters	55
2.4	Algorithm of propagation for JGO	56
2.5	Geometric interpretation of eccentric anomaly	57
2.6	Passage to perifocal frame	58
2.7	Eclipse phenomenon (3D view)	60
2.8	Eclipse phenomenon (2D view)	61
2.9	Semi-angle for eclipse condition	61
2.10	No-eclipse condition	62
2.11	Eclipse condition	62
2.12	Solid angle for eclipse condition	63
2.13	Different cases for spacecraft position	63
2.14	Geometrical considerations to calculate eclipse semi-angle	64
2.15	Particular of geometrical considerations for eclipse semi-angle	65
2.16	Fictitious Ganymede body fixed frame	66
2.17	Antenna direction	67
2.18	Azimuth angle of Jupiter mass centre respect to antenna direction	67
2.19	Eclipse condition for azimuth angle	68

INTRODUCTION

This study has been developed in Naples at Co.Ri.S.T.A (Consortium of Research on Advanced Remote Sensing System) in the framework of Europa Jupiter System Mission (EJSM), the joint international mission ESA\NASA.

EJSM consists of two primary flight operating in the Jovian system :the NASA-led Jupiter Europa Orbiter (JEO), and the ESA-led Jupiter Ganymede Orbiter (JGO).

The overarching theme for EJSM is :''*The emergence of habitable worlds around gas giant*'' , and Jupiter represents the archetype for gas giant planets of the Solar System.

JEO and JGO will execute an exploration of the Jupiter System before settling into orbit around Europa and Ganymede respectively; they carry respectively eleven and ten complementary instruments to monitor dynamic phenomena, map the Jovian magnetosphere and characterize water oceans beneath the ice shells of Europa and Ganymede.

The JEO and JGO are separated and independent spacecraft developed, launched and operated by their respective organizations to work together in the Jupiter system toward a common set of science goals and objectives.

In EJSM context Co.Ri.S.T.A is involved in the development of a Radar Sounder that will analyze Ganymede's subsurface with a high vertical resolution (order of some meters) and the topography with a Laser Altimetry with a moderate resolution, both on board of the JGO.

The purpose of this work is to realize a Ganymede Orbital Propagator to determine spacecraft state in Jupiter and in Sun eclipse phase, in order to optimize measurement planning for Radar Sounder and Laser Altimeter.

The work has been developed using SPICE library , provided by NAIF node of NASA's Planetary Data System (PDS) interfaced with software MATLAB[®].

The thesis is organized in three chapters:

- **Chapter 1** introduces a description of EJSM, JEO and JGO, principles of functioning of Laser Altimetry and Radar Sounder;

- **Chapter 2** presents the architecture of NAIF node and SPICE routines, the description of theory and algorithms on which the orbital propagator is based on;
- **Chapter 3** : shows the results about the Jupiter eclipse and Sun eclipse for the JGO.

CHAPTER 1: Europa Jupiter Sistem Mission

1.1 Mission introduction

Europa Jupiter System Mission is a joint mission ESA\NASA whose baseline consists of two primary elements operating in the jovian system; the NASA-led Jupiter Europa Orbiter (JEO) , and the ESA-led Jupiter Ganymede Orbiter (JGO).[1]

EJSM uniquely addresses several of the central theme of ESA's Cosmic Vision Programme by means of its in-depth exploration of the Jupiter system and its evolution from origin to habitability.

The overarching theme for EJSM is formulated as “*the emergence of habitable worlds around gas giant*”, and Jupiter is the archetype for the giant planets of the Solar System and for the numerous giant planets now known to orbit other stars.

To address this theme the Jupiter system will be explored, and the process leading to the diversity of its associated components and their interactions will be studied.

In particular Europa and Ganymede are singled out for detailed investigation, since , this pair of objects provides a natural laboratory for comparative analysis of the nature, evolution and potential habitability of icy worlds: in fact Europa is believed to have a saltwater ocean beneath a relatively thin and geodynamically active icy crust (*figure 1.1*).[2]

Io, Europa and Ganymede are coupled in a stable resonance which maintains their orbital period in a ratio of 1: 2: 4 and forces the orbital eccentricity of these satellites.

Europa is unique among the large icy satellites because its ocean is in direct contact with its rock mantle beneath , where the conditions could be similar to those on Earth's biologically rich sea floor .The discovery of hydrothermal fields on Earth's sea floor suggests that such areas are excellent habitats , powered by energy and nutrient that result from reactions between the sea water and silicates; consequently Europa is the prime candidate in the search for habitable zones and life in the solar system.

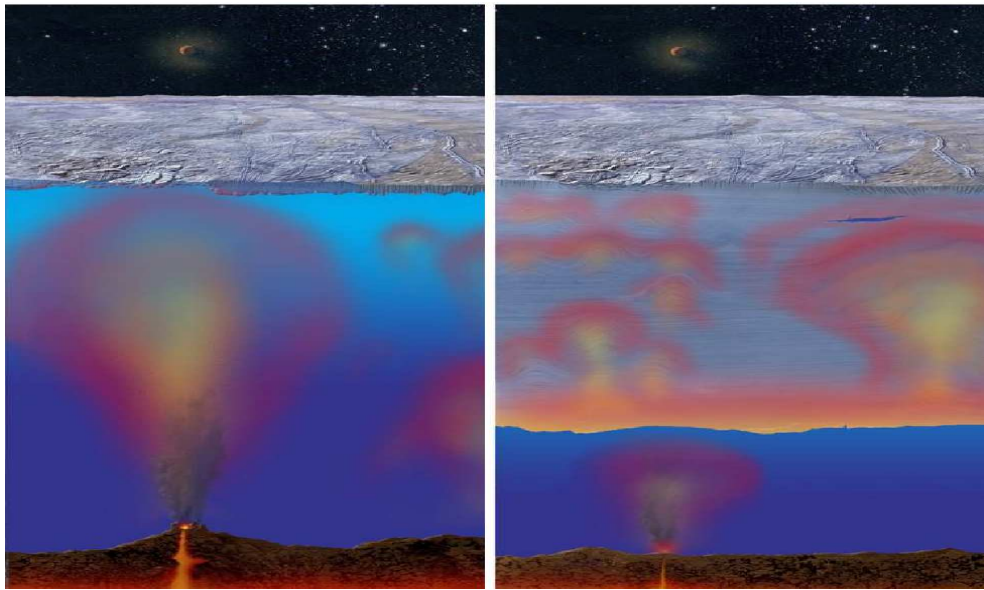


Figure 1.1 : Artistic illustration of the hypothetical saltwater ocean under icy crust of Europa's surface. [1]

Ganymede is believed to have a liquid ocean sandwiched between a thick ice shell above and high-density ice polymorphs below. It is the only satellite known to have an intrinsic magnetic field , which makes Ganymede-Jupiter magnetosphere interaction unique in the Solar System (figure 1.2)

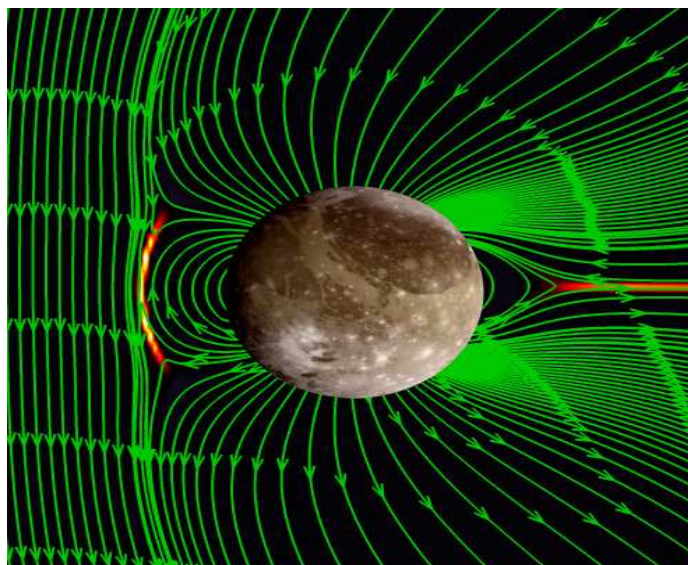


Figure 1.2 :Interaction between Ganymede and Jupiter magnetic fields [2]

EJSM will undertake in-depth comparisons of Europa and Ganymede to establish their characteristics with respect to geophysical activity and habitability .

To this end NASA's JEO spacecraft will investigate Europa in detail while ESA's JGO spacecraft will focus on Ganymede. For Europa and Ganymede both the mission elements have objectives to :

- characterize and determine the extent of sub-surface oceans and their relations to the deeper interior;
- characterize the ice shells and any subsurface water , including the heterogeneity of the ice , and the nature of surface –ice-ocean exchange;
- characterize the deep internal structure , differentiation history and (for Ganymede) the intrinsic magnetic field;
- compare the exospheres , plasma environments , and magnetospheric interactions;
- determine global surface compositions and chemistry , especially as related to habitability;
- understand the formation of the surface features , including sites of recent or current activity , and identify and characterize candidate sites for future *in situ* exploration.

JEO and JGO carry 11 and 10 complementary instruments, respectively, to monitor dynamic phenomena (such as Io's volcanoes and Jupiter's atmosphere), map the Jovian magnetosphere and its interactions with the Galilean satellites, and to satisfy the mission objectives for Europa and Ganymede.

1.2 Ganymede

Ganymede (*figure 1.3*) is a moon of Jupiter and the largest moon in the Solar System. Completing an orbit in roughly seven days, it is the seventh moon and third Galilean moon from Jupiter[3]. Ganymede participates in a 1:2:4 orbital resonance with the moons Europa and Io, respectively. It is larger in diameter than the planet Mercury but has only about half its mass. It has the highest mass of all planetary satellites with 2.01



times the mass of the Earth's moon [4]. Ganymede is composed primarily of silicate rock and water ice. It is a fully differentiated body with an iron-rich, liquid core. A saltwater ocean is believed to exist nearly 200 km below Ganymede's surface, sandwiched between layers of ice [5]. Its surface

Figure 1.3: True-color image taken by the Galileo probe [6]

comprises two main types of terrain:

- **dark regions**, saturated with impact craters and dated to four billion years ago, cover about a third of the satellite;
- **lighter regions**, crosscut by extensive grooves and ridges and only slightly less ancient, cover the remainder. The cause of the light terrain's disrupted geology is not fully known, but was likely the result of tectonic activity brought about by tidal heating [7].

Ganymede is the only satellite in the Solar System known to possess a magnetosphere, likely created through convection within the liquid iron core [8]. The meagre magnetosphere is buried within Jupiter's much larger magnetic field and connected to it through open field lines. The satellite has a thin oxygen atmosphere that includes O,

O₂, and possibly O₃ (ozone) [9]. Atomic hydrogen is a minor atmospheric constituent. Whether the satellite has an ionosphere to correspond to its atmosphere is unresolved [10]. Ganymede's discovery is credited to Galileo Galilei, who observed it in 1610 [11]. The satellite's name was soon suggested by astronomer Simon Marius, for the mythological Ganymede, cupbearer of the Greek gods and Zeus's beloved [12]. Beginning with *Pioneer 10*, spacecrafts have been able to examine Ganymede closely [13]. The *Voyager* probes refined measurements of its size, while the *Galileo* craft discovered its underground ocean and magnetic field. In Table 1.4 Ganymede's characteristics have been tabulated.

Discovery			
Discovered by	G. Galilei S. Marius		
Discovery date	January 11, 1610		
Orbital characteristics			
Periapsis	1'069'200 km		
Apoapsis	1'071'600 km		
Mean orbit radius	1'070'400 km		
Eccentricity	0.0013		
Orbital period	7.15455296 terrestrial day		
Average orbital speed	10.880km/s		
Inclination	0.20° (to Jupiter's equator)		
Physical characteristics			
Mean radius	2634.1 ± 0.3km (0.413 Earths)		
Surface area	87.0 million km ² (0.171 Earths)		
Volume	7.6×10 ¹⁰ km ³ (0.0704 Earths)		
Mass	1.4819×10 ²³ kg (0.025 Earths)		
Mean density	1.936 g/cm ³		
Equatorial surface gravity	1.428 m/s ² (0.146 g)		
Escape velocity	2.741 km/s		
Rotation period	synchronous		
Axial tilt	0–0.33°		
Albedo	0.43 ± 0.02		
Surface temp.	min	mean	max
K	70	110	152
Apparent magnitude	4.61 (opposition)		
Atmosphere			
Surface pressure	trace		
Composition	oxygen		

Table 1.4 :orbital and physic characteristics of Ganymede[6]

1.2.1 Orbit and rotation

Ganymede orbits Jupiter at a distance of 1'070'400km, third among the Galilean satellites [3], and completes a revolution every seven days and three hours. Like most known moons, Ganymede is tidally locked, with one face always pointing toward the planet [14]. Its orbit is very slightly eccentric and inclined to the Jovian equator, with the eccentricity and inclination changing quasi-periodically due to solar and planetary gravitational perturbations on a timescale of centuries. The ranges of change are 0.0009° – 0.0022° and 0.05° – 0.32° , respectively [15]. These orbital variations cause the axial tilt (the angle between rotational and orbital axes) to vary between 0° and 0.33° [16]. Ganymede participates in orbital resonances with Europa and Io: for every orbit of Ganymede, Europa orbits twice and Io orbits four times [15][17]. The superior conjunction between Io and Europa always occurs when Io is at periapsis and Europa at apoapsis. The superior conjunction between Europa and Ganymede occurs when Europa is at periapsis [15] The longitudes of the Io–Europa and Europa–Ganymede conjunctions change with the same rate, making the triple conjunctions possible. Such a complicated resonance is called the **Laplace resonance** [18].

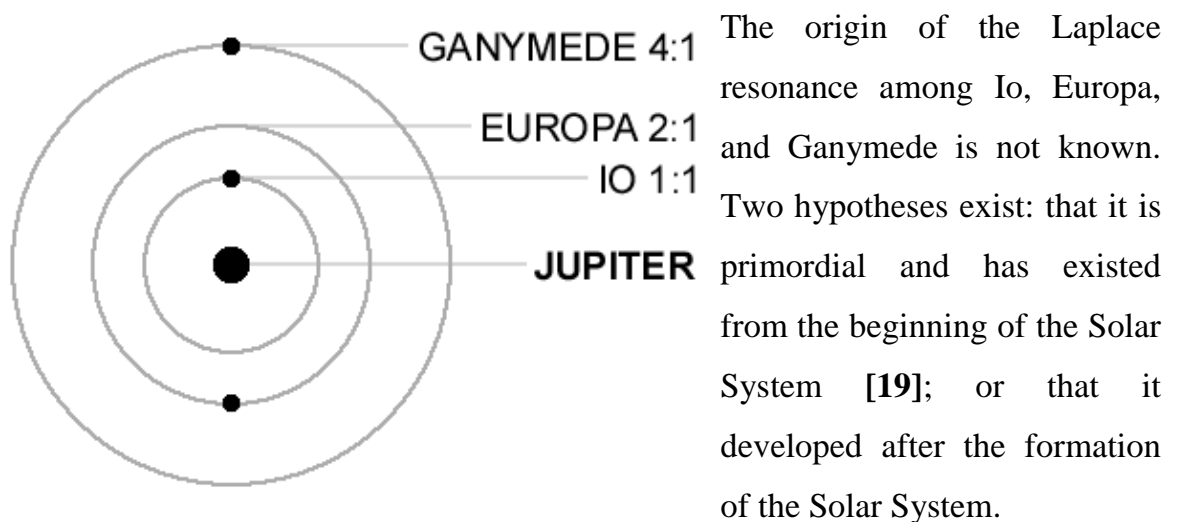


Figure 1.5 : The Laplace resonances of Ganymede, Europa, and Io [6]

A possible sequence of the events is as follows: Io raised tides on Jupiter, causing its orbit to expand until it encountered 2:1 resonance with Europa(*figure 1.5*); after that the expansion continued, but some of the angular moment was transferred to Europa as

the resonance caused its orbit to expand as well; the process continued until Europa encountered 2:1 resonance with Ganymede [18]. Eventually the drift rates of conjunctions between all three moons were synchronized and locked in the Laplace resonance [18].

1.2.2 Composition

The average density of Ganymede, 1.936g/cm^3 , suggests a composition of approximately equal parts rocky material and water, which is mainly in the form of ice [7]. The mass fraction of ices is between 46–50%, slightly lower than that in Callisto [20]. Some additional volatile ices such as ammonia may also be present [20][21]. The exact composition of Ganymede's rock is not well known [20].



Figure 1.6: Interior of Ganymede [6]

Ganymede's surface has an albedo of about 43% [22]. Water ice seems to be ubiquitous on the surface, with a mass fraction of 50–90% (*figure 1.6*) [7], significantly more than in Ganymede as a whole. Near-infrared spectroscopy has revealed the presence of strong water ice absorption bands at wavelengths of 1.04, 1.25, 1.5, 2.0 and $3.0\mu\text{m}$ [22]. The grooved terrain is brighter and has more icy composition than the dark terrain [23]. The analysis of high-resolution, near-infrared and UV spectra obtained by the *Galileo* spacecraft and from the ground has revealed various non-water materials:

carbon dioxide, sulfur dioxide and, possibly, cyanogen, hydrogen sulfate and various organic compounds [7][24]. *Galileo* results have also shown magnesium sulfate (MgSO_4) and, possibly, sodium sulfate (Na_2SO_4) on Ganymede's surface [14][25]. These salts may originate from the subsurface ocean [25]. The ganymedian surface is asymmetric; the leading hemisphere—that facing the direction of the orbital motion—is brighter than the trailing one [22]. This is similar to Europa, but the reverse is true on Callisto [22]. The trailing hemisphere of Ganymede appears to be enriched in sulfur dioxide [26][27]. The distribution of carbon dioxide does not demonstrate any hemispheric asymmetry, although it is not observed near the poles [24][28]. Impact craters on Ganymede (except one) do not show any enrichment in carbon dioxide, which also distinguishes it from Callisto.

1.2.3 Magnetosphere

The *Galileo* craft made six close flybys of Ganymede from 1995–[8] and discovered that Ganymede has a permanent (intrinsic) magnetic moment independent of the Jovian magnetic field. The value of the moment is about $1.3 \times 10^{13} \text{ T} \cdot \text{m}^3$ [8], which is three times larger than the magnetic moment of Mercury. The magnetic dipole is tilted with respect to the rotational axis of Ganymede by 176° , which means that it is directed against the Jovian magnetic moment [8]. Its north pole lies below the orbital plane. The dipole magnetic field (*figure 1.7*) created by this permanent moment has a strength of $719 \pm 2 \text{ nT}$ at the equator of the moon [8], which should be compared with the Jovian magnetic field at the distance of Ganymede—about 120 nT .

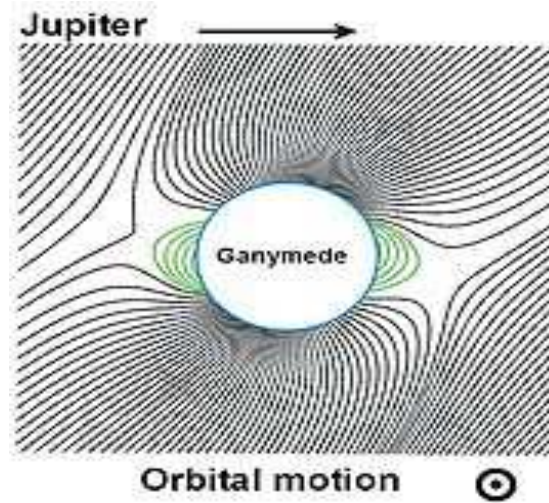


Figure 1.7 : Magnetic field of the Jovian satellite Ganymede, which is embedded into the magnetosphere of Jupiter. Closed field lines are marked with green color][6].

The equatorial field of Ganymede is directed against the Jovian field, meaning reconnection is possible. The intrinsic field strength at the poles is two times that at the equator—1440nT [8]. The permanent magnetic moment carves a part of space around Ganymede, creating a tiny magnetosphere embedded inside that of Jupiter; it is the only moon in the Solar System known to possess the feature. Its diameter is $4\text{--}5R_G$ ($R_G=2,631.2\text{km}$) [29]. The ganymedian magnetosphere has a region of closed field lines located below 30° latitude, where charged particles (electrons and ions) are trapped, creating a kind of radiation belt [29]. The main ion species in the magnetosphere is single ionized oxygen— O^+ [10]—which fits well with the tenuous oxygen atmosphere of the moon. In the polar cap regions, at latitudes higher than 30° , magnetic field lines are open, connecting Ganymede with Jupiter's ionosphere [29]. In these areas, the energetic (tens and hundreds of keV) electrons and ions have been detected [30]. which may be responsible for the auroras observed around the ganymedian poles [31]. In addition, heavy ions continuously precipitate on the polar surface of the moon, sputtering and darkening the ice [30]. The interaction between the ganymedian magnetosphere and Jovian plasma is in many respects similar to that of the solar wind and Earth's magnetosphere [29]. The plasma co-rotating with Jupiter

impinges on the trailing side of the ganymedian magnetosphere much like the solar wind impinges on the Earth's magnetosphere. The main difference is the speed of plasma flow—supersonic in the case of Earth and subsonic in the case of Ganymede. Because of the subsonic flow, there is no bow shock off the trailing hemisphere of Ganymede. In addition to the intrinsic magnetic moment, Ganymede has an induced dipole magnetic field [8]. Its existence is connected with the variation of the Jovian magnetic field near the moon. The induced moment is directed radially to or from Jupiter following the direction of the varying part of the planetary magnetic field. The induced magnetic moment is an order of magnitude weaker than the intrinsic one. The field strength of the induced field at the magnetic equator is about 60nT—half of that of the ambient Jovian field [8]. The induced magnetic field of Ganymede is similar to those of Callisto and Europa, indicating that this moon also has a subsurface water ocean with a high electrical conductivity [12][8]. Given that Ganymede is completely differentiated and has a metallic core [7][32], its intrinsic magnetic field is probably generated in a similar fashion to the Earth's: as a result of conducting material moving in the interior [8][32]. The magnetic field detected around Ganymede is likely to be caused by compositional convection in the core [32], if the magnetic field is the product of dynamo action, or magneto-convection [8][33]. Despite the presence of an iron core, Ganymede's magnetosphere remains enigmatic, particularly given that similar bodies lack the feature [7]. Some research has suggested that, given its relatively small size, the core ought to have sufficiently cooled to the point where fluid motions and a magnetic field would not be sustained. One explanation is that the same orbital resonances proposed to have disrupted the surface also allowed the magnetic field to persist: with Ganymede's eccentricity pumped and tidal heating increased during such resonances, the mantle may have insulated the core, preventing it from cooling [34]. Another explanation is a remnant magnetization of silicate rocks in the mantle, which is possible if the satellite had a more significant dynamo-generated field in the past [7].

1.3 Mission Analysis

1.3.1 Mission phases

Figure 1.8 reports the orbital tour of JGO spacecraft based on input from the EJSM Mission Analysis working group [35].

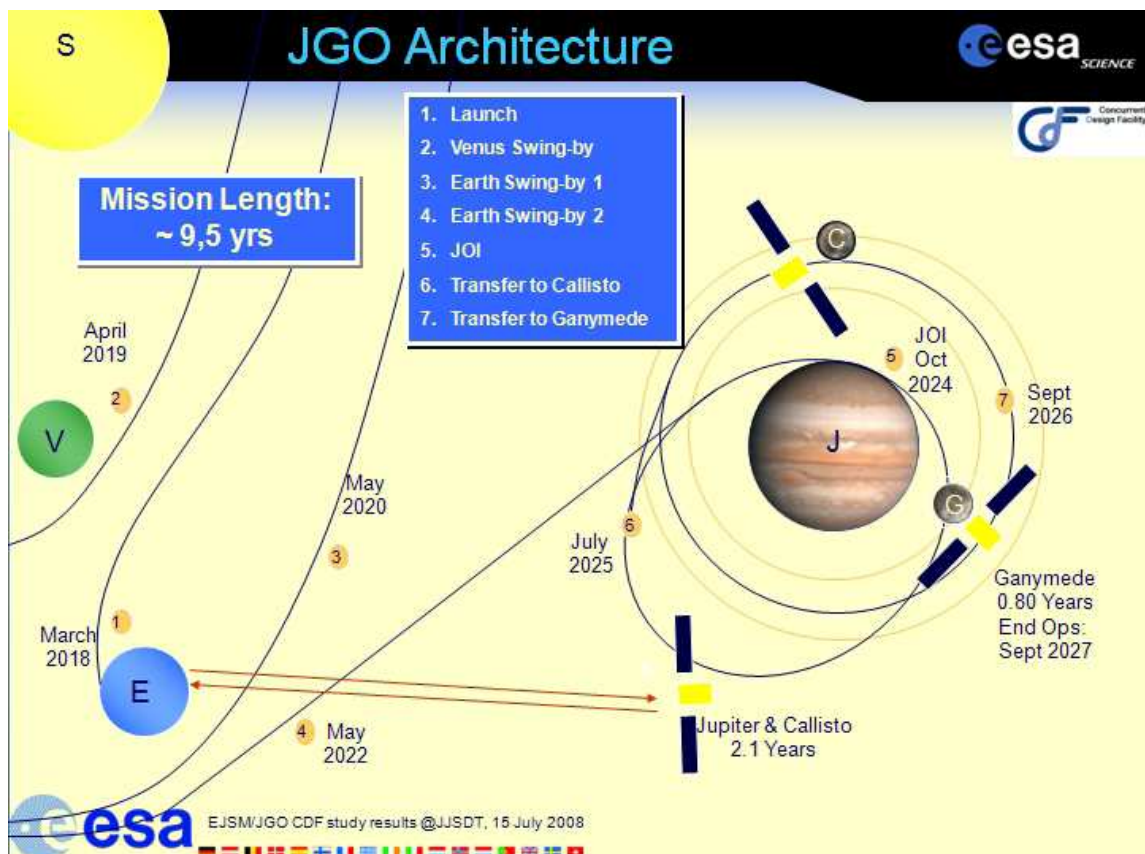


Figure 1.8 : Orbital tour of JGO spacecraft [36]

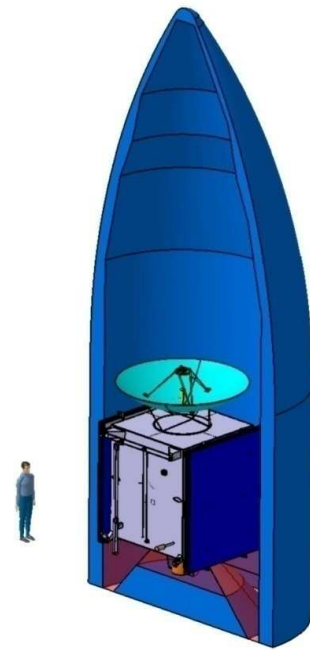
Following a description of all the different phases:

- **Launch**

Ariane 5 (figure 1.9) was selected as launch vehicle. A transfer analysis was performed and in the time frame between 2018 and 2024 three favourable launch windows were identified.



Figure 1.9 (a) Ariane 5 vector [37]



(b) Accommodation of JGO in the launcher [36]

As of this writing the baseline mission scenario foresees a launch in March 2020 from Kourou. Direct escape would be performed with an escape velocity of ~ 3.39 km/s and a declination of 0 deg. A chemical propulsion approach with gravity assists will be used.

- **The interplanetary cruise phase**

The transfer from Earth to Jupiter would be achieved by performing a series of Gravity Assists (GA). The best performance is obtained with a Venus-Earth-Earth Gravity Assist (VEEGA) sequence, with a trade-off between the minimal ΔV manoeuvres and the shortest transfer time. Figure 1.10 shows in red the VEEGA transfer trajectory for the launch of 2020.

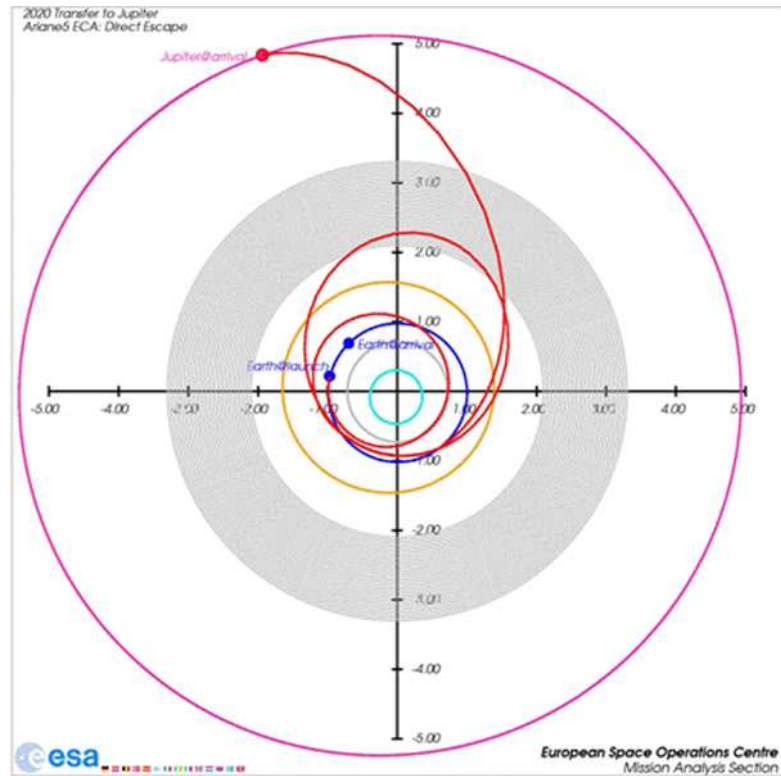


Figure 1.10 Transfer from Earth to Jupiter with an Ariane 5 [35]

- **Jupiter orbit insertion and planetocentric phase**

The arrival date for the planetocentric phase of the tour is February 2026. The V_{inf} with respect to Jupiter would be ~ 5.5 km/s and the declination with respect to Jupiter's equator would be -4.5 deg. A Ganymede Gravity Assist (GGA) would be performed before Jupiter Orbit Insertion (JOI). The JOI capture orbit is a $13 \times 245 R_j$ orbit. Gravity assist at Io and Europa are not planned in order to avoid high radiation doses. Jupiter arrival is scheduled for February 2026 with a $V_{inf} = 5.501$ km/s.

JOI would be followed by injection into a highly elliptic orbit, followed by a PeriJove Raising Manoeuvre (PRM) at apojove. Resonant GGAs are used to:

- reduce the orbital period
- reduce the inclination
- reduce the infinite velocity with respect to Ganymede

- **Callisto Science Phase**

The next phase is a Callisto science phase, where the spacecraft is placed in a resonant orbit with Callisto. These resonant orbits enable frequent passes and a good coverage of Callisto. Nineteen Callisto fly-bys are foreseen, within a total duration of 383 days. The V_{inf} remains close to 2.05 km/s and the radiation dose picked up during this phase is 21 krad.

In Figure 1.11 the Callisto science phase is shown at one of the 19 fly-by's.

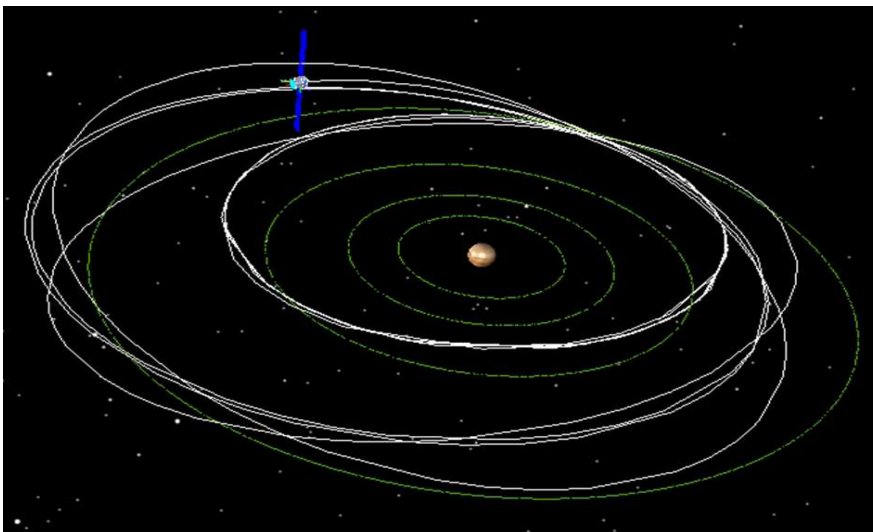


Figure 1.11 : Part of the science phase around Callisto. Jupiter is in the centre, the orbits of the Galilean moons are shown in green, Callisto and Ganymede are represented by grey spheres. A part of the trajectory of JGO is shown in white. [35]

- **Ganymede approach and orbit**

After the Callisto science phase, the spacecraft moves from Callisto to Ganymede orbit, with a Gravity Assist sequence of Callisto-Ganymede-Ganymede (CGG), taking 76 days. All GA are tuned such that they are almost all performed at the minimum altitude (200 km). Additional deep space manoeuvre cost 130 m/s in this phase. These manoeuvres result in a V_{inf} at Ganymede of 936 m/s.

This is the start of the *Ganymede science phases*, with first a near polar *elliptical* orbit followed by a *circular* phase:

Elliptical orbit: the initial argument of pericenter is set to 141.8° for the elliptical orbit of 200×6000 km (*figure 1.12*).

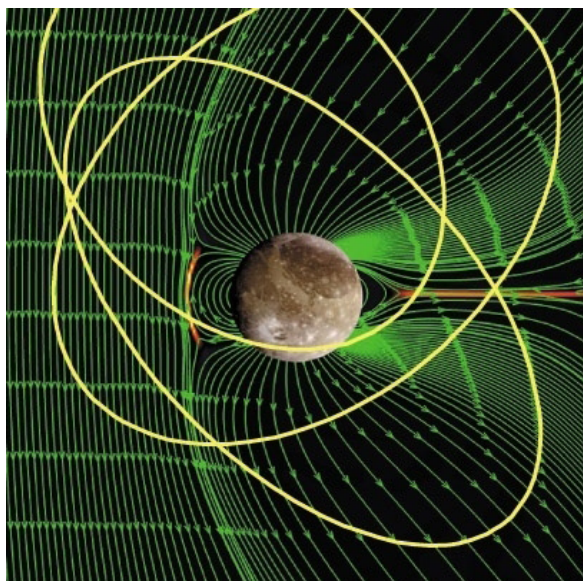


Figure 1.12 : Elliptical orbit for magnetospheric studies [38]

The natural lifetime of this orbit, before it degrades significantly, is around 190 days and limited due to Jupiter gravity disturbance. However, the maximum duration of this phase is mission phase is set to 80 days, due to radiation dose constraints. This disturbances cause the pericenter going up to 1000 km and apocenter down to 1100 km, resulting in an almost circular orbit. For this quasi polar orbit, the inclination and the ascending node remain almost constant.

The maximum eclipse duration of this phase is around 0.8 hours. The total radiation dose is 15 krad behind 8mm Al shielding within 80 days[35].

Circular orbit: the radius of the circular orbit (*figure 1.13*) would be 200km and the eccentricity remains quasi-stable at 0 for almost 150 days. After approximately 150 days, a 200 km orbit can be re-initialized with a cost of few m/s. As the circular orbit is significantly more stable than an elliptic orbit, the natural lifetime is 270 days. The maximum duration of this mission phase is set to 180 days, due to radiation dose constraints (the design point is <100 krad). For a quasi polar orbit, the inclination and the ascending node remains almost constant. The maximum eclipse duration is around 0.92 hours.

Good global coverage is achieved in less than 150 days whereby most points on the surface get more than 12 passes. Total coverage is achieved over the full life time. The total radiation dose in 180 days is 33 krad for 8mm Al shielding[35].

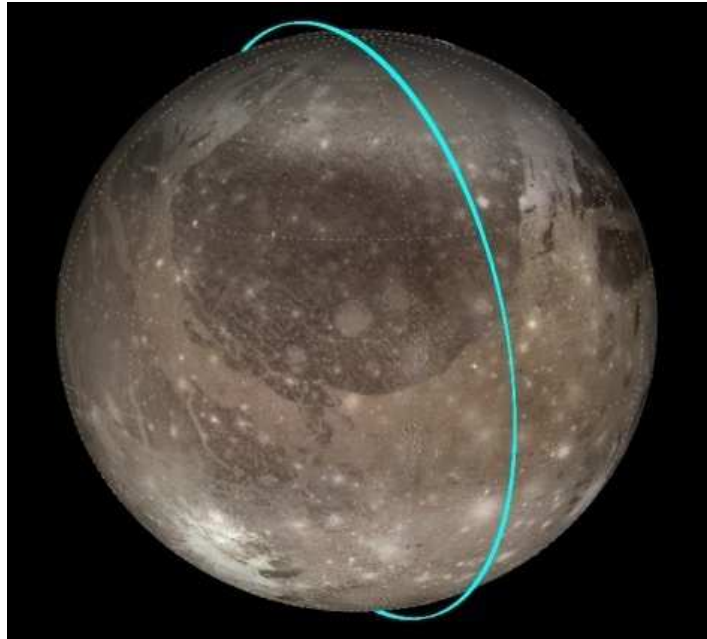


Figure 1.13 : Near-polar 200 Km altitude orbit [38]

1.3.2 End of mission options

Currently it is foreseen to impact JGO on Ganymede's surface in an *uncontrolled* way as soon as the science measurements are completed.

A *controlled impact* with a de-orbit burn would cost $\sim 15\text{m/s}$. In case of an impact the impact error would be in the order of kilometres. The *weak escape strategy* has been discarded since it would cost around 900 m/s and is not affordable[35].

1.4 Spacecraft subsystems

In this paragraph the main characteristics of the JGO spacecraft subsystems are described.

1.4.1 Structures and Configuration

The general *requirements* and **design drivers** for the configuration are:

- the overall composite configuration shall fit in the fairing of the Ariane 5;
- the configuration shall accommodate all equipment and instruments;
- the configuration shall provide unobstructed fields of view for the science instruments, the sensors and antennas, and unobstructed deployment for mechanism;
- the configuration shall provide access for the AIT (Assembly Integration and Testing), including servicing of components during ground operations;
- the complexity of the configuration shall be kept to a minimum, in order to minimise constant AIT complexity;

The major *drivers* for the **structural design** are:

- Accommodation of propellant and pressurant tanks
- Accommodation of the High Gain Antenna (HGA, 2.8 m diameter)
- Accommodation of the 500N-main engine
- Shielding of instruments and avionics

The two propellant tanks are positioned on the centre-line of the S/C within the main structural central cylinder. This concept provides stiffness for the overall spacecraft and locates the large amount of propellant mass near the centreline. The HGA is mounted at the top of the S/C with a truss structure, while the main engine is mounted at the bottom. Other subsystems are attached to the four exterior, rectangular panels, which are reinforced by interior panels. Since most of the equipment and instruments do not have high masses, the panel structure requires relatively low mass.

Figure 1.14 shows the central cylinder and structure of the body and the two main tanks that are positioned inside the main cylinder.

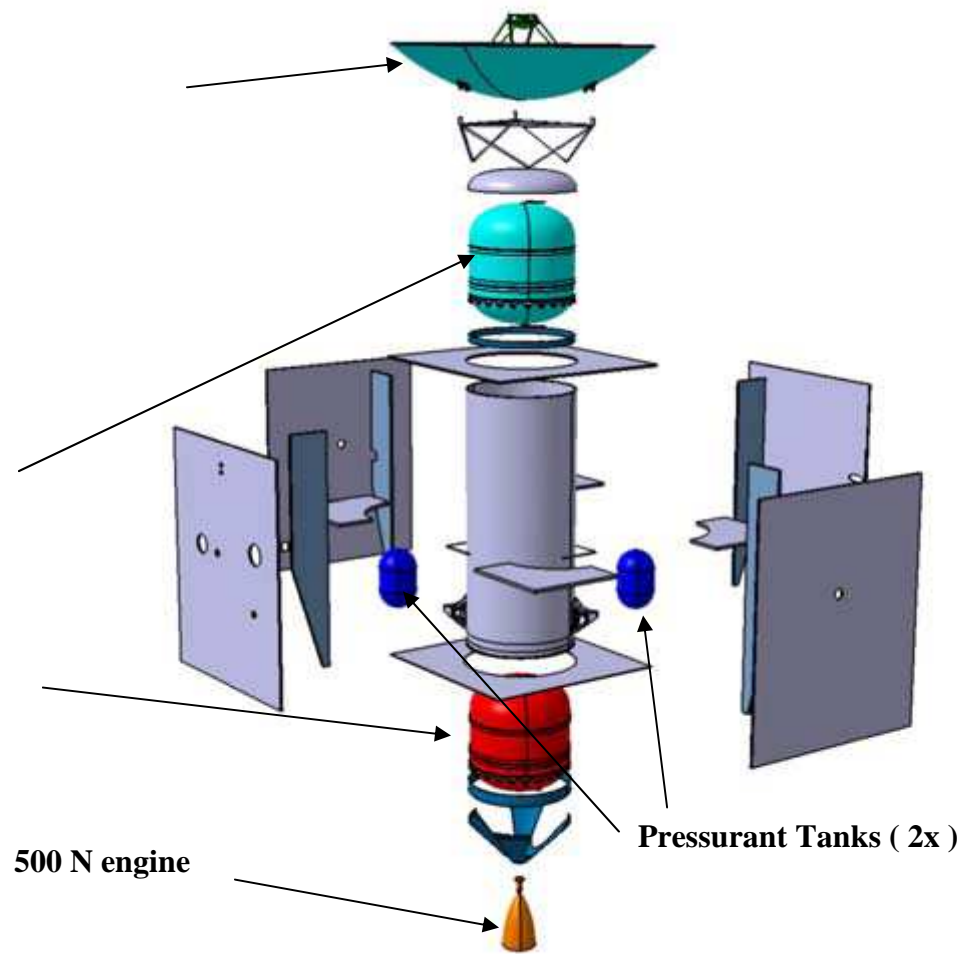


Figure 1.14: Main configuration driver, central cylinder for large propulsion tanks; exploded view.[35]

The Solar Panels of mission Rosetta have been taken as reference for the JGO configuration, but with 4 panels on each of the wings, instead of Rosetta's 5 panels each (see Figure 1.15) and using GaAs triple-junction cells. JGO requires $\sim 51\text{m}^2$ solar panels compared to 68m^2 for Rosetta.

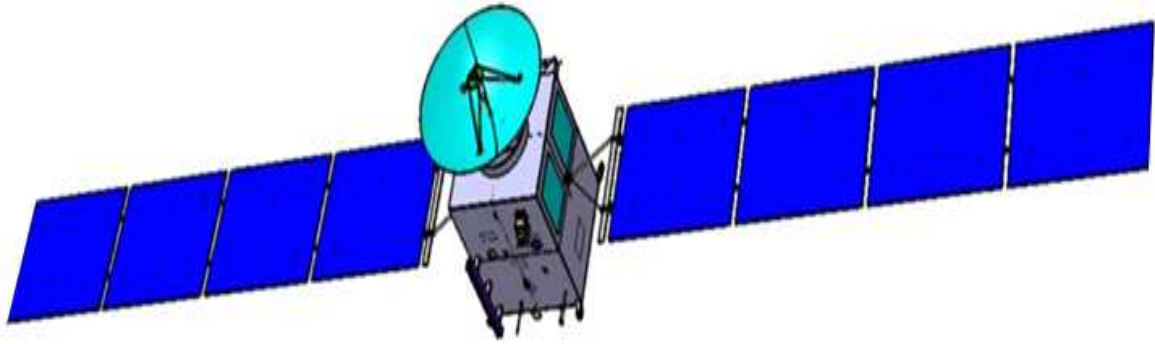


Figure 1.15: JGO with deployed solar panel [35]

Just after the deployment of the solar panels, the various instrument booms would be deployed. Figure 1.16 shows the fully deployed spacecraft, with the booms for the different instruments extended.

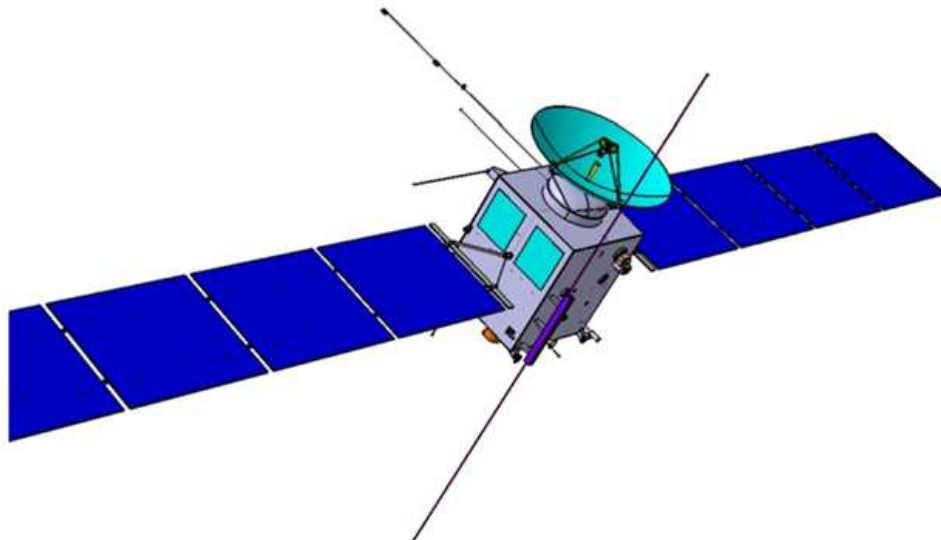


Figure 1.16: Fully deployed S/C. [35]

The tentative accommodation of science instruments on the spacecraft is shown in Figure 1.17.

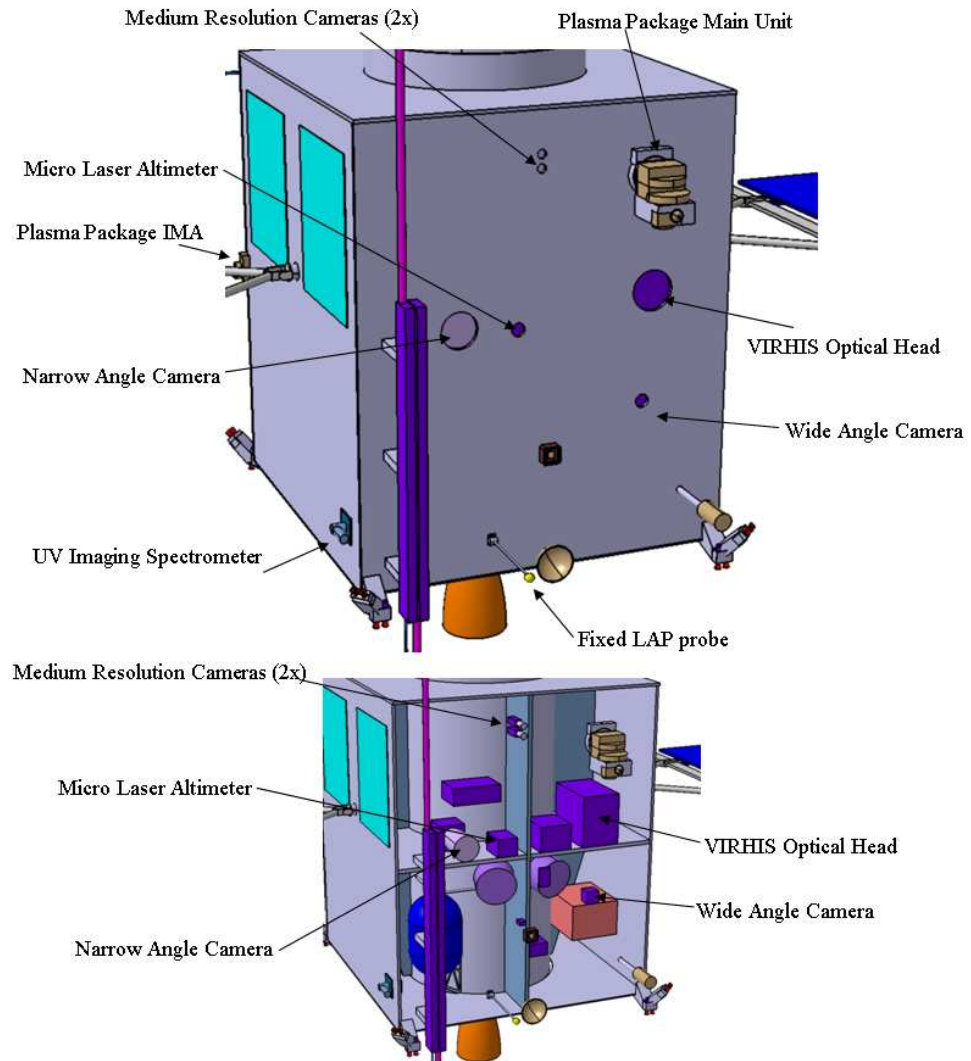


Figure 1.17 : JGO tentative instrument accommodation on the zenith side (top), and cutaway of the zenith side (bottom).[35]

1.4.2 Power subsystem

The Power subsystem consists of two main parts: solar arrays and batteries. The required Power Control and Distribution Unit (PCDU) has a mass of 12.4 kg. The regulated power bus is at 28 V.

Solar Arrays

The spacecraft is equipped with deployable, rotating solar arrays of Triple-Junction GaAs cells.

The use of solar concentrators is not foreseen. The solar array size was dimensioned for a mission to Jupiter and the Galilean moons. The power profile with respect to science operations and communications was carefully assessed. The following assumptions were considered:

- $\sim 51 \text{ W/m}^2$ Sun illumination at Jupiter orbit
- 2640 W/m^2 Sun illumination at Venus orbit
- -108°C solar array temperature at Jupiter
- solar cells: 28% efficiency of the GaAs solar cells at LILT (Low Intensity Low Temperature) conditions at beginning of life (BOL); 20% degradation during the mission life time; mass including substrate $\sim 4.94 \text{ kg}$.

The sizing case for the solar array is the Jupiter Orbit mode, requiring 417 W. Additionally, PCDU inefficiency and system margins have to be added, which results in a power requirement of **539W at end of life (EOL)** at Ganymede orbit . Taking into account the solar cell degradation , pointing losses, and path efficiency, the available maximum power (P_{max}) at Jupiter using these solar cells is reduced to 10.55 W/m^2 . The available power at the different phases of the mission is shown in Table 1.18.

Phase	Available power @ Venus [W]	Available power @ Jupiter [W]	Pmax [W/m ²] @ Jupiter	SA area [m ²]
Cruise	23763			
Jupiter to GGA2		609		
GGA2 to GGA6		607		
GGA6 to Callisto		572		
Callisto science		565		
Callisto to Ganymede		563		
Ganymede science (elliptical)		556		
Ganymede science (circular)		539	10.55	51.07

Table 1.18: Available solar array power during the mission [35]

Batteries

Batteries are required to provide power during eclipses and for safe mode. The battery sizing case was given by the science mode during eclipses (270 minutes maximum duration). During eclipse not all of the defined scientific instruments on board will operate, or at time-multiplexed operations. The most power-demanding combination

of the instruments is 70 W. During the eclipse science mode, an additional 20 W is budgeted to provide heating to the instruments. This results in 90 W power available for instruments during eclipse.

The total spacecraft power consumption during eclipses is 341 W. This results in an end-of life (EOL) battery storage capacity of 1534 Wh. The battery is Li-Ion (ABSL based) and has a mass of 25.8 kg (incl. margins).

1.4.3 Thermal control

The thermal control subsystem keeps the S/C and instruments within the specified temperature limits during the whole mission. The spacecraft must be protected both from high temperatures during the Venus fly-by, and from cold temperatures during operations around Jupiter.

Thermal control is provided by a 1.26m² Optical Solar Reflectors (OSR) radiative surface mounted on the solar arrays. OSRs are preferred to paints because less sensitivity to radiation degradation. Additionally louvers are applied on radiators to adapt emissivity as function of power dissipation and to minimize heating power demands (like for Rosetta).

High temperature MLI is applied on the S/C external surface for shielding in the hot environment in the vicinity of Venus. MLI is also applied on tanks, thruster boxes, and pipe lines. Black paint covers the internal surfaces to minimize thermal gradients.

1.4.4 Propulsion

The main drivers for the propulsion subsystem are the required ΔV to reach Jupiter, to perform the Jupiter tour with Callisto phase and orbit insertion and circularisation at Ganymede. In order to satisfy the mission ΔV of ~2990 m/s (including margins), the baseline propulsion system is a bipropellant MON/MMH system that feeds an European Apogee Motor (EAM) 500N main engine, with a specific impulse (Isp) of 323s. The 500N EAM was chosen as the main engine for the Laplace propulsion subsystem. Some of its characteristics are given in Table 1.19. The engine will be at a TRL level of 8 in 2011, when it is planned to be launched with Alphas.

PERFORMANCE : 500 European Apogee Motor	
Characteristics	
Propellant	MMH, NTO, MON-1, MON-3
Nominal thrust vac	500 ± 20 N
Nominal Isp vac	≥ 325 sec
Nominal mixture ratio	1.65
Operating Range	11 to 18 bar
Nominal chambre pressure	10 bar
Total impulse	11.85 x 10⁻⁶ Ns
Maximum burn time	10.5 h
Thermal Cycles	55
Operating Voltage	50 VDC
EAM Overall length	803 mm
Nozzle dia	382 mm
Mass	< 5 Kg
Mission design Life	15 years

Table 1.19 : EAM main engine details.[35]

The propellant and oxidiser are stored separately in two 1108-liter OST-22/X cylindrical tanks, and are supported by two He-pressurant tanks.

1.4.5 Attitude and Orbit Control Subsystem (AOCS)

The 3-axis stabilized attitude and orbit control subsystem (AOCS) allows for spacecraft pointing in particular during communication and nadir-observation phases. The AOCS consists mainly of four reaction wheels which are off-loaded regularly, two Star trackers, one internal measurement unit, and two Sun sensors. A navigation camera is used for critical manoeuvres. Correction manoeuvres and reaction wheel offloading are performed by the thrusters.

1.4.6 Mechanisms

There are five primary mechanisms on the JGO spacecraft [35]:

- ***Solar Array Deployment:*** the Solar Arrays (SA) are composed of 2 wings of 4 panels each, which must be deployed after release from the launch vehicle. The deployment mechanism includes root hinges, inter-panel hinges, synchronisation mechanisms and hold down and release mechanisms (HDRM). The JGO SA design is based on Rosetta.
- ***Solar Array Pointing:*** the Solar Arrays must be continually rotated to point to the Sun to achieve maximum power generation. It must be compatible with spacecraft manoeuvres, with a maximum speed of 27 deg/sec without exciting the SA fundamental frequency of 0.1 Hz. The JGO SA pointing mechanism design is also based on Rosetta.
- ***Magnetometer deployment:*** two magnetometers of mass 0.25 kg must be deployed on 3.3 m- and 5 m-long booms. The JGO design is based on Cluster and uses springs and hinges.
- ***Penetrating Radar dipole antenna deployment:*** a 10 m dipole antenna is created by deploying two 5 m-long booms on either side of the spacecraft. The JGO design is based on SHARAD (on board Mars Reconnaissance Orbiter), and uses elastic collapsible springs.

1.4.7 Telecommunication

The telecommunications subsystem was designed to satisfy a data rate of 40 to 66 Kbps at a distance from Earth of 5 to 6.1 AU. Science data downlink is performed at X-band and radio science experiments (measurements of gravity fields) additionally at Ka-band. X-band up-and downlink is foreseen for TC/TM.

To communicate with ground stations, the JGO is equipped with a 2.8m High Gain Antenna (HGA). In order to point the HGA towards Earth during communications, two options were examined:

- use a pointing mechanism to allow the spacecraft to point the HGA at Earth. This allows instruments to remain nadir pointed and science operations to continue;
- fix the HGA to the spacecraft. This requires the entire spacecraft to move in order to point the HGA, which interrupts science operations.

The critical phase of the mission for communications is the orbit around Ganymede. As the solar aspect angle varies by over 120 deg in this phase, to continually point the HGA at Earth would require a 2 DoF mechanism. The mass and power requirements on such a mechanism for a 2.8 m antenna were deemed to be unacceptably high. Therefore, a pointing mechanism was not baselined and instead a split was made in spacecraft operations between science observation and communication with Earth. The Cebreros ground station is foreseen for main communications. The ground station is assumed to be available for a window of 8 hours per day.

1.4.8 Data handling

The data handling subsystem is required to provide downlink data rates of 40 to 66 Kbps. The design (*Figure 1.20*) is based on a HICDS LEON2 dual redundant computer, currently prepared for ESA's Bepi Colombo mission. It consists of an integrated processor, TMTC modules including redundancies, and an integrated mass memory board and controller.

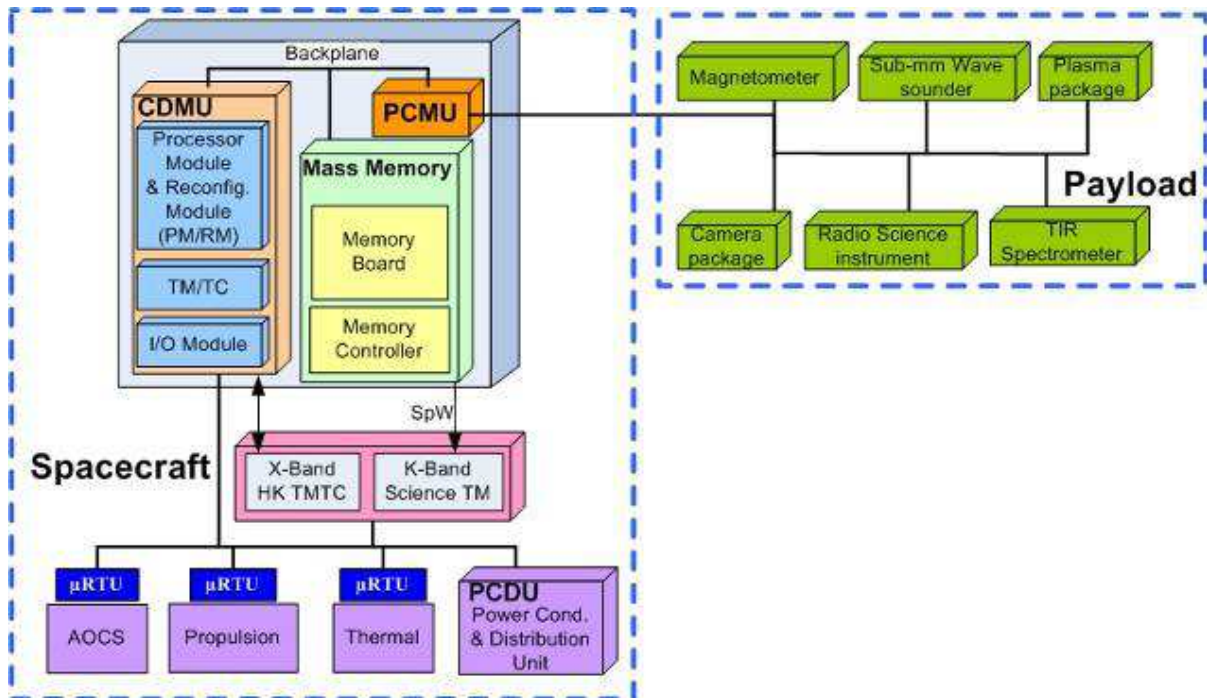


Figure 1.20 : Simplified schematics of data handling system..[35]

The data handling subsystem is required to store all science data and telemetry for up to 10 days in case of interruption of communications. It has been estimated that a board with FLASH technology could contain up to 1024/2048 Gbits of data space. For JGO, a very conservative approach is retained which leads to a single memory board of 256Gbits of size, which gives plenty of extra storage space and margin, while being very small in size.

1.5 Laser Altimetry and Radar Sounder performance

In this paragraph information about Laser Altimetry (LA) and Radar Sounder (RS) on board the JGO will be given. The analysis of the Ganymede subsurface with a **Radar Sounder** instrument can bring new detailed data of this icy body that, matched with the Europa sounder, will provide evidence and clues on the genesis and behavior of this exotic type of planetary body. The **Laser Altimetry** will contribute to the characterization of the mission target in the areas of geodesy and geophysics, and will also be crucial for studies of the spacecraft orbit in the gravity field of satellite by providing accurate range data[39].

1.5.1 Laser Altimetry

The proposed instrument is a Laser Altimetry with time-of flight measurement and pulse-waveform analysis capability. The former measures the range from the spacecraft to the satellite's surface; the latter allows for determination of surface characteristics.

The vertical measurement accuracy of the instrument is <1 m. At Ganymede, ranging will be possible at altitudes of about less than 400 Km and at Callisto of about less than 300 Km.

The active Q-switched Nd: YAG laser will have adjustable pulse repetition rates and output energies in order to work power-efficiently, but with high quality data generation even in different operation scenario [40].

1.5.1.1 Science goals related to Laser Altimetry

The Laser altimetry on-board JGO would contribute to the following mission goals that have been defined by the EJSM Joint Definition Team (JSDT) [40]:

- *Characterize Ganymede as a planetary object including its potential habitability*

With respect to habitability the Laser altimeter will mainly contribute in determining whether or not a subsurface ocean exists in the interior of Ganymede. There is theoretical and experimental evidence (from the Galileo Mission) that Ganymede, Callisto and Europa may harbor internal oceans underneath their cold surface ice shells. Each of those would contain more liquid water than Earth's oceans combined. The tidal surface deformation to be measured with laser altimetry crucially depends on the presence of liquid shells in the interior and will determine whether these oceans exist or not. To localize and characterize liquid water reservoirs is essential to understand the habitability and prospects for the evolution of life in the Jovian system. LA will characterize the geology of Ganymede and Callisto by obtaining height profiles of tectonic features, craters and other landforms, e.g. the grooved terrain on

Ganymede. Especially in combination with subsurface radar sounding and stereo imaging this will tell us how these features were formed and how they are linked to the internal dynamics and thermal evolution of the moons. Additionally, surface characteristics on small scales (roughness, albedo) can be derived from wave-form analysis of the reflected signal)[40];

- *Study the Jovian System, its origin and evolution*

The laser altimeter will contribute to Jupiter system by studying the topography of two major satellites, Ganymede and Callisto. Topography data is required for interpretation of the gravity signals to infer the interior structure of the moons. The state of differentiation of Ganymede and Callisto are completely different although they are similar in size and composition. To understand how such different evolution scenarios came to be is one major goal of the mission.

Precise characterization of geodetic properties of Ganymede and Callisto like shape, rotational state and orientation in space, as a basis for all other dynamical models of the moons is another important task for the laser altimeter.

If JGO should be equipped with a laser receiver allowing for range-measurements from Earth or from JEO, the receiver electronics could be shared. The ranging would allow for very precise orbit determination significantly improving the interpretation of the above measurements but also for other experiments where precise positioning is of concern, e.g. gravity measurements.

The Ganymede orbit phase over several months would allow for constraining the tidal acceleration (or deceleration) of Ganymede. This will yield important constraints on the evolution of the three inner Galilean satellites Io, Europa, and Ganymede which are locked in the Laplace resonance, a stabilized 1:2:4-ratio of the orbital periods of these moons.

1.5.1.2 Sun radiation effects for LA

Very important issues for EJSM mission are considerations about the radiation environment that can compromise data capture.

The harsh radiation environment in the Jupiter System is a challenge for any instrument on-board JGO. The high-energy electrons and protons trapped in the rotating magnetosphere of Jupiter are limiting factors for the total ionizing dose and, presumably for false detections.

The solar radiation represents the greater disturbing source for a correct data acquisition for Laser Altimetry, for this reason, it is important to estimate when spacecraft JGO is in a condition of Sun eclipse .

1.5.2 Radar Sounder

The Radar Sounder system on board JGO will work at low frequency (20-50 MHz). The Sounder system is based on a robust and mature technology that was already used successfully for two different Mars Missions (Mars Express, with the MARSIS instrument; NASA Reconnaissance Orbiter with SHARAD).

A Radar Sounder, thanks to the relatively low frequency of its impulse, has the capability to penetrate the surface and to perform a sub-surface analysis with a penetration ability of few kilometers (which depends on the specific selected central frequency of the pulse) with a vertical resolution in the order of some meters. The Radar Sounder can range between different intervals of depth depending on the choice of the central frequency. We can expect to have a minimum depth of about 3Km at about 50MHz (with a range of resolution of 10m in the vacuum). The instrument requirements are reported in Table 1.21[39] .

Orbiter altitude	200 Km (in the circular phase around Ganymede)
Transmitted central frequency	In the range 20-50 MHz
Transmitted bandwidth	10 MHz
Antenna dimension	< 10 m
Peak transmitted power	20 W
Along track resolution	<1 km
Across track resolution	< 5 Km
Penetration depth	< 5 Km
Vertical resolution	15 m (vacuum)
Data rate	300 kbps
Mass (without antenna)	10 Kg
Pointing requirements	$\pm 5^\circ$ for optimal measurements

Table 1.21: Main instrument requirements[39]

The RS is nadir-looking radar sounder. The antenna should illuminate the surface according to a nadir view. The optimal conditions for the measurements are associated with a nadir pointing with an accuracy of $\pm 5^\circ$.

The acquisition strategy should be defined taking into account both the data rate of the other remote sensing instruments on the JGO and also the synergy with the sounder on board of the JEO.

Signal power can be evaluated by using a classic “radar equation” that expresses the received power by a generic radar as a function of transmitted power, antenna gain, path losses and target reflectivity. In the path losses also the attenuation of the crossed terrain layers should be considered. Therefore, the received signal is strongly dependent on either the geometric parameters characterizing each crossed interfaces (supposed random rough surfaces) and dielectric properties of layers. The noise contributions arise from thermal noise, surface clutter, and environmental noise. The first one is the classic noise common to all electronic devices and its effect can be reduced by increasing either the pulse repetition frequency (PRF) for allowing a high degree of pulse integration, and the so called compression factor (the product of transmitted bandwidth and pulse duration). The second one refers to the fact that the surface echo coming from lateral directions (off-nadir clutter) may interfere with the subsurface echo in the same range cell. The ratio between these two contributions is

called signal to noise ratio (SNR). The phenomenon is pictorially shown in Figure 1.22. The off-nadir clutter power is weighted by antenna pattern and depends on terrain backscattering coefficient behaviour. Since in low frequency range the antenna is poorly directive, the only method for reducing the effect of clutter is to perform a Doppler beam sharpening in the along track direction like done for MARSIS and SHARAD. In this way, isodoppler curves allow one to improve azimuth resolution and to filter out surface clutter by reducing the area subtended by the isorange curves (see Figure 1.22)[41].

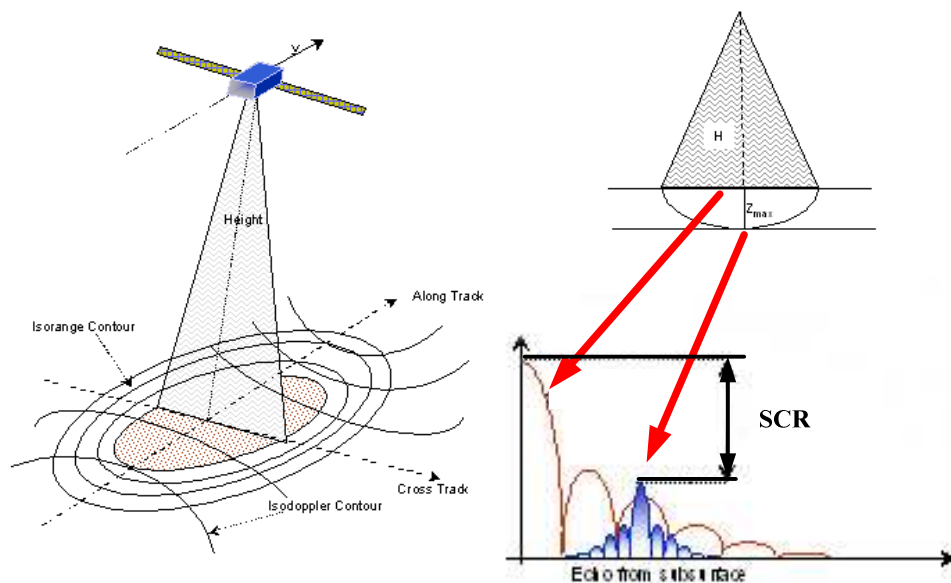


Figure 1.22 – Off-nadir clutter phenomenon[41]

1.5.2.1 Science goals related to Radar Sounder

The detailed scientific goals related to Radar Sounder for JGO are[39]:

1. Identification of the stratigraphic and structural pattern of Ganymede:

- Reconstruct the stratigraphic geometries of the ice strata and bodies and their internal relations
- Recognition, analysis and mapping of the tectonic features

2. Crustal behavior:

- Utilizing the stratigraphic and structural data identify the mode of accretion of the crust and its consumption matched by the deformational processes.
- Estimation of the ice depositional rate.
- Identification of evidences for degassing of the Ganymede's interior.

3. Matching the surface geology with subsurface features:

- Synergetic analysis of the surface and subsurface geology in order to understand the depositional and tectonic processes active in the uppermost icy crust and infer in areas without radar data the subsurface nature.

4. Global tectonic setting and Ganymede's geological evolution:

- Understanding the large scale geological processes active in the Ganymede at the global scale.
- Global map of the different geological realms based on the surface and subsurface geology.
- Reconstruction of the geological evolution of Ganymede

5. Comparison between Ganymede and Europa :

- Definition of the differences and common geological patterns of the two planetary bodies leading to a better understanding of the general development of the icy bodies and the geological principles on which the icy bodies formation evolution are based.

1.5.2.2 Jupiter radiation effects for RS

Jupiter radiation environment provides disturbance noise source for a correct working of RS: the jovian radiation can compromise data acquisition at the RS working frequency. For this reason it is necessary to establish when spacecraft JGO is in condition of Jupiter eclipse.

CHAPTER 2 : JGO orbital propagator

2.1 Planetary Data System , NAIF and SPICE

The Navigation and Ancillary Information Facility (NAIF) serves as the Navigation Node of NASA's Planetary Data System (PDS) archiving and providing the science community access to SPICE data from NASA's planetary exploration missions.

NAIF provides the information system SPICE which assist scientists in planning and interpreting scientific observations from space.

The SPICE system is focused on *solar system geometry* (figure 2.1): it includes a collection of data , tools , routines and a large suite of software , mostly in the form of subroutines , that customers can incorporate in their own applications to compute derived observations geometry.

The version of SPICE Toolkit used in this work ,is N00063 released on April 17th, 2009.

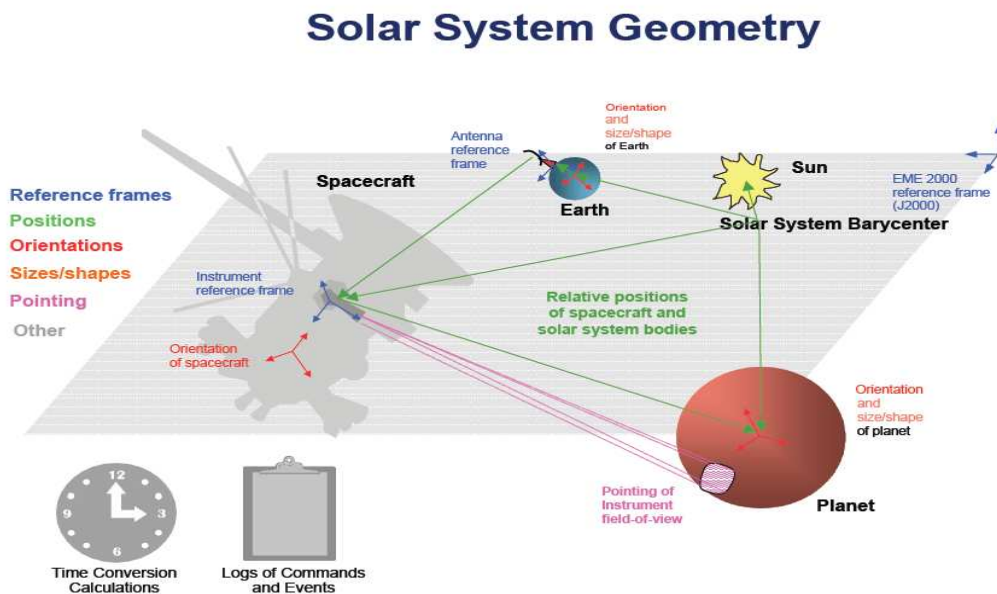


Figure 2.1: Solar System Geometry on which SPICE system is based on.[42]

2.1.1 Spice kernels

The primary SPICE data sets are often called "*kernels*" or "*kernels file*" [43]: they are produced by the most knowledgeable sources of space information, usually located at a mission operation centre.

SPICE kernel file contents and characteristics are summarized below, starting from its acronyms:

S- Spacecraft ephemeris , given as a function time (SPK).

P-Planet satellite asteroid or comet ephemeris given as function of time (PCK).

I-Instrument description kernel containing descriptive data peculiar to a particular science instruments (IK).

C-Pointing kernel containing a transformation matrix, traditionally called the C-matrix, which provides time-tagged pointing (orientation) angles for a spacecraft structure with respect to science instruments are mounted (CK).

E-Events kernel, summarizing mission activities both planned and unanticipated. Events data are contained in the SPICE EK file set, which consists of three components: Science Plans, Sequence , and Notes (EK).

Frame Kernel contains specifications for the assortment of reference frames that are typically used by flight projects (FK).

Spacecraft Clock Kernel and **Leapseconds kernel** are used in converting time tags between various time measurement systems.

SPICE kernel files can be downloaded from

http://naif.jpl.nasa.gov/pub/naif/generic_kernels

All the previous description is summarized in Figure 2.2.

SPICE Components

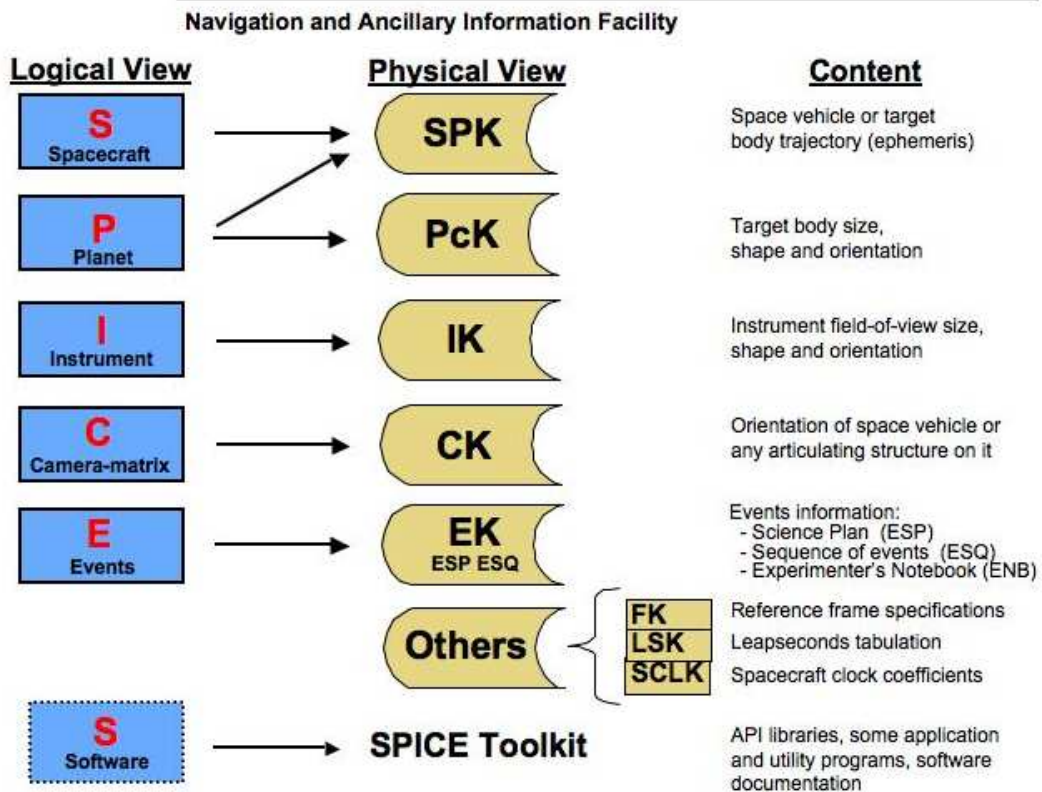


Figure 2.2: SPICE kernels architecture [44]

2.1.2 SPICE Toolkit

As mentioned above, SPICE toolkit is a collection of software and its principal component is a library of subroutines needed to read kernel files and to calculate observation geometry parameters of interest.

Users can integrate these SPICE toolkit subroutines into their own applications such as IDL, FORTRAN 77, C, ANSI and MATLAB.

The SPICE toolkit can be downloaded from <http://naif.jpl.nasa.gov/naif/toolkit>.

In this study we analyse by means interface MICE with the compiler MATLAB 7.3.1 (it has to be noted that NAIF built and tested MICE using MATLAB version 7.4). on a PC platform for WINDOWS.

NAIF distributes MICE as a complete, standalone package. The package includes:

- the CSPICE source files;
- the MICE interface source code;
- platform specific build scripts for MICE and CSPICE;
- an HTML based help system for both MICE and CSPICE;

- the MICE MEX shared library and the M wrapper files.

The system is ready for use after installation of the library. The toolkit directory (directory structure for different interface is almost identical) consists of:

- **data**: cookbook example kernel (used only for training);
- **doc**: text documents and HTML documentation. A toolkit User's Guide, where everything about executable and SPICE software is explained. The extensions of these files can be *.ug (as User's Guide) and *.req (as "Required Reading" reference documents). These docs, which can be opened with a common text editor, contains:

- **include**: header files;
- **lib**: toolkit libraries;
- **src**: source code directories for executables and libraries;
- **exe**: utility programs. They allow to make several operations on kernel files, such as taking out comments, converting a binary format in a "transfer" one (to transfer files on computers that use different binary files storage). These programs are:

- **brief.exe**: command line program that displays a contents and time coverage summary for SPK or binary PCK files;
- **ckbrief.exe**: command line program that summarizes the pointing coverage for CK files;
- **commnt.exe**: command line program that reads, adds, extracts or deletes comments from SPICE binary kernel files;
- **chronos.exe**: command line program that converts between several time systems and time formats;
- **inspect.exe**: interactive program that examines the contents of an events component (ESQ) of an E-kernel;
- **mkspk.exe**: program that creates an SPK file from a text file containing trajectory information ;
- **msopck.exe**: command line program that converts attitude data provided in a text file as UTC, SCLK or ET-tagged quaternions, Euler angles or matrices, optionally accompanied by angular velocities;
- **simple.exe**: program that calculates the angular separation of two target bodies as seen from an observing body;

- **spacit.exe**: program that converts kernel in transfer format to binary format, converts binary kernels to transfer format and summarizes the contents of binary kernels;
- **spkdiff.exe**: program that computes differences between geometric states obtained from two SPK files and either displays these differences or shows statistics about them;
- **spkmerge.exe**: program that subsets or merges SPK files into a single one;
- **states.exe**: program that demonstrates the use of SPK files and subroutines by computing the state of a target body as seen from an observing body at a number of epochs within a given time interval;
- **subpt.exe**: program that demonstrates the use of CSPICE in computing the apparent sub-observer point on a target body;
- **tictoc.exe**: program that demonstrates the use of CSPICE time conversion utility routines string2ET and ET2UTC;
- **tobin.exe**: command line program that converts transfer format SPK, CK and EK files to binary format;
- **toxfr.exe**: command line program that converts binary format SPK, CK, EK files to transfer format.[45]

Of In this thesis we used *mkspk.exe* in order to get in output of the orbital propagator the binary file *eph.bsp* in which Ganymede's ephemeris, for the set propagation time, are contained.

To create the file *eph.bsp* it is necessary before to have from the propagator the file *ephemerisdata.txt* and then to compile the file called *setup.txt* as follows :

```
\begindata
INPUT_DATA_FILE = 'ephemerisdata.txt'
OUTPUT_SPK_FILE = 'eph.bsp'
INPUT_DATA_TYPE = 'STATES'
OUTPUT_SPK_TYPE = 5
OBJECT_ID      = -177
CENTER_NAME    = 'GANYMEDE'
```

```

REF_FRAME_NAME   = 'IAU_GANYMEDE'
PRODUCER_ID      = 'ARMANDO MAROTTA'
DATA_ORDER       = 'EPOCH X Y Z VX VY VZ'
INPUT_DATA_UNITS = ('ANGLES=RADIANS' 'DISTANCES=km')
DATA_DELIMITER   = 'TAB'
LINES_PER_RECORD = 1
IGNORE_FIRST_LINE = 0
LEAPSECONDS_FILE = 'naif0009.tls'
PCK_FILE         = 'Gravity.tpc'
TIME_WRAPPER     = '# ETSECONDS'
SEGMENT_ID       = 'PROVA_SPK_MIO_SAT'
APPEND_TO_OUTPUT = 'YES'
\begin{text}

```

When the file *setup.txt* is compiled, it can be recalled from the *mkspk.exe* software to generate the ephemeris file *eph.bsp*. This binary file can be recalled as a SPICE kernel-file by means the command *cspace_furnsh*('C:\current directoy\eph.bsp'): in this way the ephemeris of satellites in orbit around Ganymede are recognized by all SPICE routines.

2.1.3 Temporal reference.

Very important is to clarify some fundamental concepts about time, in particular the concept of **Ephemeris Time (ET)**.

ET is an uniform timescale used in ephemerides of celestial bodies. Two kinds of ephemeris time exist: Barycentric Dynamical Time (TDB) and Terrestrial Dynamical Time (TDT). ET and TDB are used synonymously in SPICE documentation. The TDB standard is used to describe the motion of celestial bodies relative to Solar System barycentre, while the TDT standard is used to describe the motion of bodies next to the Earth. These standard are linked by the relation :

$$\mathbf{TDB = TDT + 0.001657 \sin (E + 0.01671\sin(E))}$$

TDB is also linked with TAI by a constant values, in other words their difference is always 32.184 seconds:

$$\mathbf{TDB - TAI = 32.184 \text{ s}}$$

ET (or TDB) counts seconds past the reference epoch indicated with J2000 (approximately 1 January 2000, 12:00:00 at Greenwich). For example, the precedent string

26 JULY 1986 1:30:07.162 (UTC)

correspond to

-424002537.65 seconds past the ephemeris epoch J2000

Most of spacecrafts has onboard clocks (**Spacecraft Clock**, SCL) to control time coverage of instruments. These clocks don't have linear time progress, so relations between SCLK, ET and UTC can't be described by linear functions.

Mission lifetimes are divided in several partitions where the clock works continuously. So time strings in spacecraft clocks are always preceded by the partition number, such as

1/4132564.034

where "1" is the partition number and the left numbers indicate the seconds of that partition.

Sometimes, in SPICE documentation the concept of **Julian Date** occurs to determine easily the number of days between two different epochs. This standard counts days and day fractions (in Julian Proleptic Calendar) past the noon (Greenwich time) of 1st January 4713 b.C. [46]

2.1.4 Spatial reference frames

In order to individuate the position of the satellite in a precise instant of time, it is necessary to define opportune reference coordinate systems.

To reach our purpose we have used several types of reference frame, such as :

- perifocal frame
- inertial reference frame
- body-fixed reference frame

Perifocal frame is a cartesian reference system in which the fundamental plane is the plane of the spacecraft's orbit. The x_ω -axis, which points towards the periapsis and the y_ω -axis, rotated of 90° in orbital motion direction, lie in the fundamental plane, while z_ω -axis, normal to the orbital plane, is oriented to complete a right-handed system. The versors associated with these axis are respectively p , q and w . This frame is particularly useful for describing and computing the motion of the satellite along the orbit .

Inertial reference frame is the frame in which the axis are indicated with x , y and z with x and y lying on Ganymede's equator (reference plane) and z coinciding with the rotational axis of the moon. The x -axis direction is given by the ascending node of the Ganymede's equatorial plane on the Earth equatorial plane (coinciding with Celestial equator), while the y -axis is defined to complete the right-handed Cartesian tern.

The unit vectors associated with x , y and z are indicated respectively with I , J and K .

This frame is important for an absolute knowledge of satellite's position and to link it with latitude and longitude of the corresponding point on Ganymede's surface

With the help of *SPICE kernel files*[38], it is possible to relate the position of these axis with those of the *Earth Mean Equator* and *Equinox of Epoch J2000* inertial reference system (*EME 2000*) [38], a right-handed Cartesian set of three orthogonal axis with origin in the centre of the Earth, z_E -axis normal to the Earth mean equator at 2000, x_E -axis parallel to the Vernal Equinox of the Earth mean orbit at 2000 and y_E -axis to complete the right-handed system. This definition, using mean quantities at 2000, allows to exclude the effects of equinox precession interesting the Earth. From

SPICE kernel file relative to *Galileo* mission, we deduce the right ascension (α) and the declination (δ) in *EME 2000* of the north pole of Ganymede at a generic instant of time [38]:

$$\alpha = 268,20^\circ - 0,009 \cdot T$$

$$\delta = 64,57^\circ + 0,003 \cdot T$$

where T is the centuries past from 2000. The multiplied coefficients of T take in account the effects due to the equinox precession of Ganymede. With α and δ the position of rotational axis is individuated and then the reference plane is normal to this axis.

In this way the inertial Ganymede-centred inertial system is fully defined.

Body-fixed frame. This spherical frame is used to locate a point on the surface of Ganymede through the specification of two angles: the *longitude* φ (the angle between the prime meridian and the projection in the equatorial plane of the vector individuating the point) measured towards East in the sense of rotation and comprised between 0° and 360° , and the *latitude* λ (the angle between the vector individuating the point and the equator) ranging from 0° at the equator and 90° at the poles and considered positive for the northern hemisphere and negative for the southern one . The third coordinate is fixed and equal to the main radius of Ganymede, which we suppose spherical, being the difference between equatorial and polar radius very small [38].

Obviously we need a reference point from which starting the estimation of longitude, that is the intersection between the prime meridian and the equator. In particular, because this reference system rotates together with Ganymede, in order to locate this point at a certain time it is necessary to know the prime meridian position at a reference time and its angular velocity. From *SPICE .kernel file*, we find that the position of Ganymede's prime meridian at a particular time is [47][48]:

$$PM = PM_{J2000} + PM_{rate} \cdot d + 0,033 \cdot \sin(\mathbf{J4}) - 0,389 \cdot \sin(\mathbf{J5}) - 0,082 \cdot \sin(\mathbf{J6})$$

that is:

(2.1)

$$PM = 44,04^\circ + 50,3176081^\circ \cdot d + 0,033 \cdot \sin(\mathbf{J4}) - 0,389 \cdot \sin(\mathbf{J5}) - 0,082 \cdot \sin(\mathbf{J6})$$

with

$$\mathbf{J4} = 355,80^\circ + 1191,3^\circ \cdot \mathbf{T}$$

$$\mathbf{J5} = 119,90^\circ + 262,1^\circ \cdot \mathbf{T}$$

$$\mathbf{J6} = 229,80^\circ + 64,3^\circ \cdot \mathbf{T}$$

and \mathbf{T} is the number of Julian centuries from epoch J2000 ($1 \cdot \mathbf{T} = 36'525$ days).

In formula 2.1 PM_{J2000} is the position at J2000 (the angle on the equator between the x -axis of inertial frame and the prime meridian in the verse of rotation), PM_{rate} is the angular displacement in a terrestrial day, d represents the days past from J2000 and PM is the position at the time indicated with d (geometrical interpretation in analogous to that of PM_{J2000}) [47][48]

The knowledge of the satellite position and of prime meridian location, both in the inertial frame, allows to locate the point on the surface pointed by the satellite.

In SPICE library this kind of reference frame is called IAU-GANYMEDE where the prefix "IAU" indicates that the orientation of this frame is typically determined from the IAU (International Astronomical Union) model for the celestial body considered. The constants associated with this model are stored in one or more text PCK files, which have to be loaded in order to use the information of reference frame.

2.1.5 SPICE routines of interest

SPICE library permits to use a lot of routines to reach several objectives, but in this sub-paragraph we described only more important routines used in this thesis. [49]

The routines are listed in the following:

1. `et = cspice_str2et(str)`

converts a string representing an epoch to a double precision value representing the number of TDB seconds past the J2000 epoch corresponding to the input epoch.

Input:

str any scalar or NxM character array of strings recognized by SPICE as an epoch.

Output:

et the scalar or 1XN-vector of double precision number of TDB seconds past the J2000 epoch that corresponds to the input 'str'

2. [state, lt] = **cspice_spkezr**(targ, et, ref, abcorr, obs)

returns the state (position and velocity) of a target body relative to an observing body, optionally corrected for light time (planetary aberration) and stellar aberration.

Input:

targ the scalar string name of a target body. Optionally, you may supply the integer ID code for the object as an integer string.

et the scalar or 1XN-vector of double precision ephemeris epochs, expressed as seconds past J2000 TDB.

ref the scalar string name of the reference frame relative to which the output state vector should be expressed.

abcorr a scalar string that indicates the aberration corrections to apply to the state of the target body to account for one-way light time and stellar aberration.

Output:

state a double precision 6x1 array or double precision 6xN array representing the state of the target body in kilometers and kilometers-per-second of the target body relative to the specified observer, (the first three

components of 'starg' represent the x-, y- and z-components of the target's position; the last three components form the corresponding velocity vector)

lt the double precision scalar one-way light time or double precision 1xN array of one-way light times between the server and target in seconds; if the target state is corrected for aberrations, then 'lt' is the one-way light time between the observer and the light time corrected target location.

3. [range, ra, dec] = **cspice_recrad**(rectan)

converts rectangular (Cartesian) coordinates to right ascension, declination coordinates

Input :

rectan a double precision 3x1 array or double precision 3xN array containing the rectangular coordinates of the position or set of positions.

Output:

radius a double precision scalar or 1xN-vector describing the distance of the position from origin.

ra a double precision scalar or 1xN-vector describing the right ascension of the position as measured in radians.

dec a double precision scalar or 1xN-vector describing the declination of the position as measured in radians.

4 [sep] **cspice_vsep**= (V1 , V2)

returns the scalar double precision separation angle in radians between two double precision , 3-vectors. This angle is defined as zero if either vector is zero.

Input :

v1 is an arbitrary double precision, 3-dimensional vector or 3xN array

v2 is also an arbitrary double precision, 3-dimensional vector or 3xN array

'v1' or 'v2' or both may be the zero vector.

Output:

sep the double precision, positive definite, scalar or 1xN array of the angular separation(s) between 'v1' and 'v2' expressed in radians. If either 'v1' or 'v2' is the zero vector, then **cspice_vsep** return value has value 0 radians.

2.2 Orbital propagator structure

In this paragraph we will describe the developed orbital propagator. The following analysis is made for Ganymede science phase described in paragraph 1.3.1, for a duration of 180 days.

The propagator objectives are an estimation of spacecraft state as function of time, in order to retrieve information about the azimuth angle of Jupiter with respect to antenna direction (always pointed toward Ganymede's centre) and to verify when the satellite is in a condition of Jupiter and Sun eclipse.

These results are very important since the collected data of the Radar Sounder and Laser Altimeter, mounted on the spacecraft, are very biased respectively by cosmic noise that Jupiter radiates and by Sun illumination.

The orbital propagator, developed in Matlab language, is composed by the following *.m files :

- **main_program**: it contains records in which input parameters are introduced, calls for utilized functions, and records for output results.
- **orbital_propagator**: the M-file-function where a code to determine spacecraft ephemeris has been developed.
- **calculate_angular_coordinates**: the function in which spacecraft right ascension and declination are determined.
- **eclipse_in_linda** (linda is a fictitious name used for a reference frame): the function used to impose the first condition to determine Jupiter eclipse.
- **eclipse_in_mery** (mery is a second fictitious name used for a second reference frame): the function used to impose the second condition to determine azimuth angle of Jupiter with respect to antenna direction in Jupiter eclipse phase.
- **sun_eclipse_murphy** (murphy is a third fictitious name for a third reference frame): the function used to determine the first condition for Sun eclipse phase.
- **sun_eclipse_mery**: the function used to determine the second condition for Sun eclipse phase.
- **jup_sun_eclipse**: the function in which duration of Jupiter and Sun eclipse are determined.
- **coordinates_in_out_eclipse**: the function in which are calculated the spacecraft planetocentric coordinates for which JGO is in eclipse condition.
- **coord_sat_J2000**: the function in which the spacecraft angular coordinates in Earth Inertial Frame J2000 are computed.

The code of orbital propagator is reported in the ANNEX.

In details, orbital propagator input data are the following (*figure 2.3*):

- *altitude h [Km]*, the height of the orbit or, analogously, of the spacecraft above the surface;
- *eccentricity e* , gives information about orbital shape;

- *inclination i [°]*, the angle of orbital plane with respect to Ganymede's equatorial plane;
- *right ascension of the ascending node Ω [°]*, the angle on Ganymede's equatorial plane between vector joints the center of Ganymede with ascending node and X axis in inertial frame;
- *argument of periapsis ω [°]*, the angle on the orbital plane, between eccentricity vector and nodes line measured in anticlockwise sense from ascending node;
- *initial true anomaly ν [°]*, the angle on orbital plane between eccentricity vector and the vector that joints Ganymede's center with spacecratposition.
- *initial date*, the time for starting propagation in terms of year, month, day, hour, minute and second;
- *step time of propagation dt [s]*, the increment of time counted from initial time;

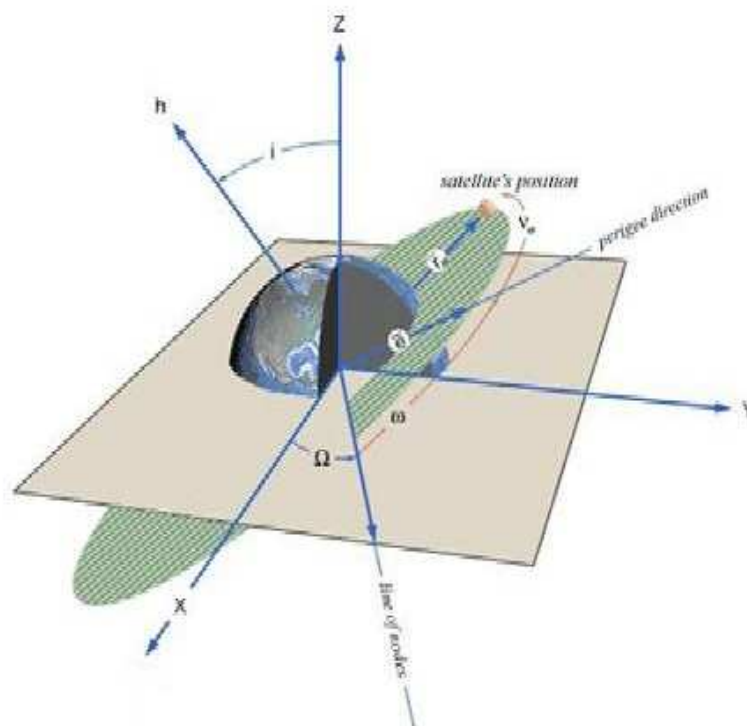


Figure 2.3 : Orbital parameters [50]

The user has the possibility to set and change the values of the following parameters:

- $h = 200 \text{ Km}$
- $e = 0$
- $i = 87.5^\circ$
- $\Omega = 0^\circ$
- $\omega = 0^\circ$
- $\nu = 0^\circ$

In addition to that, the user can also choose if to consider an ideal Keplerian orbit or a perturbed one taking into account the effects J_2 due to the non-sphericity of Ganymede, to set the initial propagation time eti and the step time dt .

2.2.1 Spacecraft ephemeris

Set the input parameters the algorithm is developed following the block diagram below (figure 2.4).

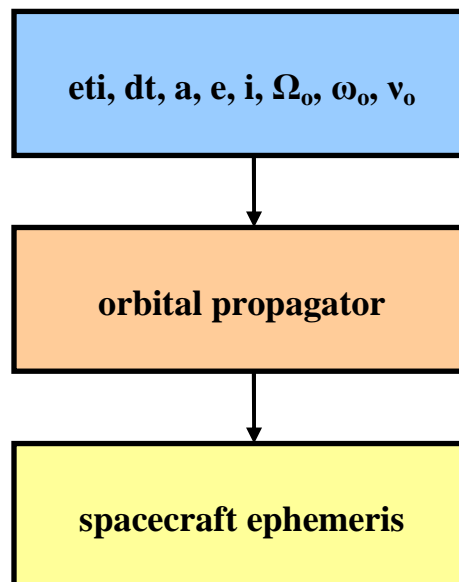


Figure2.4: Algorithm of propagation for JGO

Introduced input parameters , the orbital propagator determines the spacecraft's cartesian coordinates in a frame fixed in the center of the conical (in our case a circumference) passing true the eccentric anomaly .

In *figure 2.5* is represented the case of a generic conical.

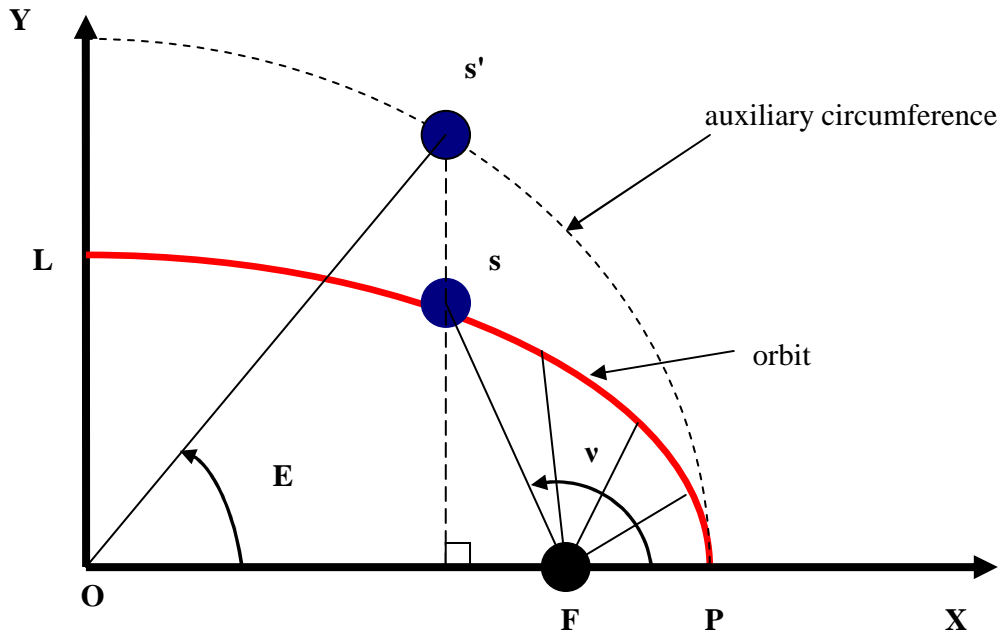


Figure 2.5 :Geometric interpretation of eccentric anomaly[51]

Note that referring to *figure 2.5* [51]:

$$x_s = x_{s'} = a \cos E \tag{2.2}$$

$$y_s = b \sin E$$

$$z_s = 0$$

The perifocal frame is oriented as the system in figure 2.5 with the difference that it is centered in the focus of orbit (*figure 2.6*)

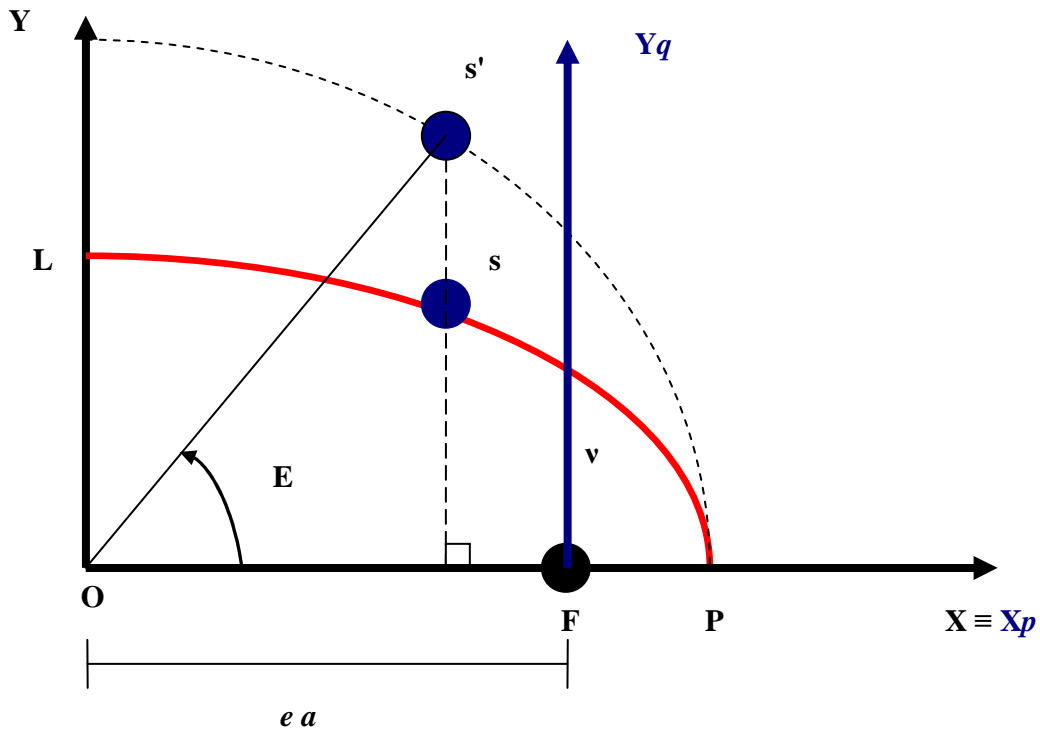


Figure 2.6: Translation of perifocal frame respect to this in which Cartesian coordinates (2.2) are calculated

The cartesian coordinates of spacecraft in perifocal frame are:

$$x_s = x_{s'} = a \cos E - ea = a (\cos E - e) \quad (2.3)$$

$$y_s = b \sin E$$

$$z_s = 0$$

Known spacecraft coordinates in perifocal frame it is possible to determine spacecraft Cartesian coordinates for Ganymede inertial frame using the rotation matrix $\mathbf{T}(I \Omega \omega)^T$:

$$[\mathbf{a}]_{IJK} = [\mathbf{T}(I \Omega \omega)]^T [\mathbf{a}]_{PQW} \quad (2.4)$$

where :

$$[\mathbf{T}(i \Omega \omega)]^T = \begin{pmatrix} c\Omega c\omega - s\Omega s\omega ci & -c\Omega s\omega - s\Omega c\omega ci & s\Omega si \\ s\Omega c\omega + c\Omega s\omega ci & -s\Omega s\omega + c\Omega c\omega ci & -c\Omega si \\ s\omega si & c\omega ci & ci \end{pmatrix} \quad (2.5)$$

with $c = \cos$ and $s = \sin$. [51]

It is possible to use SPICE routines for Ganymede in Ganymede's centered fixed frame: for this reason it is necessary to know the spacecraft coordinates in this frame. We can calculate these coordinates knowing the amplitude of the angle, indicated with θ , between the \mathbf{X} -axis of inertial frame and the \mathbf{X} -axis at i -instant of body fixed one using (2.1), that is the right ascension of intersection point of prime meridian with Ganymede's equatorial plane. In this way the orientation of first meridian can be determined using elementary rotation matrix consisting of an elementary rotation around Z-axis of inertial frame [51]:

$$\mathbf{T}_z(\theta) = \begin{pmatrix} \cos \theta & \sin \theta & 0 \\ -\sin \theta & \cos \theta & 0 \\ 0 & 0 & 1 \end{pmatrix} \quad (2.6)$$

Applying this procedure and using the respective SPICE routines (1) and (2) mentioned in the sub-paragraph 2.1.5, Ganymede's cartesian coordinates in body fixed frame and planetocentric coordinates, are determined.

2.2.2 Jupiter and Sun eclipses

The next step of propagator is to locate the spacecraft position in a condition of Jupiter and Sun eclipses to optimize data acquisition during *Ganymede Science Phase*.

We start to analyze the Jupiter eclipse, describing the concept of eclipse and theory implemented in the orbital propagator.

The *eclipse* is an astronomic event that recurs when a celestial body (in our case Ganymede) places itself between a celestial body considered a body source (Jupiter now and Sun in the following) and a third body (in our case the JGO).

In according with the analysis performed, Jupiter is the cosmic noise source and the Sun is the heat source .

The condition for eclipse is showed in *figures 2.7* and *2.8* in case of Jupiter eclipse.

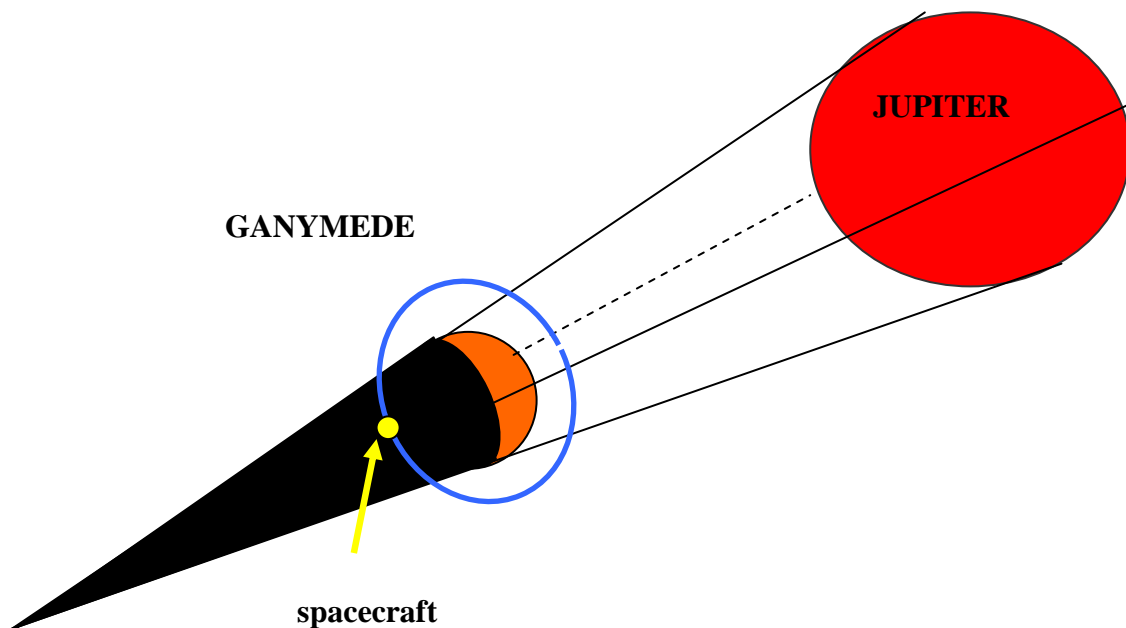


Figure 2.7 : Astronomical phenomenon of eclipse.

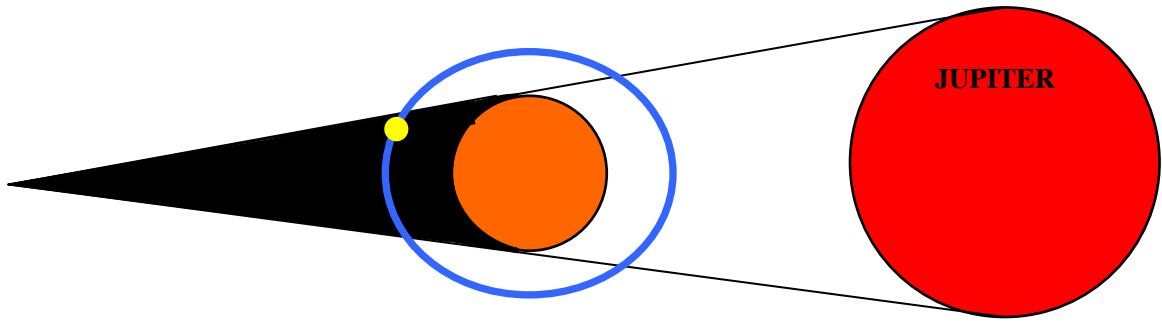


Figure 2.8 :Eclipse phenomenon.

Our scope is the estimation of angle α showed in *figure 2.9* , which will help to impose the condition of eclipse and estimate Jupiter eclipse duration for JGO:

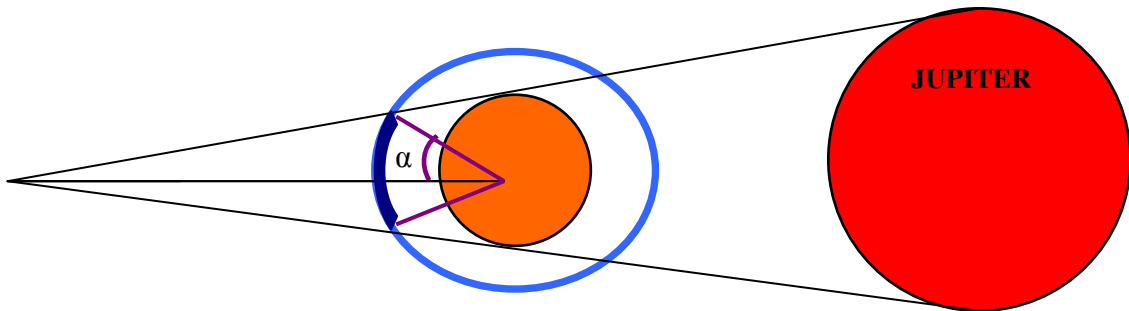


Figure 2.9 :The semi-angle α fore eclipse condition.

According to *figure 2.9* it is possible to affirm that a generic point of orbit (blue circumference) that represents the spacecraft position at the *i-istant* is not in eclipse condition if, indicating with \underline{r} the spacecraft position vector respect to centre of Ganymede, l the distance of Ganymede' mass centre respect to Jupiter' mass centre and β the angle between \underline{r} and l direction, with $0 < \beta < 180^\circ$, the following condition is satisfied:

$$\beta < 180^\circ - \alpha \quad (2.7)$$

where β is counted in anticlockwise sense (*figure 2.10* .)

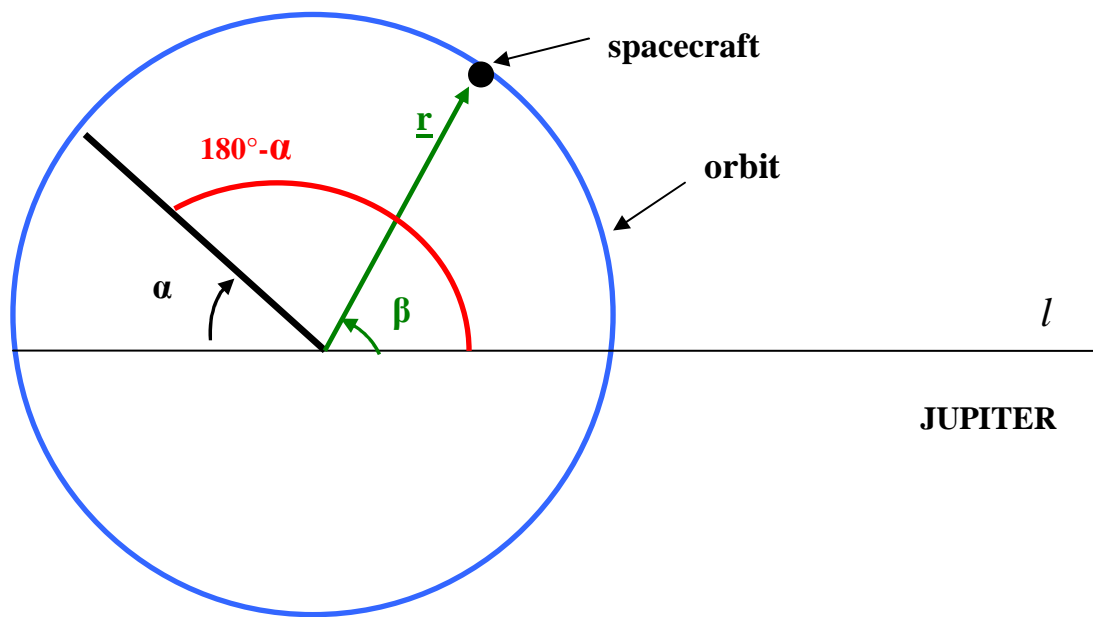


Figure 2.10 : Not- eclipse condition

On the contrary if the point (or better the spacecraft) belongs to eclipse zone the condition to be satisfied is (figure 2.11):

$$\beta \geq 180^\circ - \alpha \quad (2.8)$$

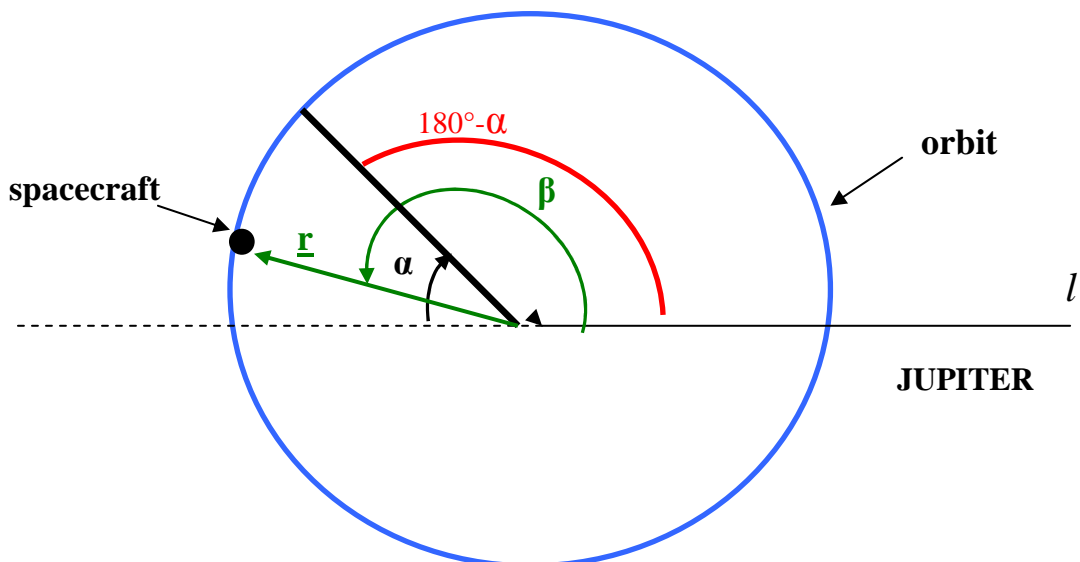


Figure 2.11 : Eclipse condition

Where the sign “ = “ is valid at the instant during which the spacecraft is entering into eclipse zone.

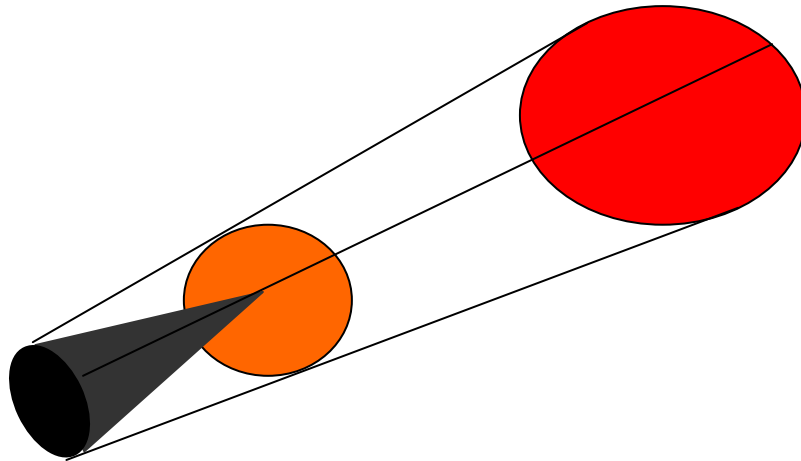


Figure 2.12 : Solid angle for eclipse

According to figure 2.12 we can consider the celestial sphere (an ideal sphere around Ganymede) and make this consideration for three different cases considered as examples for three several conditions.

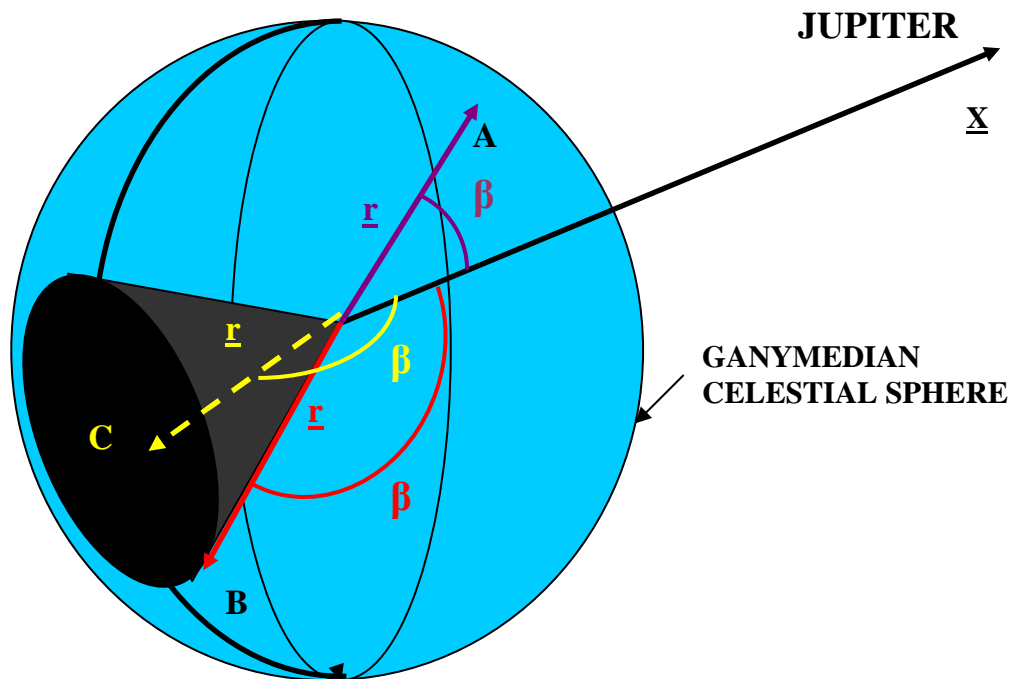


Figure 2.13: Geometrical conditions for eclipse , no-eclipse , and entering in eclipse

For a point located in **A** (figure 2.13) the angle β satisfies the condition $\beta < 180^\circ - \alpha$ that is the satellite is not in eclipse, while for a point located in **B** is verified the condition $\beta = 180^\circ - \alpha$ (\underline{r} coincides with cone apotema) and the satellite is just

entering in eclipse zone, for the point located in **C** the satellite is in a condition of total eclipse since $\beta > 180^\circ - \alpha$. Obviously the orbit will be a *maximum circle* of the sphere in figure 2.13.

The value of angle α is obtained making the following geometrical considerations (figure 2.14).

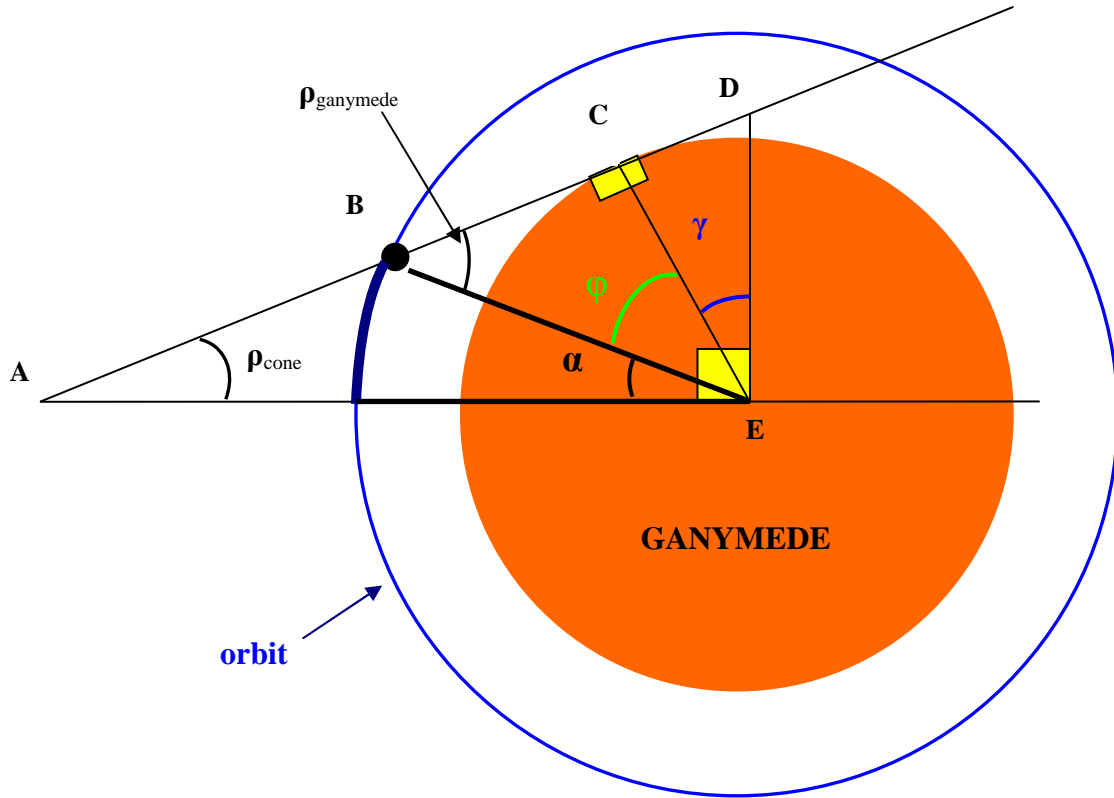


Figure 2.14: Geometrical consideration to calculate α

$$\rho_{\text{cone}} = \text{asin} \left[\frac{(\mathbf{R}_{\text{jup}} - \mathbf{R}_{\text{gany}})}{\mathbf{L}} \right] \quad (2.9)$$

$$\rho_{\text{gany}} = \text{asin} \left[\frac{(\mathbf{R}_{\text{gany}})}{(\mathbf{R}_{\text{gany}} + \mathbf{h})} \right] \quad (2.10)$$

Where :

- ρ_{cone} = semi-angle of the opening of cone
- ρ_{gany} = spacecraft angle of view
- \mathbf{R}_{jup} = mean radius of Jupiter

- R_{gany} = mean radius of Ganymede
- L = distance between Ganymede's and Jupiter's mass centres .

A detail of triangle **ADE** is reported in *figure 2.15*.

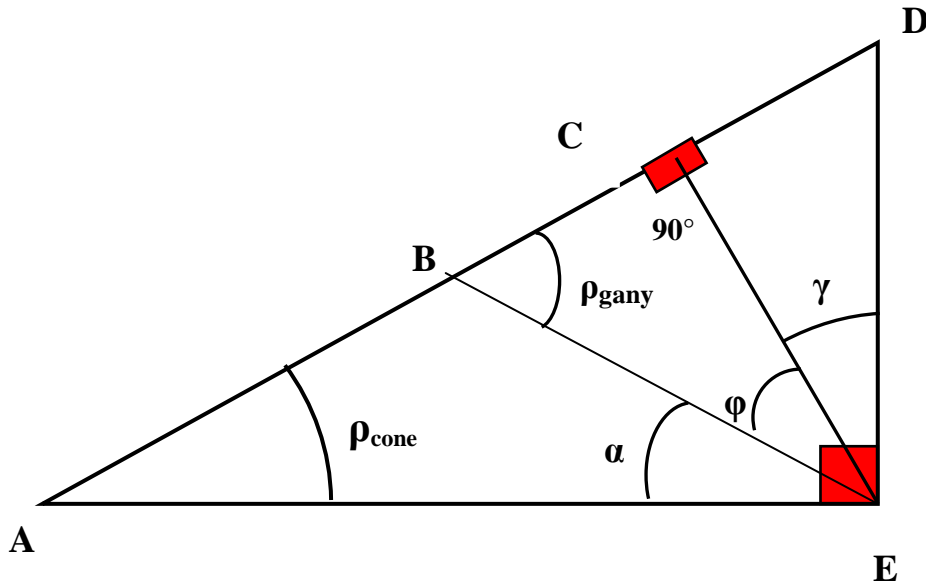


Figure 2.15 :Particular of triangle AED for geometrical considerations

Since $\underline{EC} \perp \underline{AD}$ and $\underline{ED} \perp \underline{AE}$ then $\gamma = \rho_{cone}$, and for the angle angles the following equations can be written:

$$\begin{cases} \varphi = 180^\circ - 90^\circ - \rho_{gany} = 90^\circ - \rho_{gany} \\ \alpha = 90^\circ - \varphi - \gamma \end{cases} \quad (2.11)$$

from which:

$$\alpha = 90^\circ - (90^\circ - \rho_{gany}) - \rho_{cone} = \rho_{gany} - \rho_{cone} \quad (2.12)$$

It is easy to understand the dependence of α from ρ_{gany} and consequently from altitude h of orbit .

After this detailed description of the theoretical concepts on which the orbital propagator is based we wish to describe how it has been possible to execute the propagator with SPICE routines.

Among the SPICE routines, listed in paragraph 2.1.5, the routine `sep=cspice_vsep(v1, v2)` has been described above. This routine permits to calculate the amplitude of the angle included between two vector, generically called **V1** and **V2**. To determine eclipse condition we have set a reference frame centered in Ganymede with the **Xr** – axis constantly pointing toward Jupiter’ s center , with **Yr** – axis directed according Ganymede ‘s speed direction and the **Zr**-axis such as to form a right handed oriented frame(*figure 2.16*)

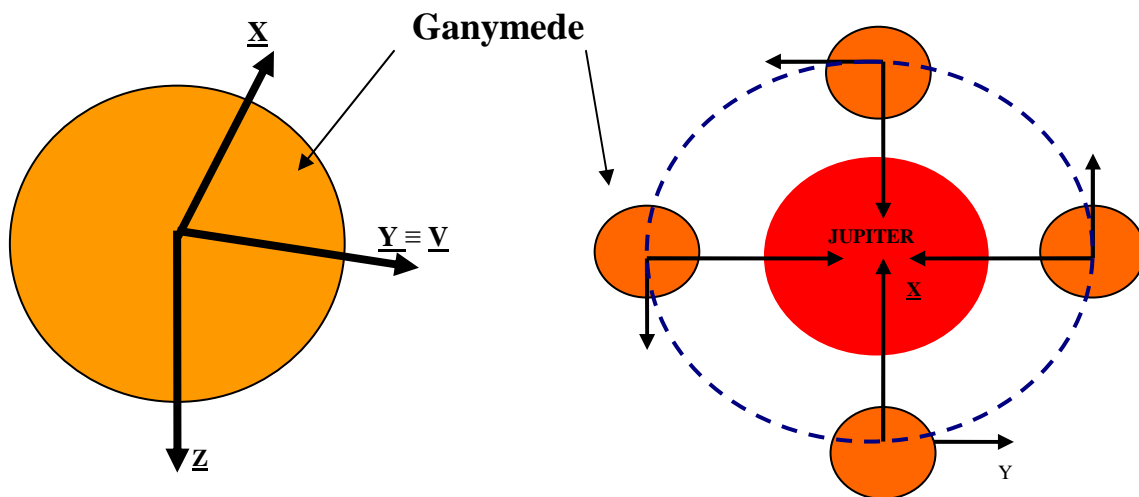


Figure 2.16: Ganymede fictitious body fixed frame

Using this reference system only the **X** component is not null, while **Y** and **Z** components are equal to zero computing in it Jupiter state.

At the *i-istant* we can measure the amplitude of β using the mentioned SPICE routine `cspice_vsep` and imposing the condition of equation (2.8) it is possible to determine if spacecraft is in eclipse or not.

On spacecraft the pointing of antenna Radar Sounder is nadir as showed in *figure 2.17*).

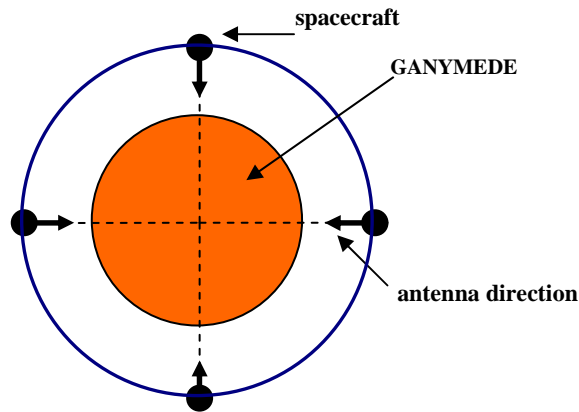


Figure 2.17: Antenna direction at the *i*-instant

Due to antenna pointing it is necessary to know the azimuth angle of Jupiter mass centre with respect to the antenna direction: this angle is indicated with λ (figure 2.18);

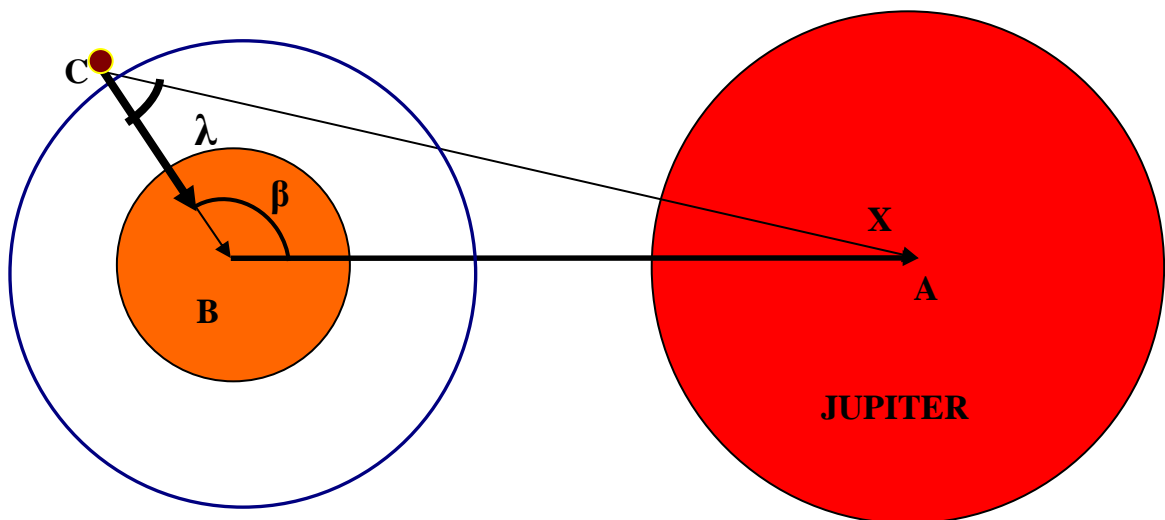


Figure 2.18: Definition of λ angle

The angle λ is estimated by `cspice_vesp` routine , creating another fictitious reference frame centred on spacecraft and with axis \mathbf{X}_s pointing to Ganymed's centre mass.

In figure 2.19 is reported the triangle **ABC** of figure 2.18.

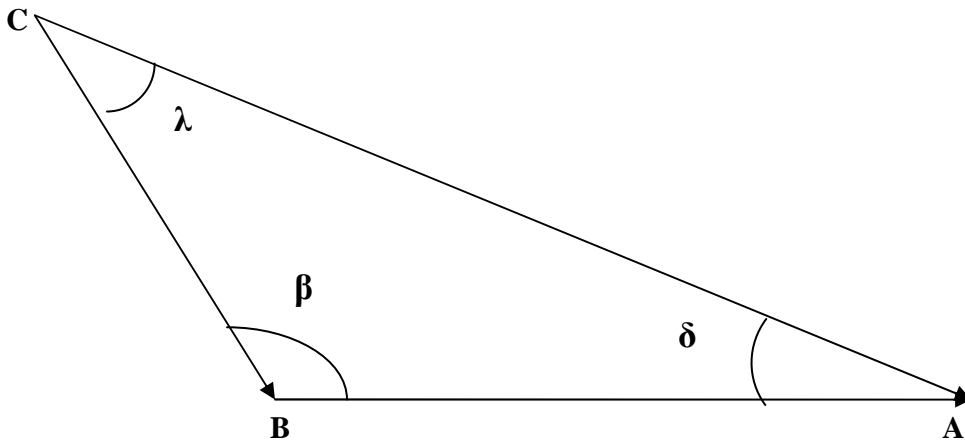


Figure 2.19: Details of the three angles needed to calculate eclipse condition based on amplitude of λ

Knowing the values of amplitude of β and λ , in every instant the amplitude of δ is:

$$\delta = 180^\circ - \beta - \lambda \quad (2.13)$$

Note that according to the condition (2.8) the spacecraft is in total eclipse zone if:

$$\beta \geq 180^\circ - \alpha \quad (2.14)$$

Hence from relationship (2.13)

$$\beta = 180^\circ - \lambda - \delta \quad (2.15)$$

we have

$$180^\circ - \lambda - \delta \geq 180^\circ - \alpha \quad (2.16)$$

or better

$$\lambda \leq \alpha - \delta \quad (2.17)$$

The azimuth angle λ of Jupiter' s mass centre with respect to antenna direction is known and in addition we are able to understand if spacecraft is in total eclipse phase or not .

The same considerations can be replaced to analyze the spacecraft position in Sun eclipse: it is necessary substitute all the parameters relative to Jupiter with which relative to Sun.

CHAPTER 3 Validation and results

In this chapter validation data for spacecraft propagation and results for Jupiter and Sun eclipses are presented.

3.1 Validation graphs

Validation data have been plotted for one orbital period ($T_{\text{orb}} \approx 2,64\text{h}$) and then for a period of propagation of around 7 terrestrial day (i.e. one ganymedian revolution period).

3.1.1 Validation graphs for one spacecraft orbital period

The following graphs have been plotted for one orbital period with a step time $\mathbf{dt} = 60\text{s}$, having an interpolated curve of around 158 points per orbit.

In Figure 3.1(a) and Figure 3.1 (b) are represented the curve of spacecraft right ascension as function of time propagation, and spacecraft right ascension as function of number of orbital periods, respectively, both in ganymedian inertial frame. In the graphs it is possible to distinguish different trends. At starting the curve presents a slowly increasing trend in the range $0 \div 0.6 \text{ h}$ (around $0 \div 0.2 T_{\text{orb}}$), then it quickly increases in range $0.6 \div 0.7 \text{ h}$ ($0.2 \div 0.3 T_{\text{orb}}$) because of the passage of spacecraft at *orbit's north pole*; in range $0.7 \div 1.78 \text{ h}$ ($0.3 \div 0.68 T_{\text{orb}}$) the curve has the same characteristics described in the range $0 \div 0.6 \text{ h}$; in range $1.8 \div 2.15 \text{ h}$ ($0.7 \div 0.8 T_{\text{orb}}$) the curve increases again due to the passage of spacecraft around *orbit's south pole*; finally the curve repeats its trend in a new time range interval.

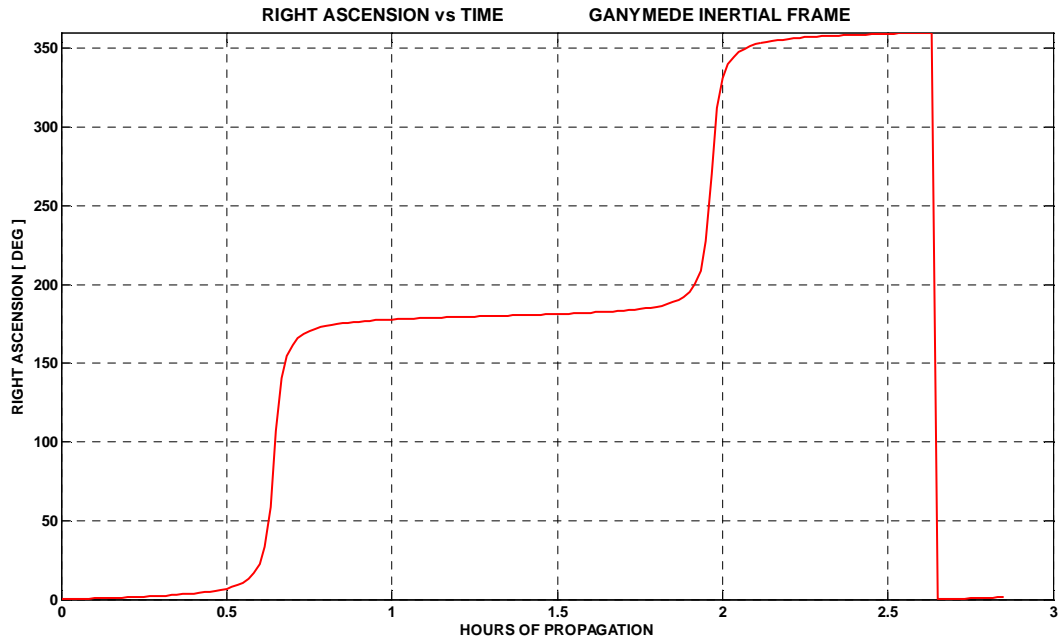


Figure 3.1: (a) Spacecraft right ascension vs time in ganymedian inertial frame.

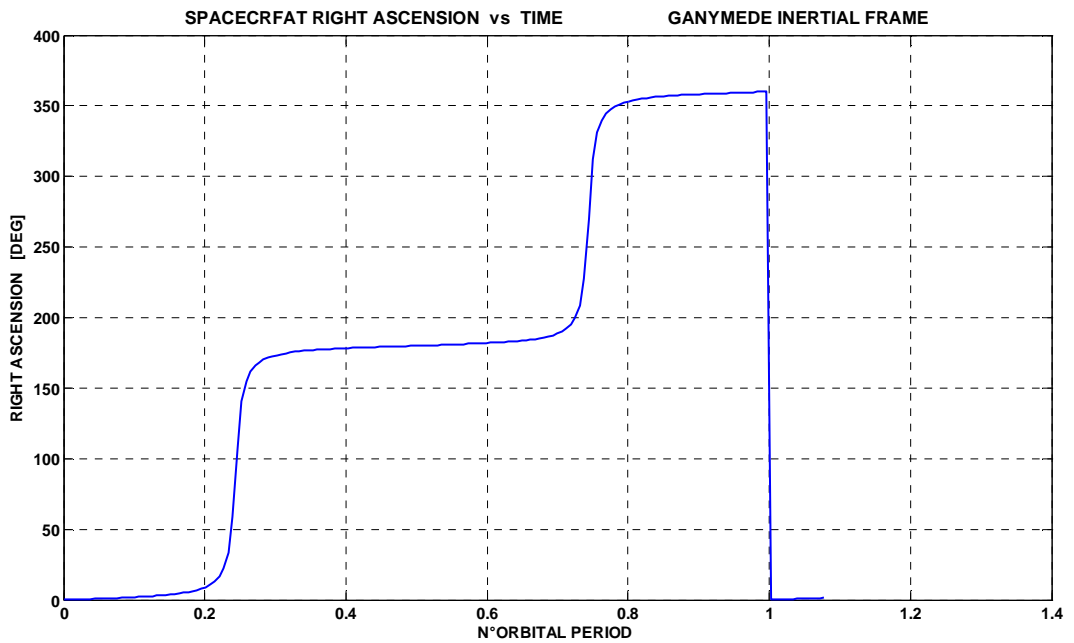


Figure 3.1: (b) Spacecraft right ascension vs n^* orbital periods in ganymedian inertial frame.

In figure 3.2 it is possible to observe the spacecraft declination comprised in a range of $[-90^\circ, 90^\circ]$.

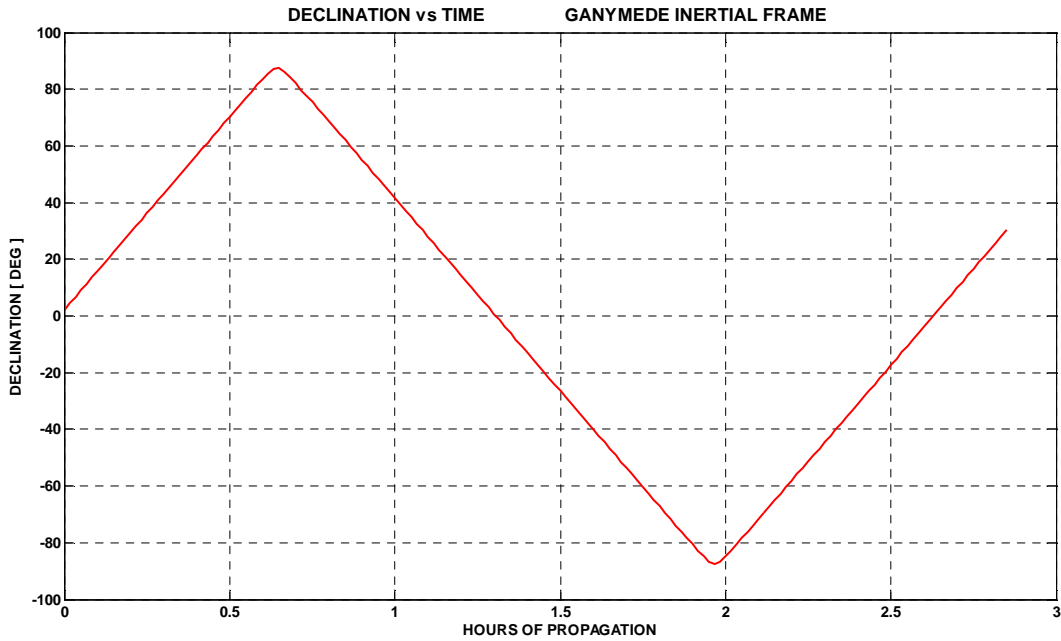


Figure 3.2: *Spacecraft declination vs time in ganymedian inertial frame.*

Figure 3.3 shows the graph of declination as function of right ascension plotted for one orbit; the starting point is indicated with the simbol "o".

It is possible to note that the values of longitude increase reaching a maximum value of declination of 90° , then they decrease: this trend is due to combination of results show in figure 3.1 and figure 3.2.

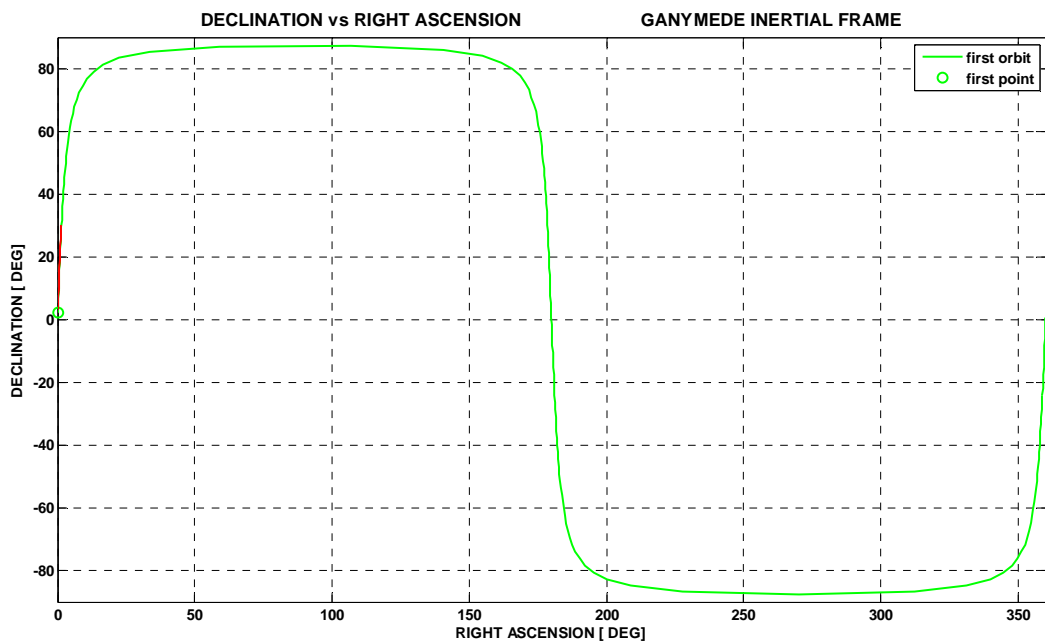


Figure 3.3: *Spacecraft declination vs right ascension in ganymedian inertial frame.*

For Figure 3.4 (spacecraft longitude vs time) remain valid the same explanations of figure 3.1, but now the starting value of longitude is not zero since the prime meridian of body-fixed frame (in which longitude is computing) is rotated of an angle with an amplitude not equal to zero respect to X-axis of ganymedian inertial frame.

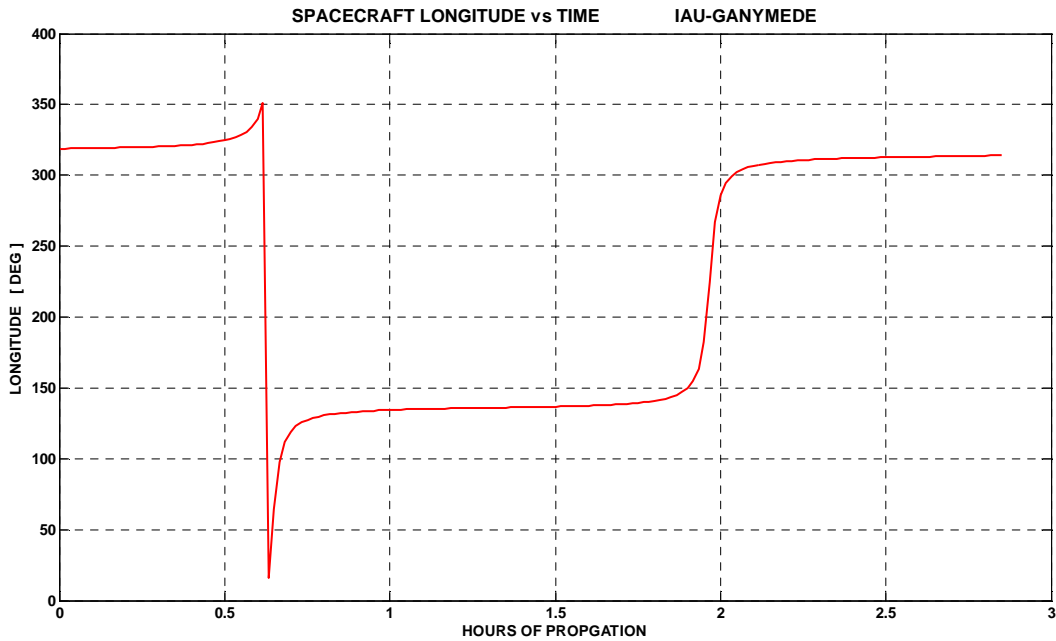


Figure 3.4: Spacecraft longitude vs time in ganymedian body-fixed frame.

Figure 3.5 shows usual curve progress of latitude in range $-90^{\circ} \div 90^{\circ}$ in ganymedian body fixed frame.

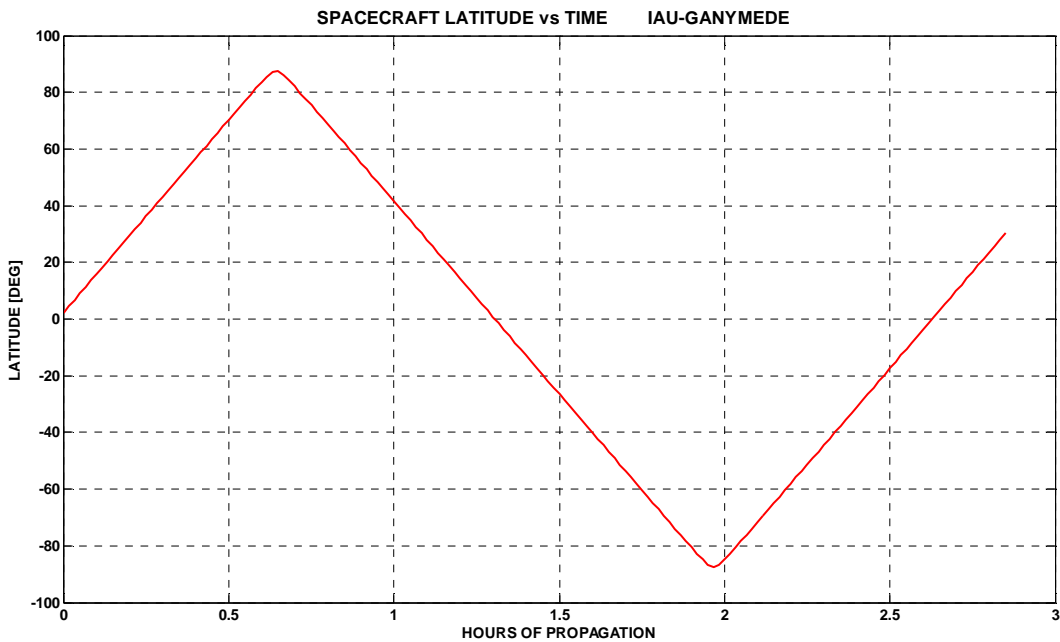


Figure 3.5: Spacecraft latitude vs time in ganymedian body-fixed frame.

In Figure 3.6 latitude as function of longitude for JGO is represented in ganymedian body-fixed frame.

The graph starts at point indicated with the symbol “o”, then it goes on toward east and the graph continues on the left side of image.

It is possible to note that when a full orbit is completed, the successive orbit is deviated toward west: this is due to the east rotation of Ganymede around its own Z-axis and consequently from rotation of ganymedian body-fixed frame.

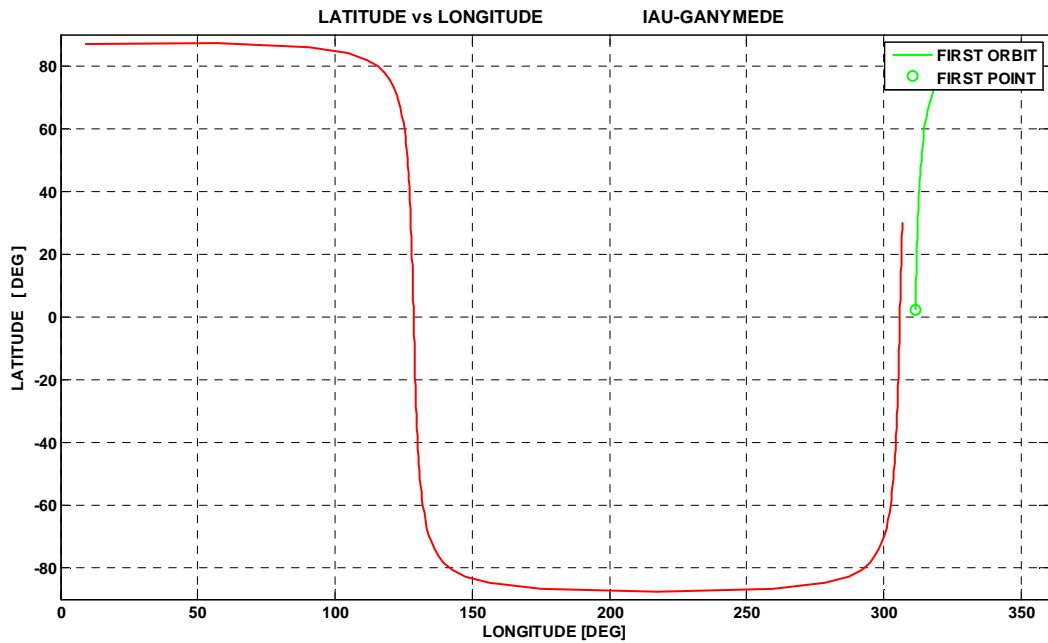


Figure 3.6: Spacecraft latitude vs longitude in ganymedian body-fixed frame.

Figure 3.7 shows the curve progress of spacecraft X-coordinate in ganymedian inertial frame. It is possible to note that, since the starting right ascension $\Omega_0 = 0^\circ$, initial direction of *node line* coincides with the direction of X-axis of ganymedian inertial frame: as consequence, the X-component of spacecraft vector position is equal to orbit radius, i.e. 2831.2Km. The graph provides also the periodicity of curve in a single spacecraft orbital period: around 2,64 h.

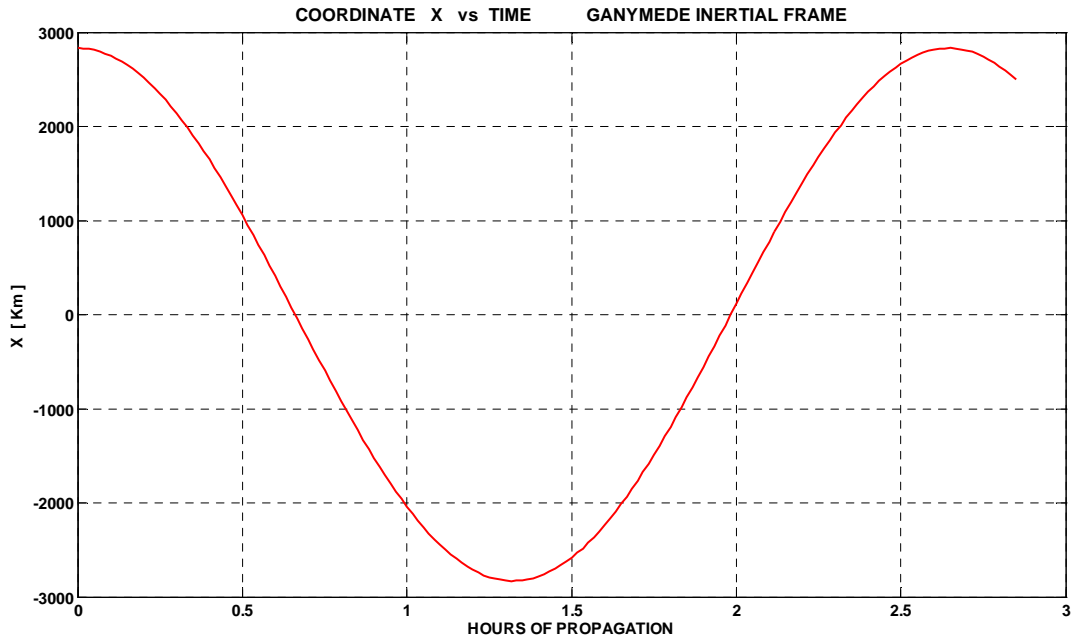


Figure 3.7: *Spacecraft X- coordinate vs time in ganymedian inertial frame.*

In figure 3.8 the spacecraft Y-coordinate in ganymedian inertial frame is showed. Since the considerations made for figure 3.7 remain valid it is justified that the starting point for this graph is $Y=0$. The periodicity in a propagation time is around 2,64h, of course.

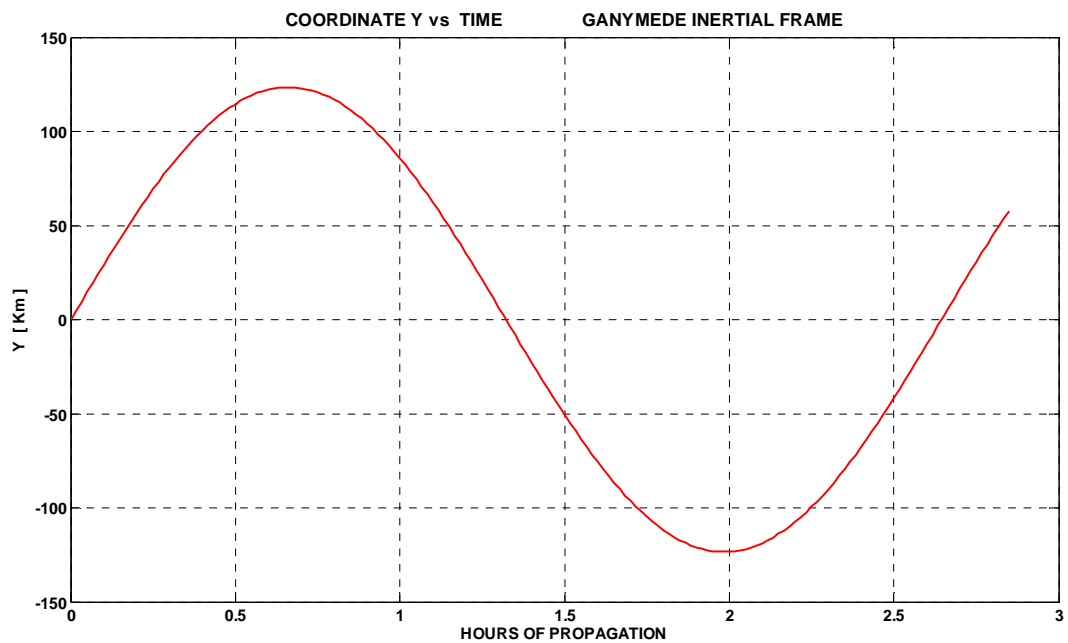


Figure 3.8: *Spacecraft Y - coordinate vs time in ganymedian inertial frame.*

For graph in figure 3.9 all the consideration made about figure 3.8 remain valid.

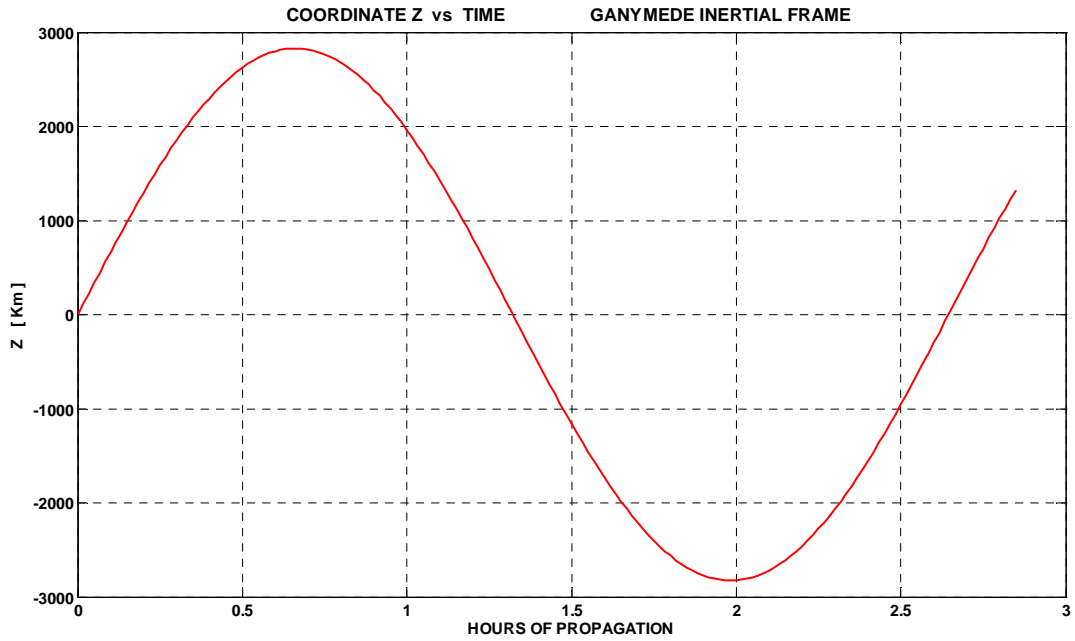


Figure 3.9: Spacecraft Z-coordinate vs time in ganymedian inertial frame.

Figure 3.10 shows the curve progress for Jupiter right ascension as function of time of propagation in ganymedian inertial frame. To get information about this trend it is necessary to analyse figure 3.27.

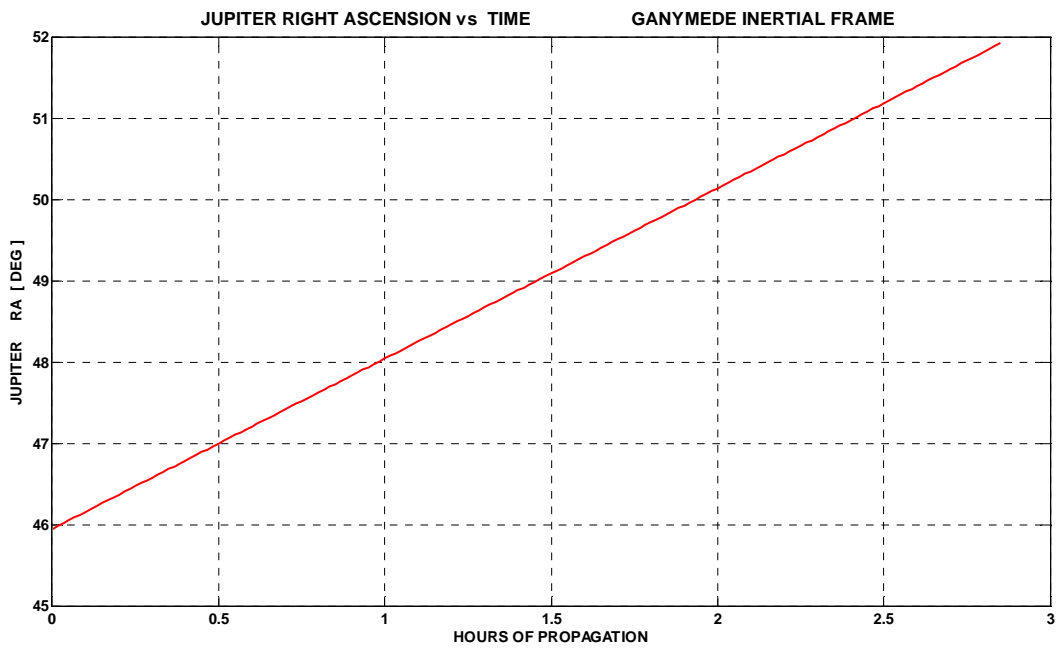


Figure 3.10: Jupiter right ascension vs time in ganymedian inertial frame.

Figure 3.11 shows the curve progress for Jupiter declination as function of time of propagation in ganymedian inertial frame. Also in this case to have major information it is necessary to see figure 3.28.

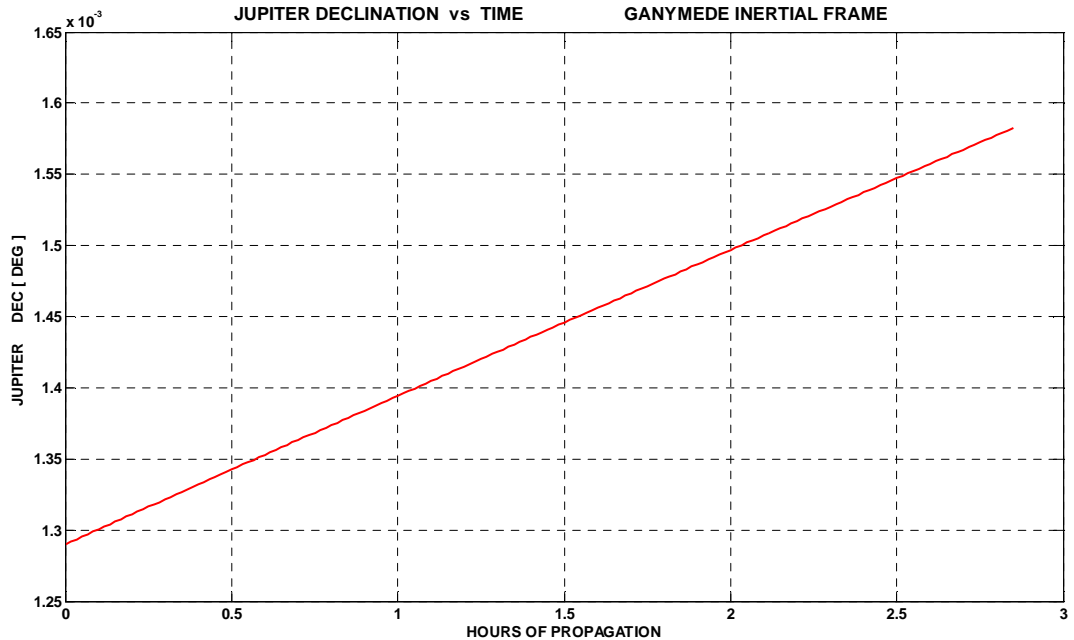


Figure 3.11: Jupiter declination vs time in ganymedian inertial frame.

Figure 3.12 shows the curve progress for Sun right ascension as function of time of propagation in ganymedian inertial frame. To have major information it is necessary to see figure 3.35.

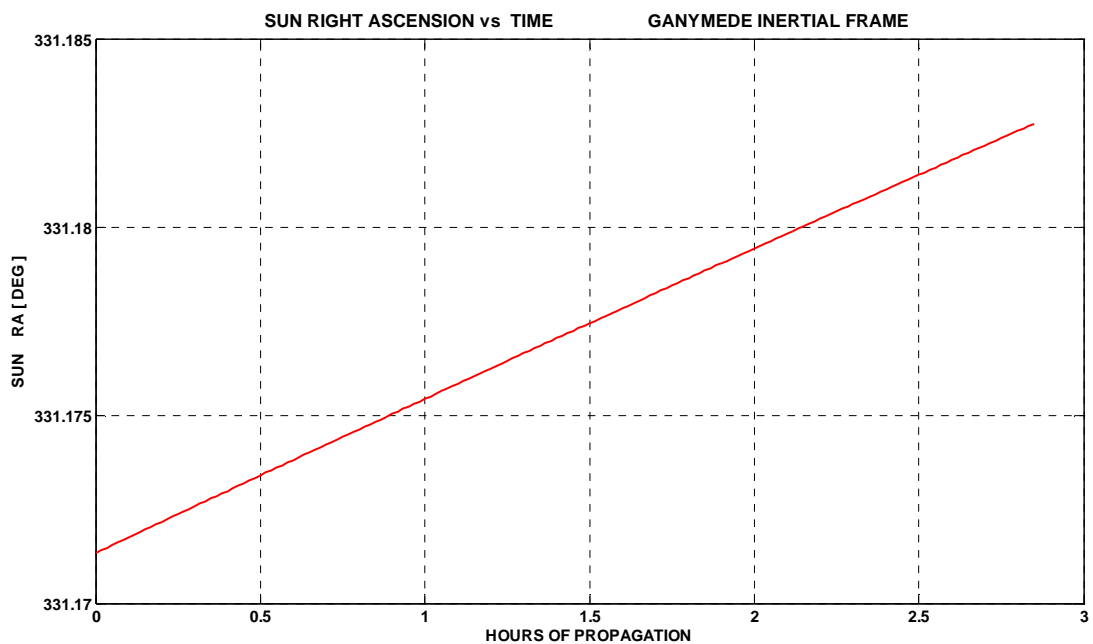


Figure 3.12: Sun right ascension vs time in ganymedian inertial frame.

Figure 3.13 shows the curve progress for Sun declination as function of time of propagation in ganymedian inertial frame. To have major information it is necessary to see figure 3.36.



Figure 3.13: Sun declination vs time in ganymedian inertial frame.

Figure 3.14 and figure 3.15 show Sun right ascension and Sun declination as time function respectively in Earth inertial frame J2000. For a more detailed description it is recommended to see respectively figure 3.37 and figure 3.38

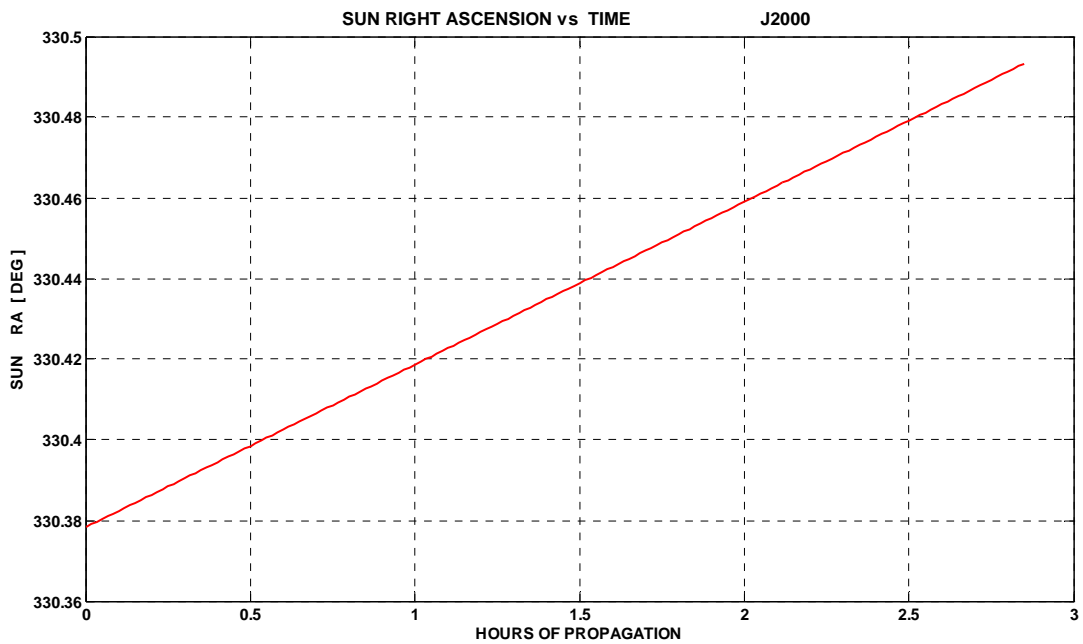


Figure 3.14 Sun right ascension vs time in Earth inertial frame J2000.

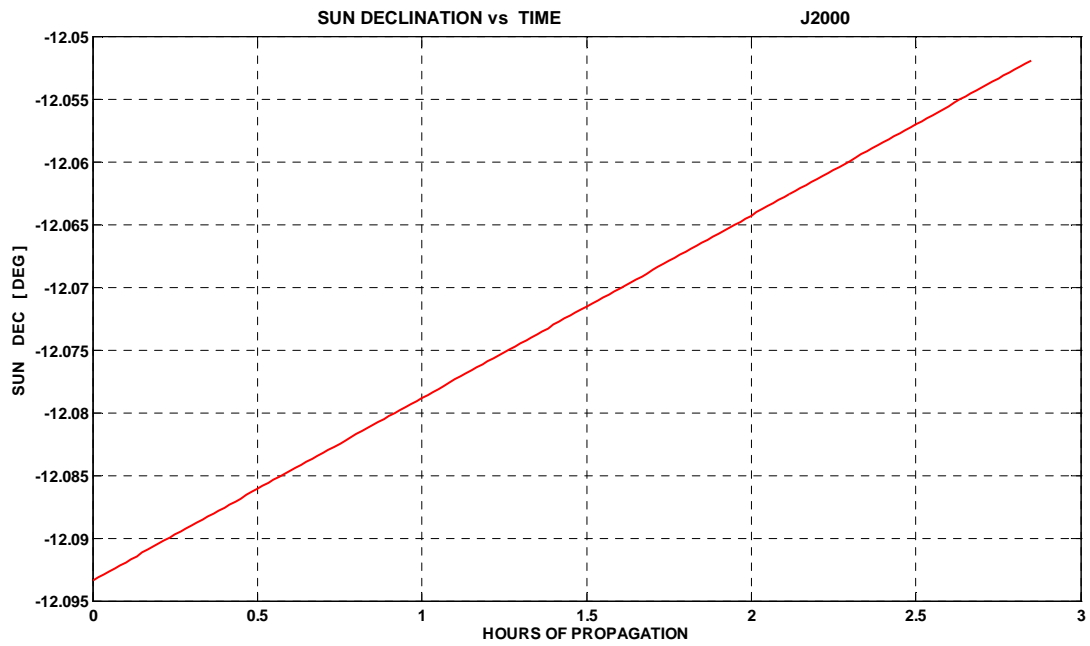


Figure 3.15: Sun declination vs time in Earth inertial frame J2000

In the following figure 3.16, where spacecraft orbital trajectory in ganymedian inertial frame is illustrated, it is possible to note that the orbit is almost a polar orbit ($i_o=87,5^\circ$).

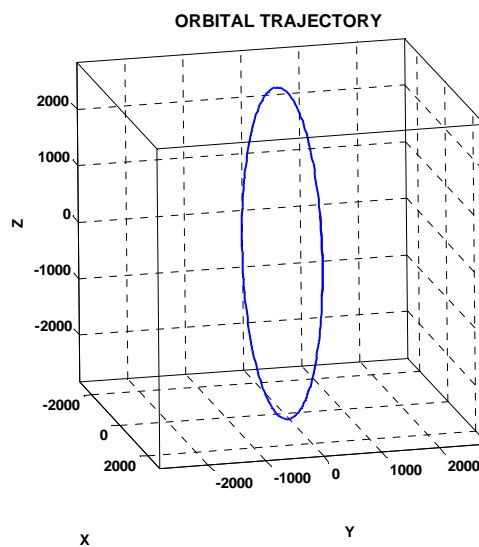


Figure 3.16: Spacecraft orbital trajectory in ganymedian inertial frame.

In the following figure 3.17, spacecraft orbital trajectory in ganymedian body-fixed frame is showed. Its deviation toward west is due to the fact that the ganymedian body-fixed rotates toward east because of ganymedian angular speed.

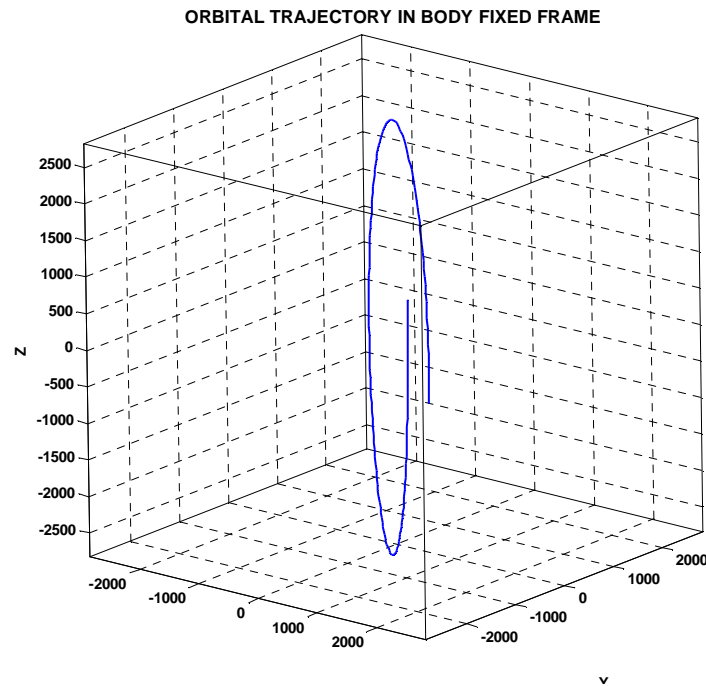


Figure 3.17: Spacecraft orbital trajectory in ganymedian body-fixed frame.

3.1.2 Validation graphs for one ganymedian revolution period

All the following graphs are plotted for one ganymedian revolution period (around 7 terrestrial days) with a step time $\mathbf{dt}= 60\text{s}$, having an interpolated curve passing true around 158 points per orbit. For figures 3.18, 3.19, 3.20, 3.21, 3.22, 3.23 all the considerations made for the same curves around one orbital period (paragraph 3.1.1) are valid.

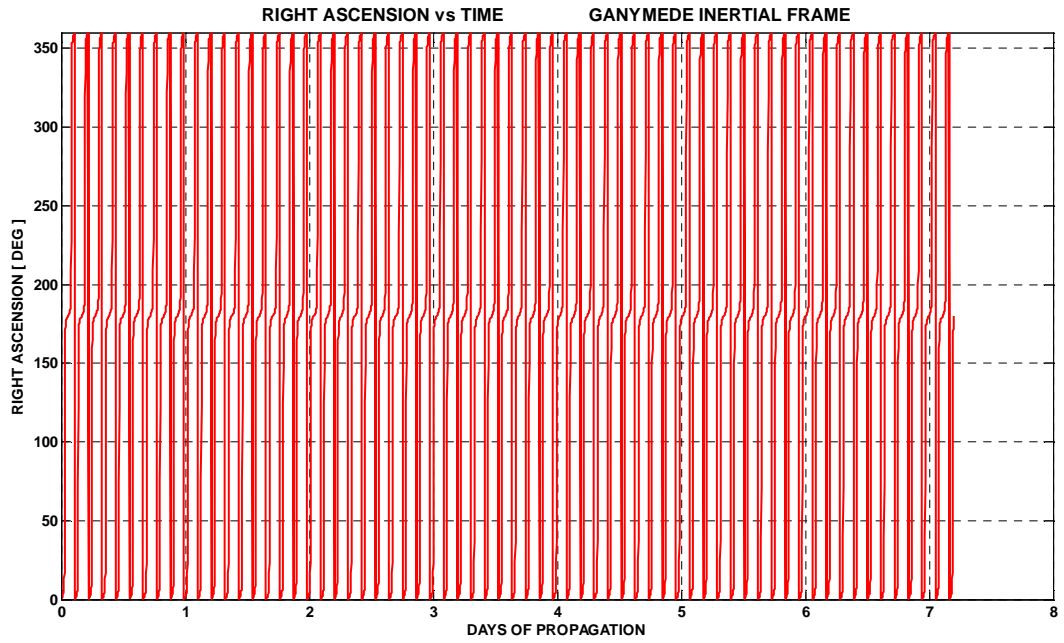


Figure 3.18: *Spacecraft right ascension vs time in ganymedian inertial frame.*

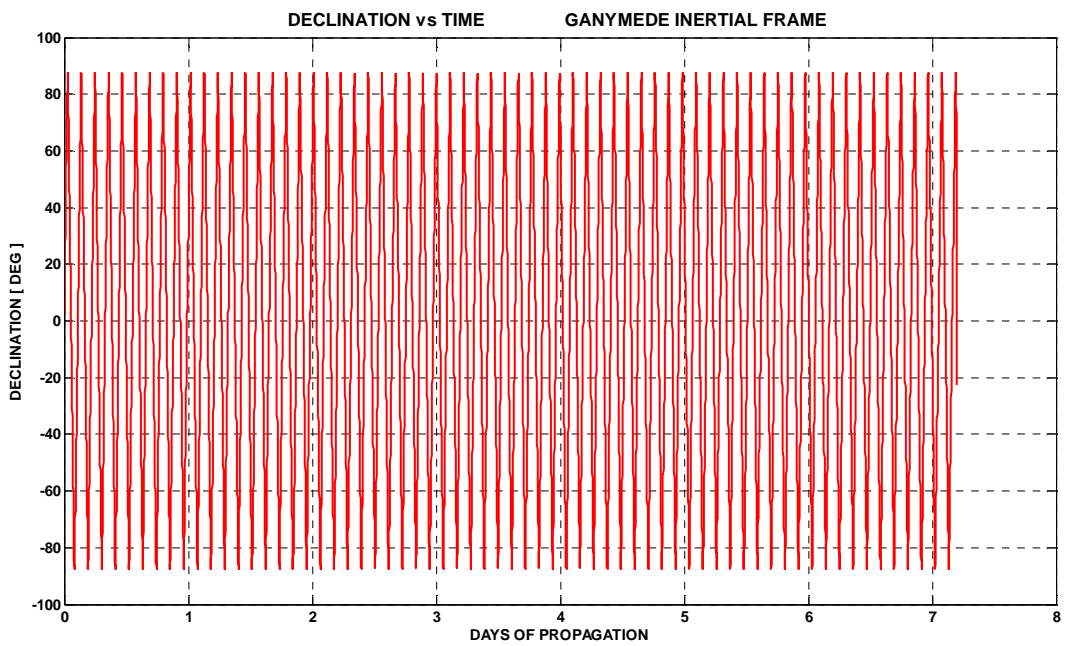


Figure 3.19: *Spacecraft declination vs time in ganymedian inertial frame.*

In next figure 3.20 it is possible to note that the curve lays upon itself during propagation.

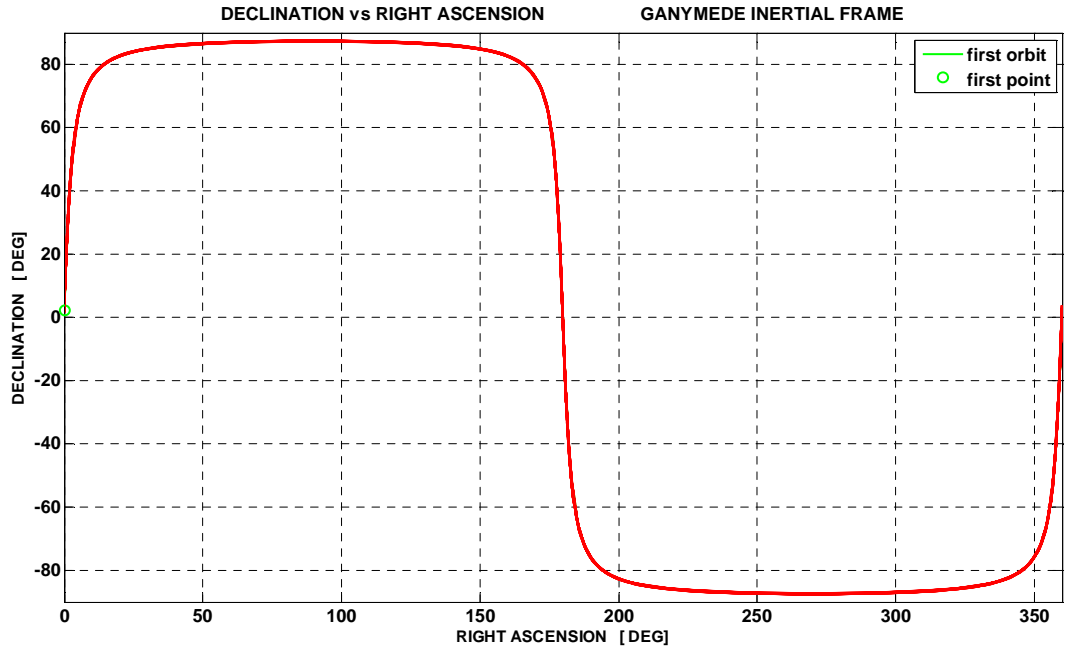


Figure 3.20: Spacecraft declination vs right ascension in ganymedian inertial frame.

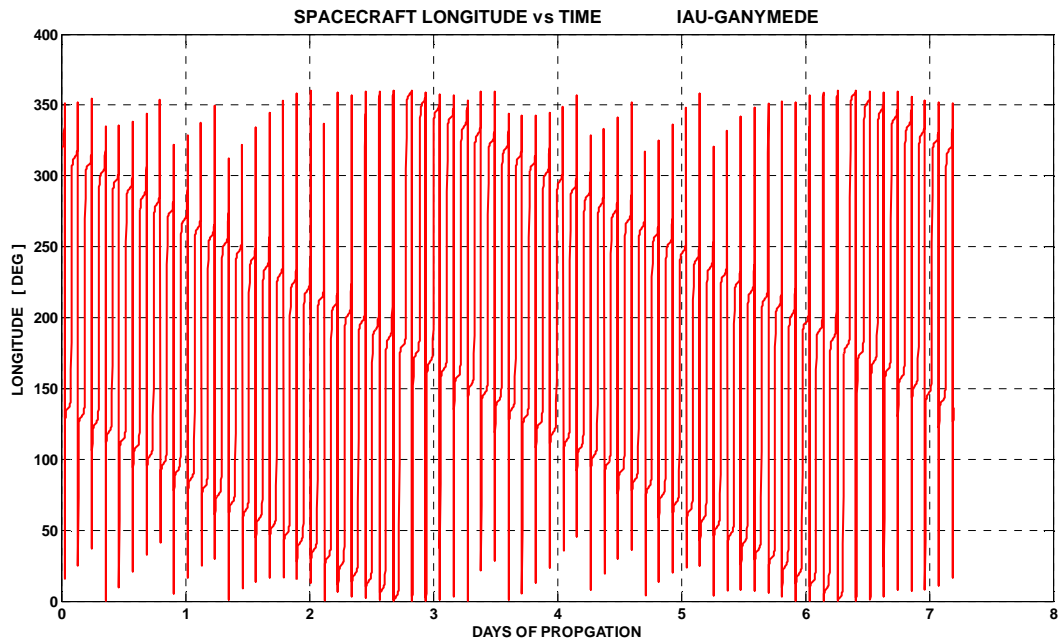


Figure 3.21: Spacecraft longitude vs time in ganymedian body-fixed frame.

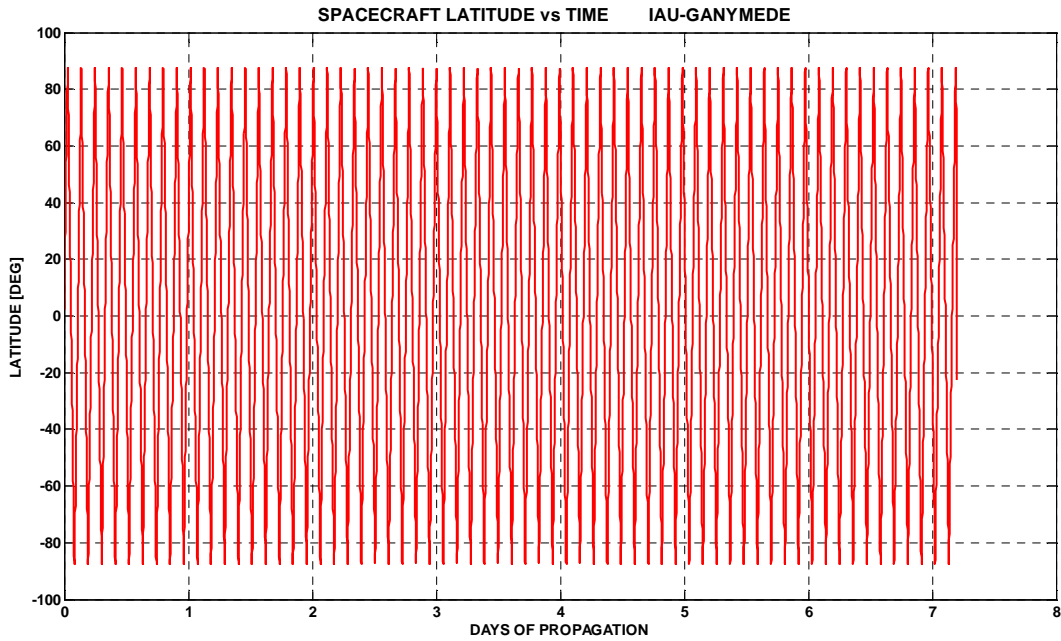


Figure 3.22: Spacecraft latitude vs time in ganymedian body-fixed frame.

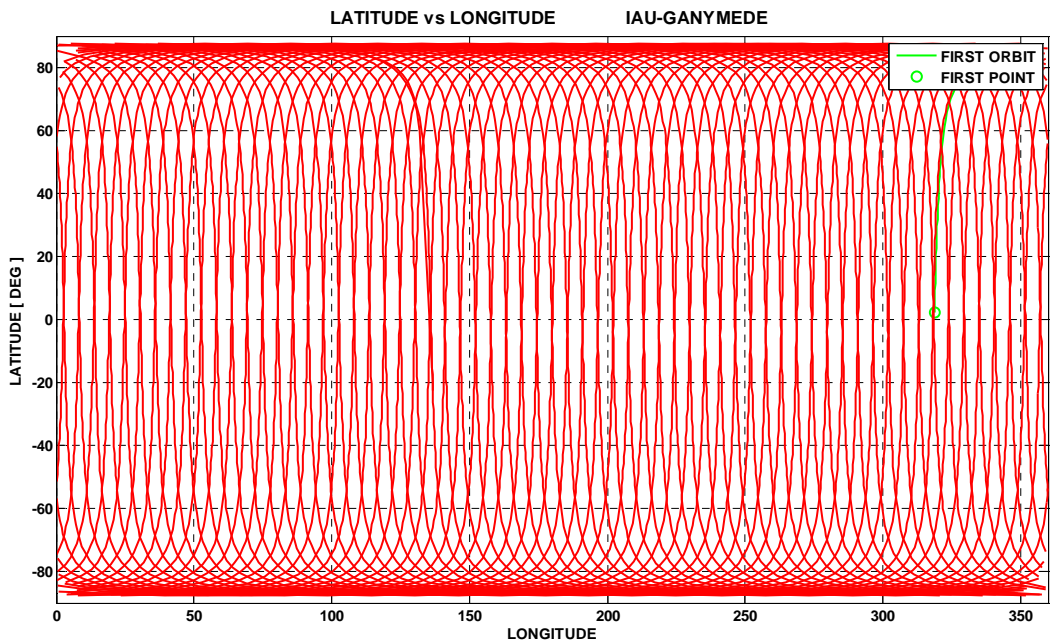


Figure 3.23: Spacecraft latitude vs longitude in ganymedian body-fixed frame.

In figure 3.24 spacecraft curve progress of X-coordinate as function of time in ganymedian inertial frame is illustrated. Note that the curve is always comprised in a range $[-2831,2 ; 2831,2]$ Km, i.e. equal to orbital radius. This is due to the value of starting right ascension of ascending node value $\Omega_o=0^\circ$ together with starting value of inclination $i=87,5^\circ$.

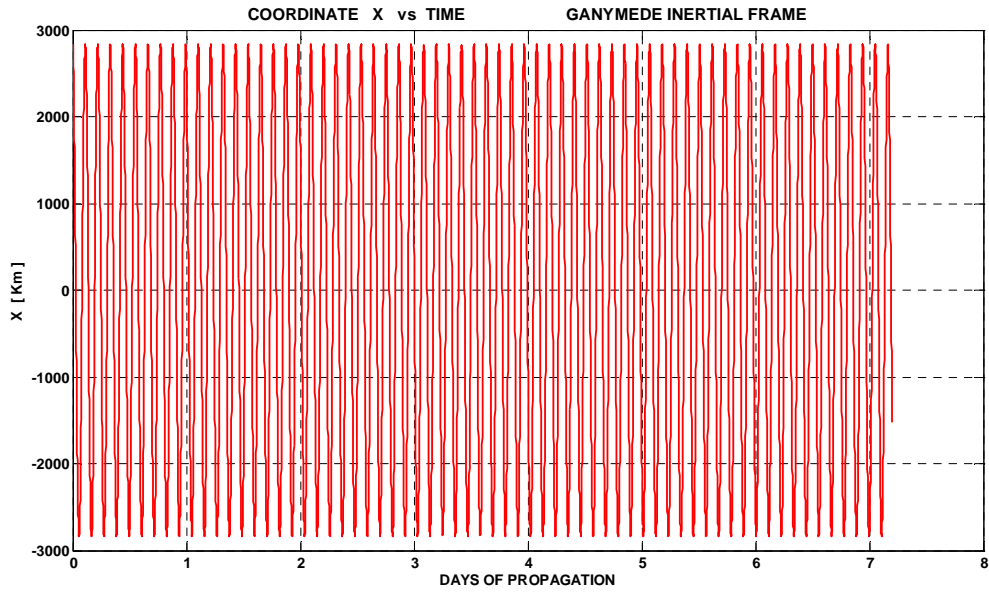


Figure 3.24: Spacecraft X-coordinate vs time in ganymedian inertial frame.

In figure 3.25 spacecraft curve progress of Y-coordinate as function of time in ganymedian inertial frame is illustrated. Note that the curve is always comprised in a range smaller respect to that one of X-coordinate: this is due to the starting values of right ascension of ascending node and orbital plane inclination.

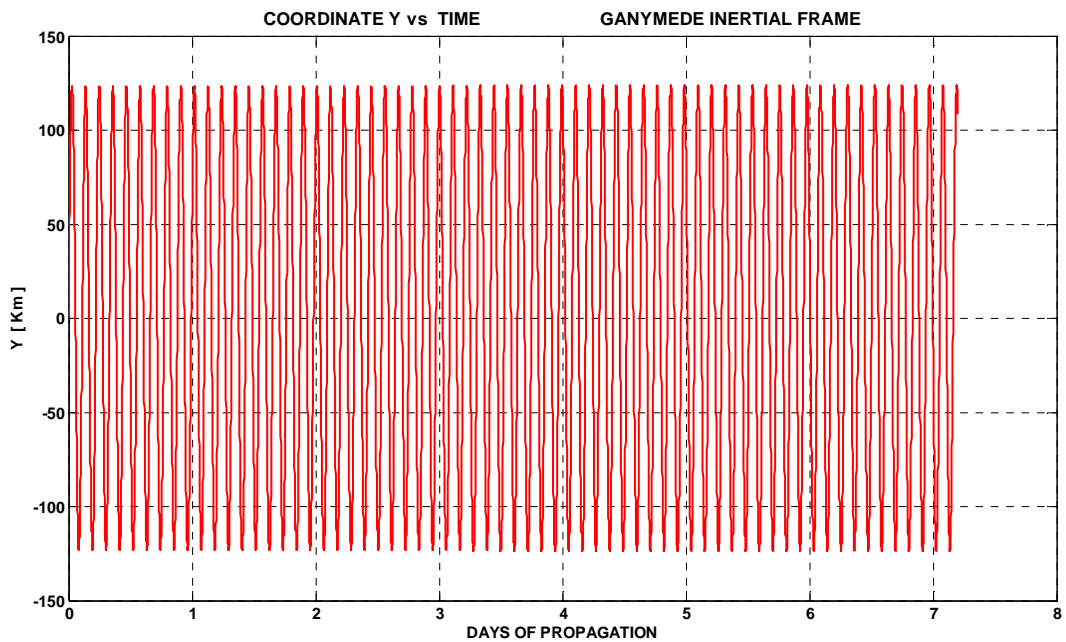


Figure 3.25: Spacecraft Y- coordinate vs time in ganymedian inertial frame.

Figure 3.26 shows curve progress for spacecraft Z-coordinate as function of time in ganymedian inertial frame. Also in this case the trend depend of the starting values of right ascension of ascending node and orbital plane inclination.

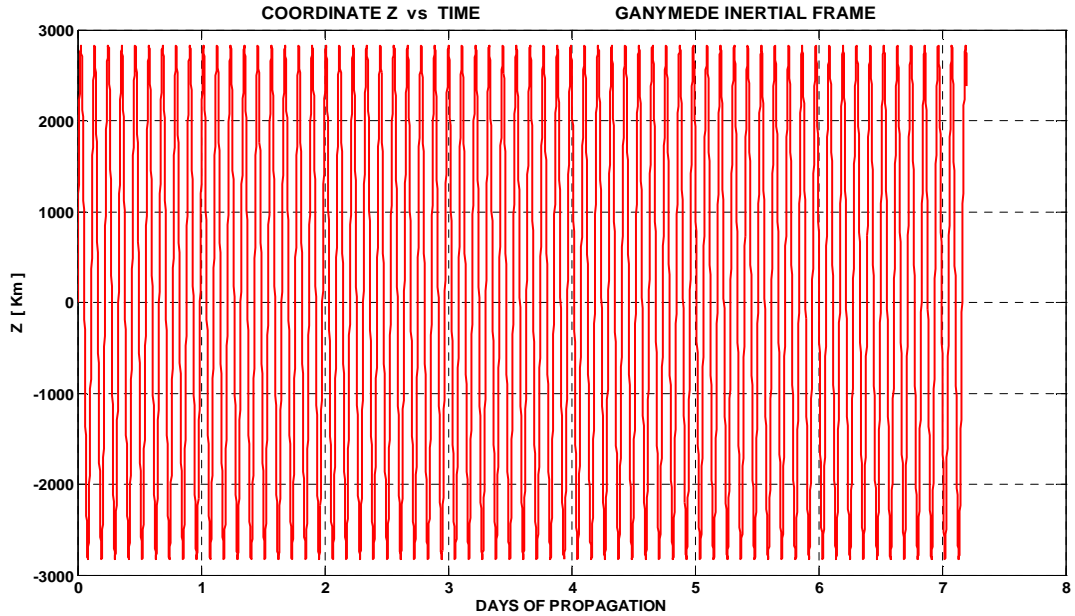


Figure 3.26: Spacecraft Z-coordinate vs time in ganymedian inertial frame.

In figure 3.27, it is possible to note the periodicity of curve progress of Jupiter right ascension in ganymedian inertial frame for an orbital period of propagation of around 7 terrestrial day (i.e. one ganymedian revolution period).

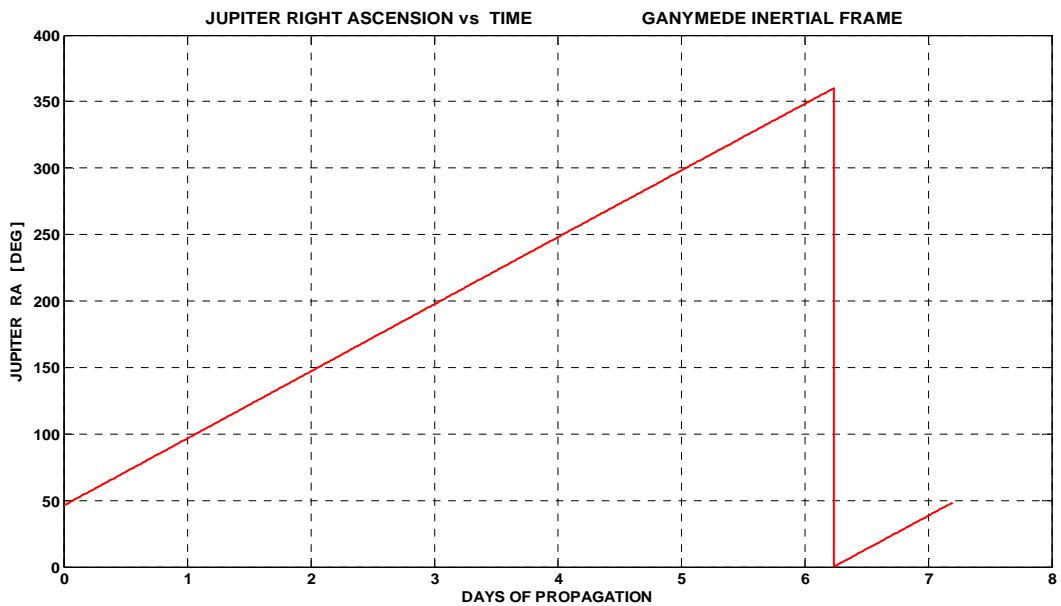


Figure 3.27: Jupiter right ascension vs time in ganymedian inertial frame.

In figure 3.28, it is possible to note the periodicity of curve progress of Jupiter declination, in ganymedian inertial frame, for an orbital period of propagation around 7 terrestrial day (i.e. one ganymedian revolution period).

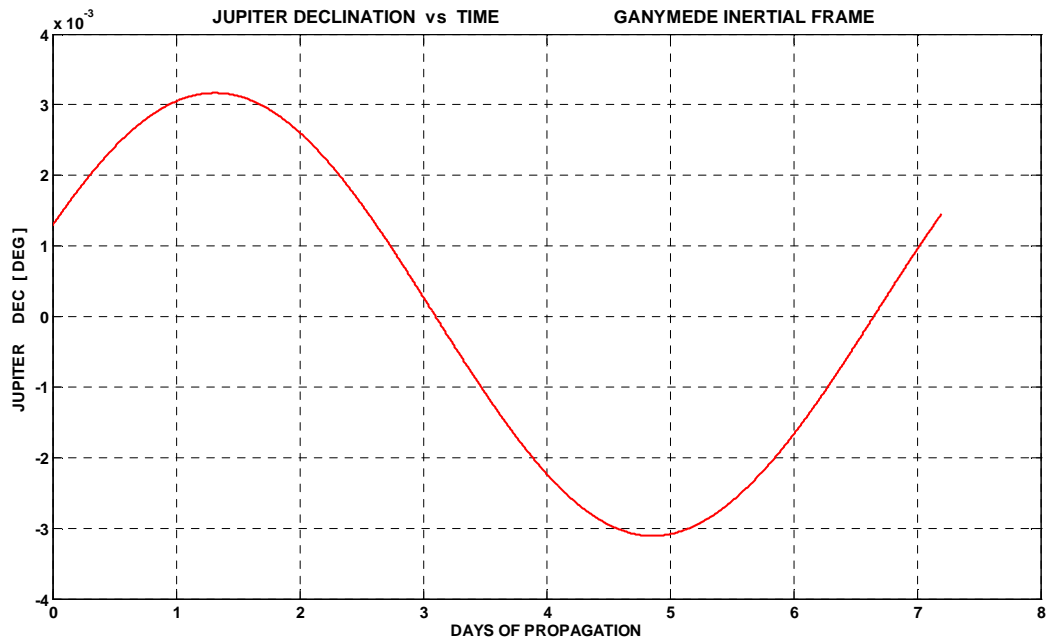


Figure 3.28: Jupiter declination vs time in ganymedian inertial frame.

Figures 3.29 and 3.30 illustrate Sun right ascension and sun declination as function of time, respectively, in ganymedian inertial frame. In figure 3.29 the increasing mean value of function is due to the orbital revolution motion of Jupiter around Sun, and the oscillations are a consequence of the orbital revolution motion of Ganymede around Jupiter, so, the curve is the result of combination of the two relative motions.

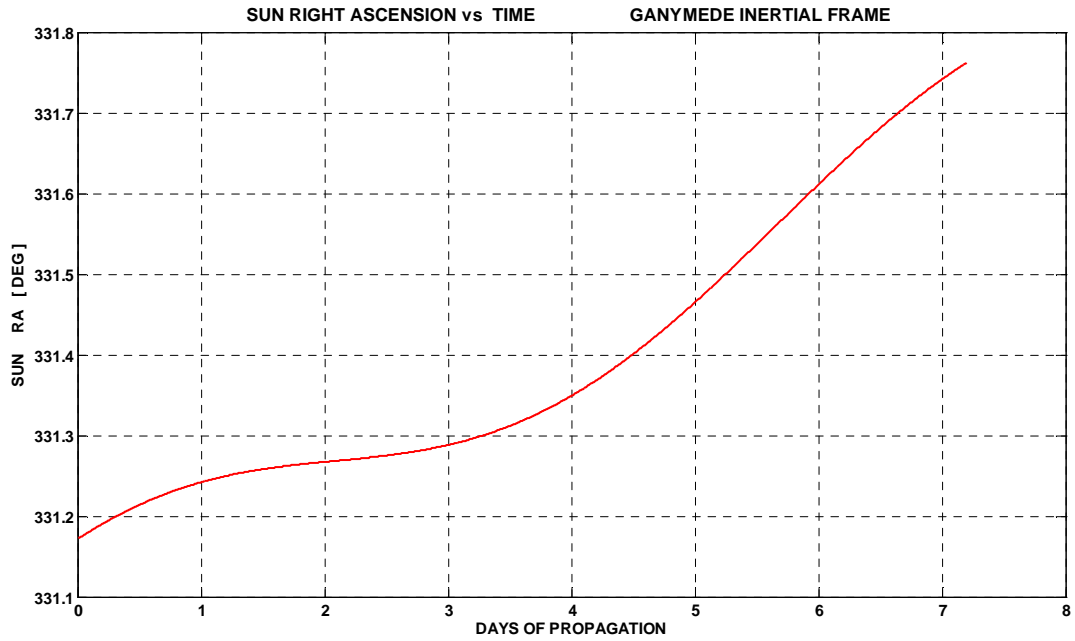


Figure 3.29: Sun right ascension vs time in ganymedian inertial frame.

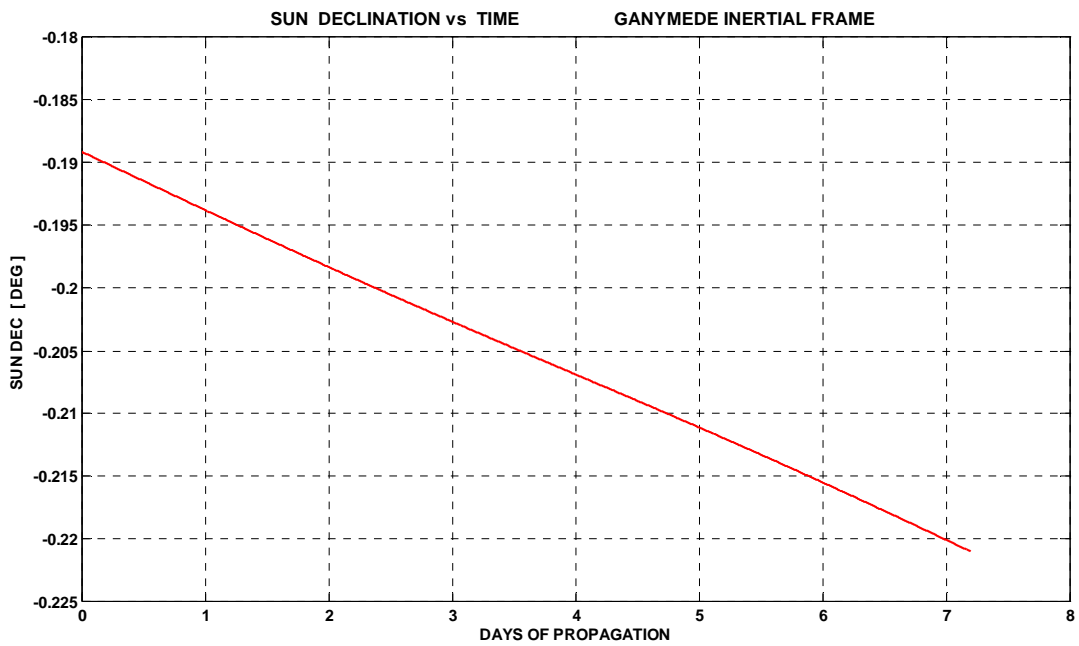


Figure 3.30: Sun declination vs time in ganymedian inertial frame

Figure 3.31 and figure 3.32 show the curve progress of sun right ascension and sun declination as function of time, respectively, in Earth inertial frame J2000.

It is recommended to refer figure 3.37 and figure 3.38, where the same functions are reported but for a period of time of 12 years: there it is to note a periodicity in one terrestrial year.

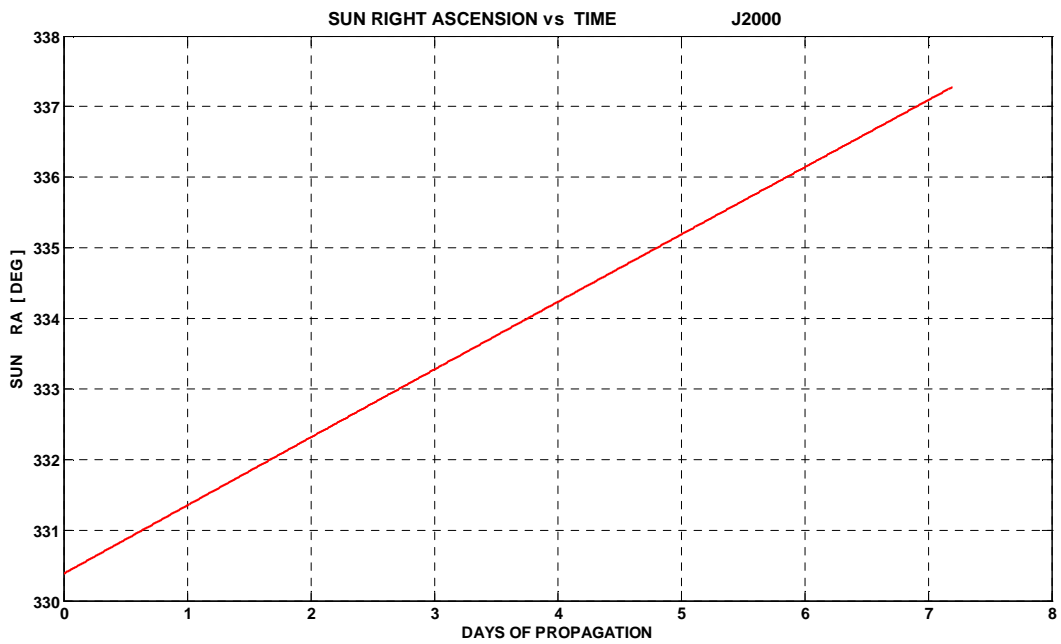


Figure 3.31: Sun right ascension vs time in Earth inertial frame J2000.

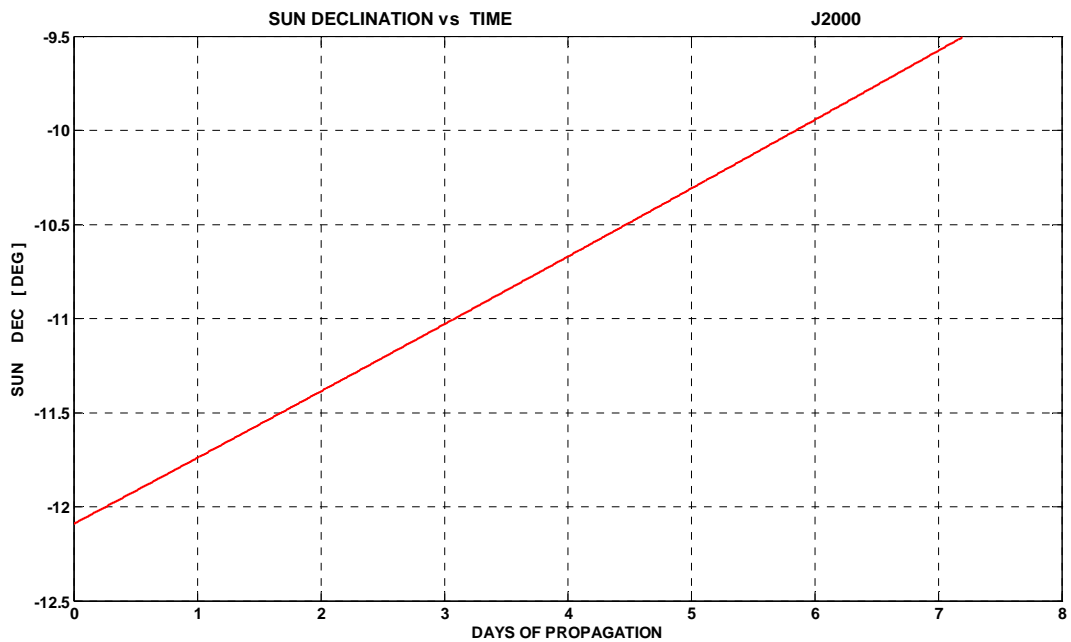


Figure 3.32: Sun declination vs time in Earth inertial frame J2000.

Figure 3.33 shows spacecraft orbital trajectory in ganymedian inertial frame for a period of propagation of almost 7 terrestrial days.

Observing this figure it is possible to note that the trajectory, neglecting the ascending node right ascension variation, repeat its trend.

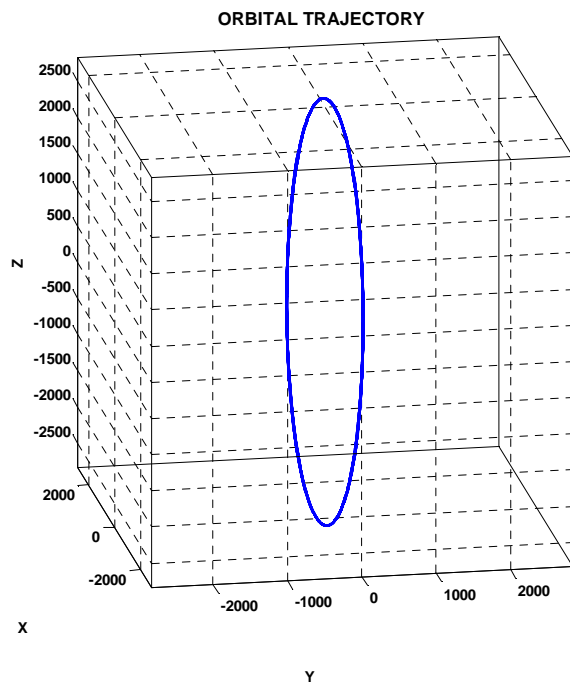
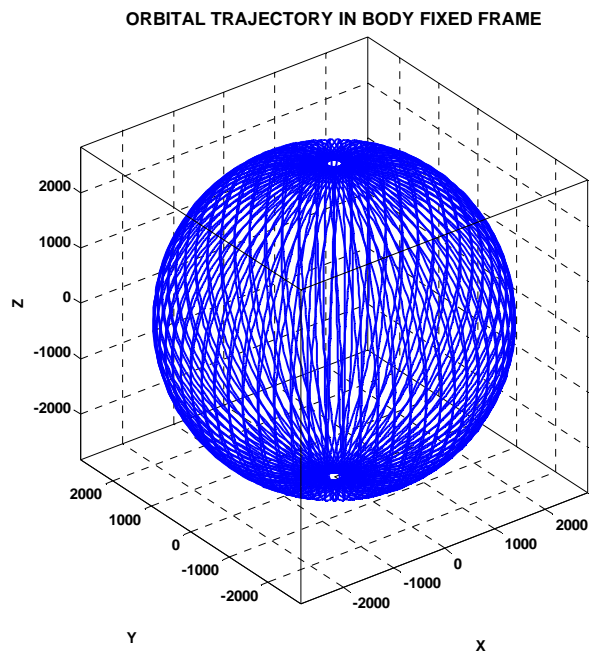


Figure 3.33: Spacecraft orbital trajectory in ganymedian inertial frame.

Figure 3.34 is illustrated the spacecraft coverage for an orbital period of one ganymedian revolution period (around 7 terrestrial days).



3.34: Spacecraft orbital trajectory in ganymedian body-fixed frame.

3.1.3 Sun useful plots

In figure 3.35 the periodicity of the Sun right ascension as function of time in ganymedian inertial frame, in an period of propagation of around 12 terrestrial years (i.e one Jupiter year).

The periodicity is given by the periodicity of Jupiter motion around the Sun (almost 12 terrestrial years), neglecting the revolution motion of Ganymede around Jupiter.

The same considerations are valid also for figure 3.36, in which Sun declination as function of time is represented.

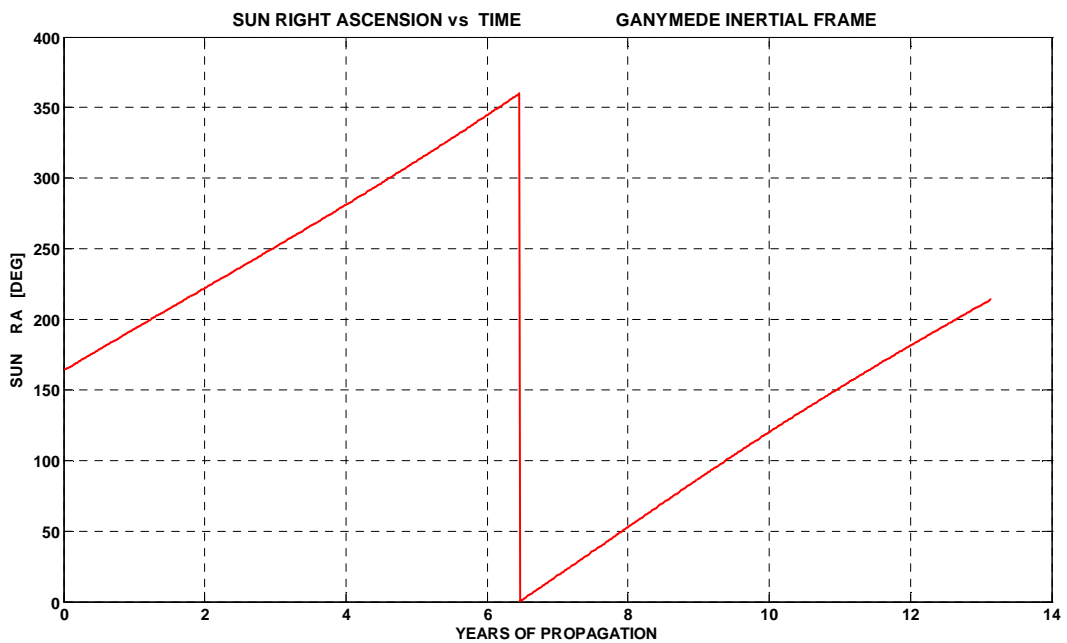


Figure 3.35: Sun right ascension vs time in ganymedian inertial frame.

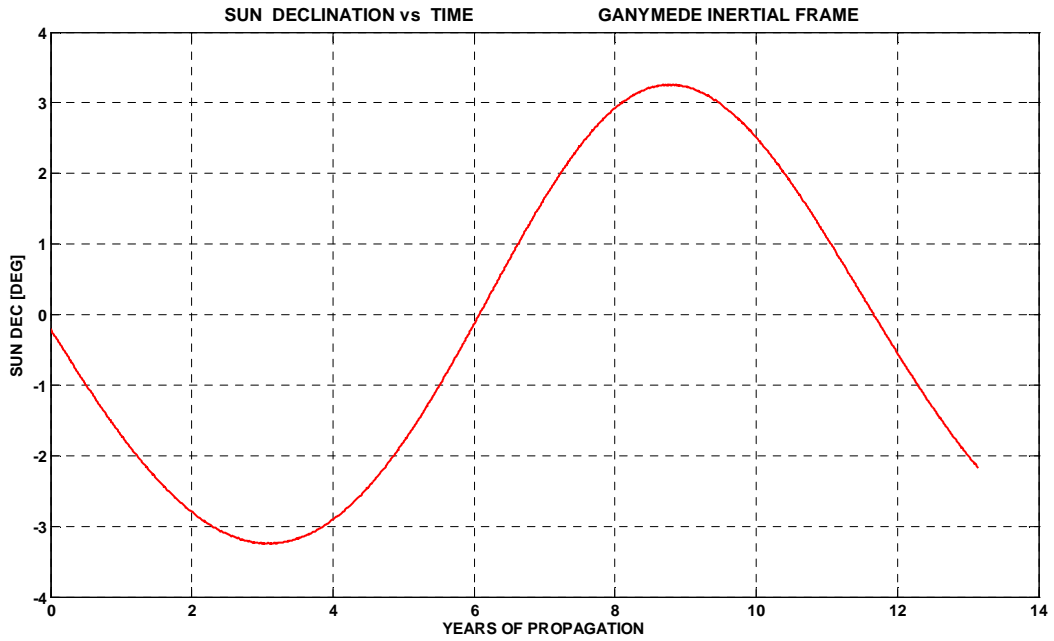


Figure 3.36: Sun declination vs time in ganymedian inertial frame.

In figure 3.37 and figure 3.38 Sun right ascension and Sun declination as function of time are showed. The graph is plotted for a time of propagation of around 12 terrestrial years (i.e one Jupiter year). The graphs show that the periodicity of the two curves is one terrestrial year.

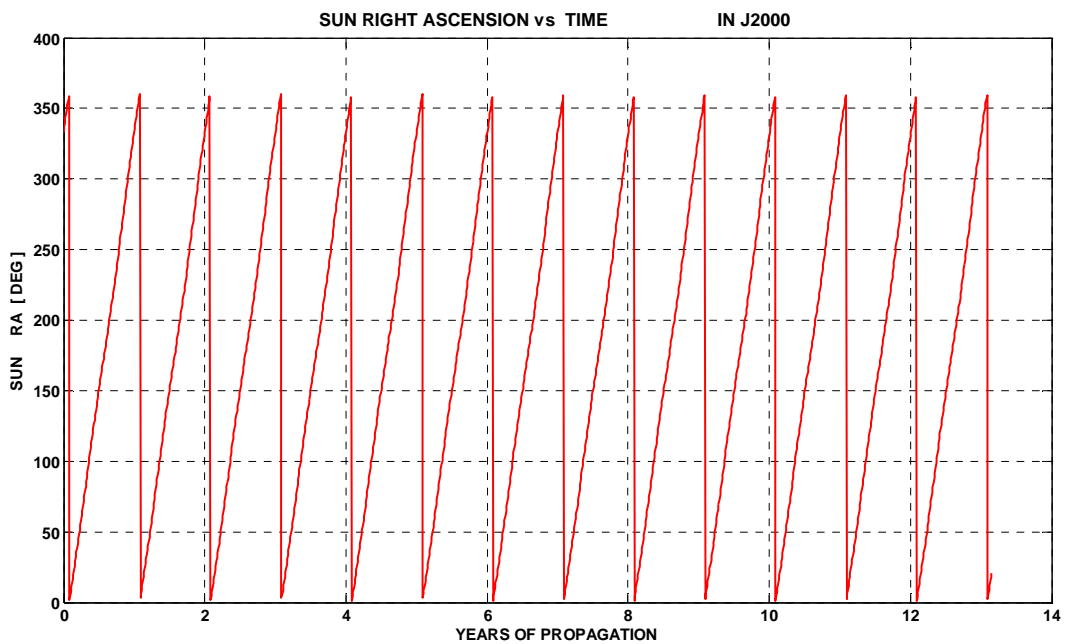


Figure 3.37: Sun right ascension vs time in Earth inertial frame J2000.

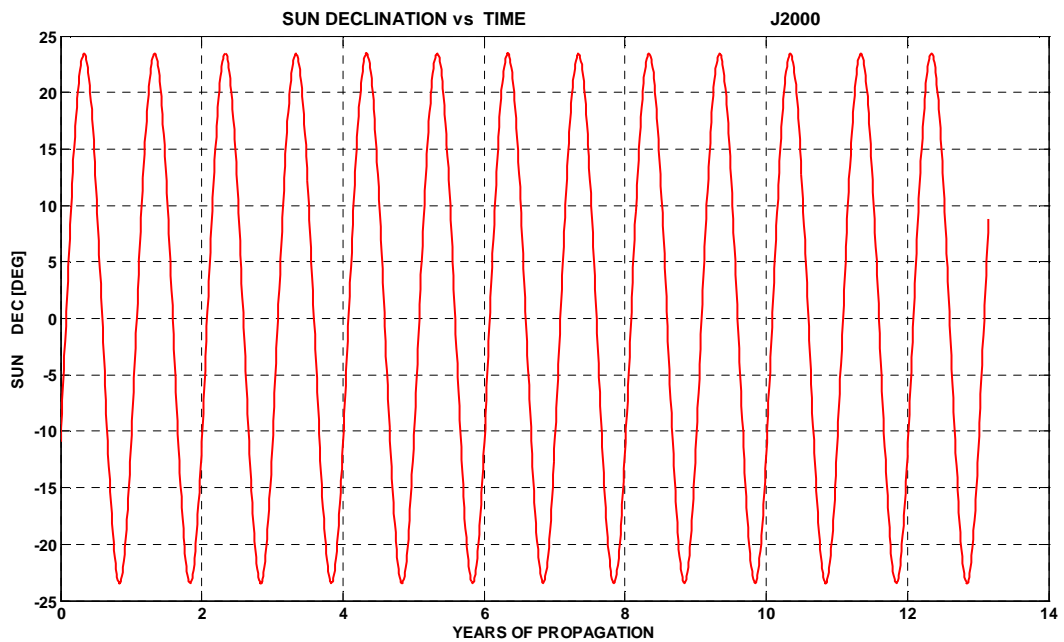


Figure 3.38: Sun declination vs time in Earth inertial frame J2000.

3.2 Graph results for Jupiter eclipse

This chapter provides the results obtained for Jupiter eclipse condition for JGO during the set propagation time.

It is opportune to remember that the Ganymede science phase (data collection phase) has a duration of 180 days.

The showed graphs are plotted for 180 days of propagation and then, for a clearer presentation of curve trends, also for around 7 terrestrial days of propagation , i.e. for one ganymedian revolution period.

3.2.1 Graph results for 180 terrestrial days of propagation

The following graphs are obtained for an orbit propagation starting in date February 17st 2009 12:00:00, with step time $dt = 15$ min; the obtaining curves interpolated around 10 points per orbital period. From figure 3.39 it is possible to note that for a

period of propagation of 180 terrestrial days the semi-angle α (see figures 2.9, 2.10) for Jupiter eclipse is contained into a range [64.744 ° , 64.726°].

As showed in relationship 2.12, this negligible variation is due to the dependence of eclipse semi-angle α from ρ_{cone} , and from the distance Ganymede-Jupiter (L).

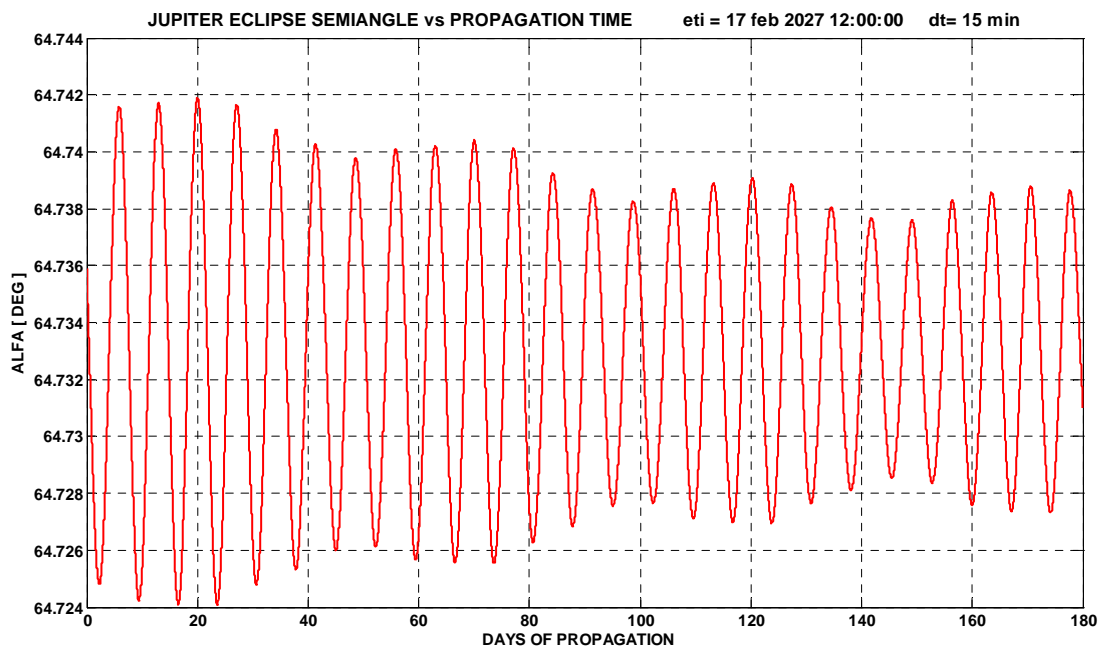


Figure 3.39: Semi-angle for Jupiter eclipse.

In figure 3.40 is showed the curve progress for azimuth angle (λ) (see figure 2.18) of Jupiter mass centre respect to antenna 's direction.

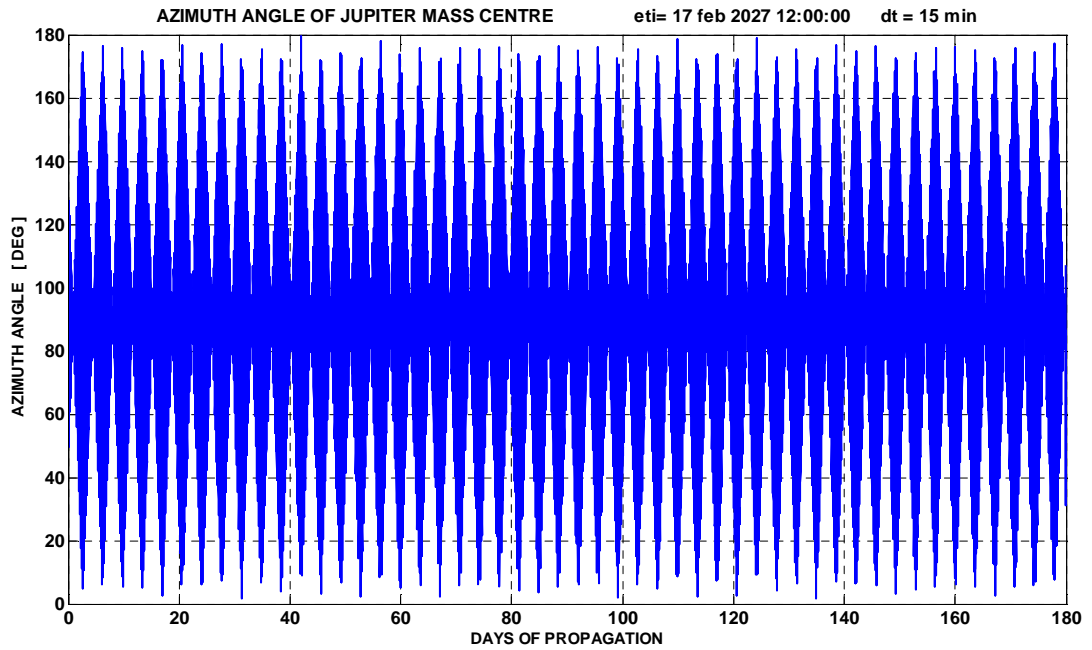


Figure 3.40: Azimuth angle of Jupiter's mass centre respect to antenna direction.

The Figure 3.41 represents the trend of the same angle of figure 3.40, but here it is possible to distinguish when the spacecraft is (blue) or not (red) in Jupiter eclipse condition.

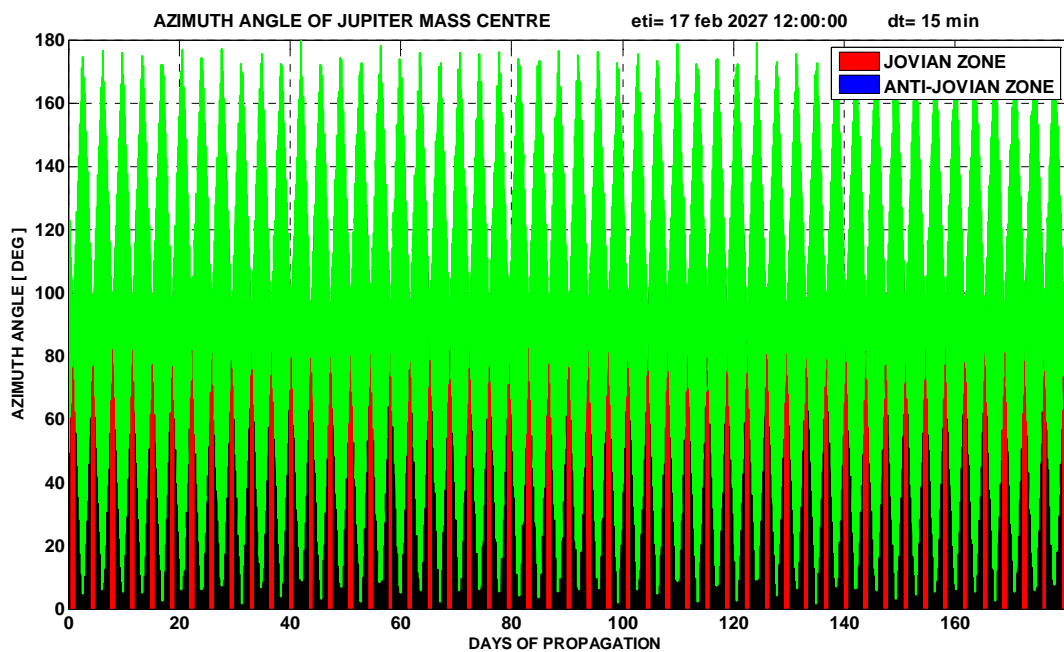


Figure 3.41: The green curve represents the azimuth angle trend showed in figure 3.40; the blue and red zones give information about no-eclipse and eclipse conditions respectively.

Figure 3.42 shows the duration of every single eclipse presented in previous image.

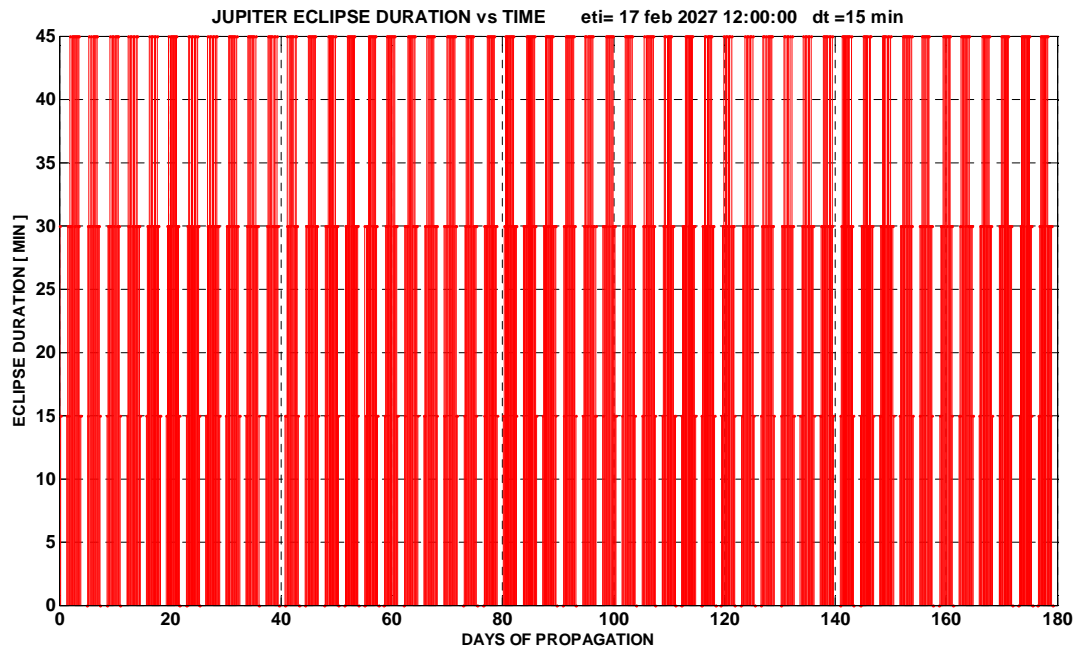


Figure 3.42: Jupiter eclipse duration vs time.

3.2.2 Graph results for one ganymedian revolution period

For a more detailed visual perception we will to show in next figures the curve progress for around 7 days (one ganymedian revolution period) of orbit propagation with a restrict step time $dt = 1$ min, that is to say 158 points per orbit.

In figure 3.43 it is possible to note the periodicity for eclipse semi-angle α in ganymedian inertial frame for around 7 days of propagation (i.e. ine ganymedian revolution period).

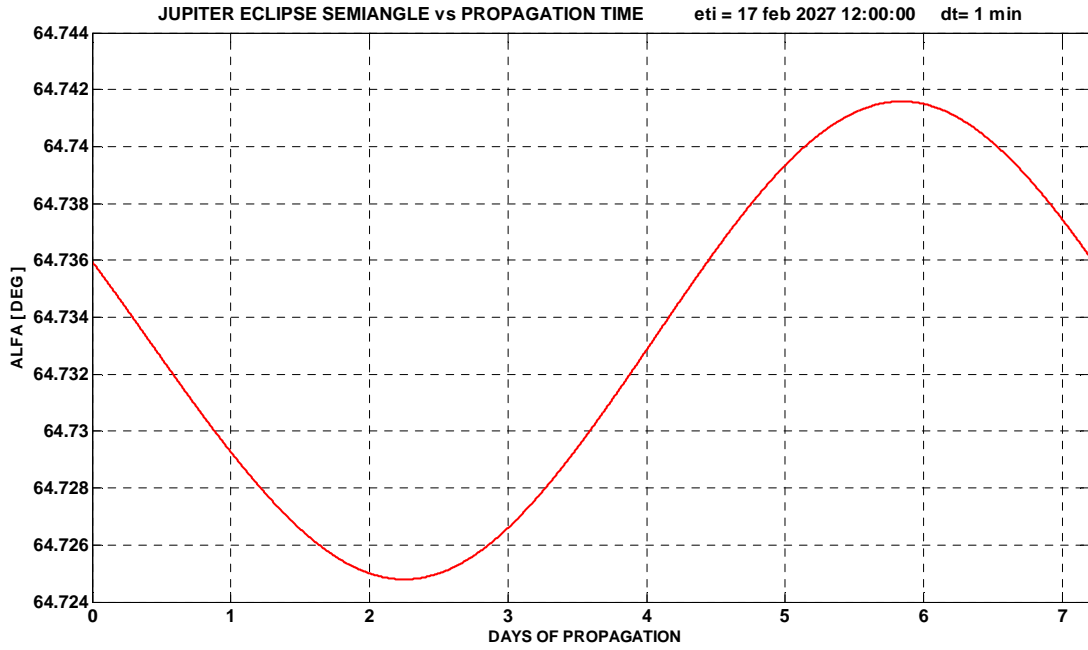


Figure 3.43: Eclipse semi- angle for Jupiter eclipse around 7 days of propagation.

In figure 3.44 curve-progress for azimuth angle of Jupiter mass centre respect to antenna direction is showed.

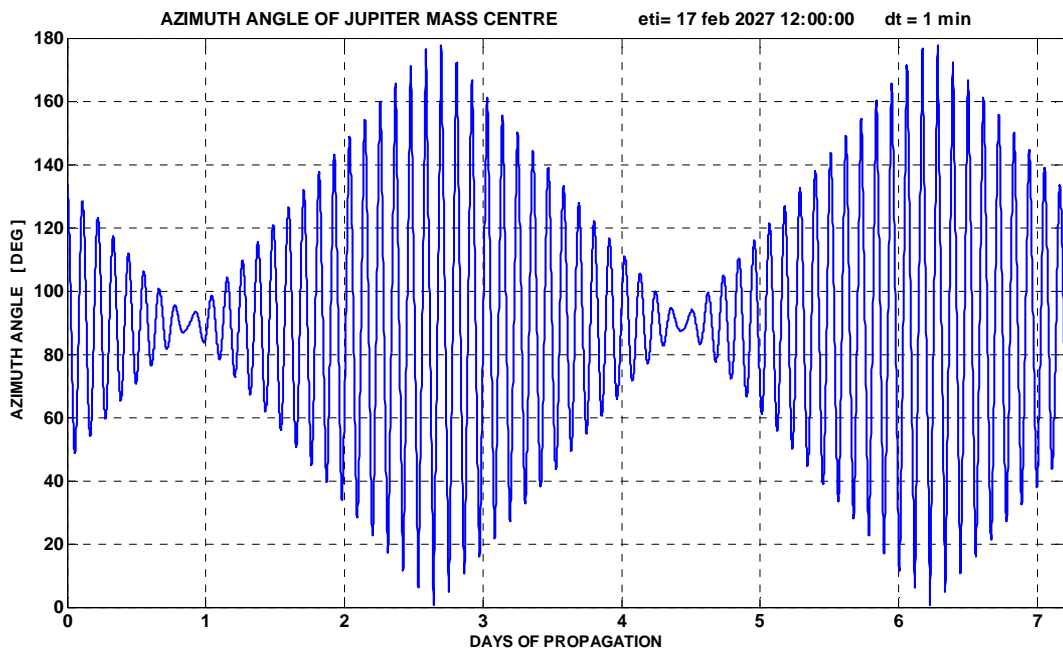


Figure 3.44 : Azimuth angle of Jupiter mass centre respect to antenna direction.

In next Figure 3.45 it is possible to distinguish *eclipse (anti-jovian zone)* from *not-eclipse(jovian zone)* conditions about previous graph.

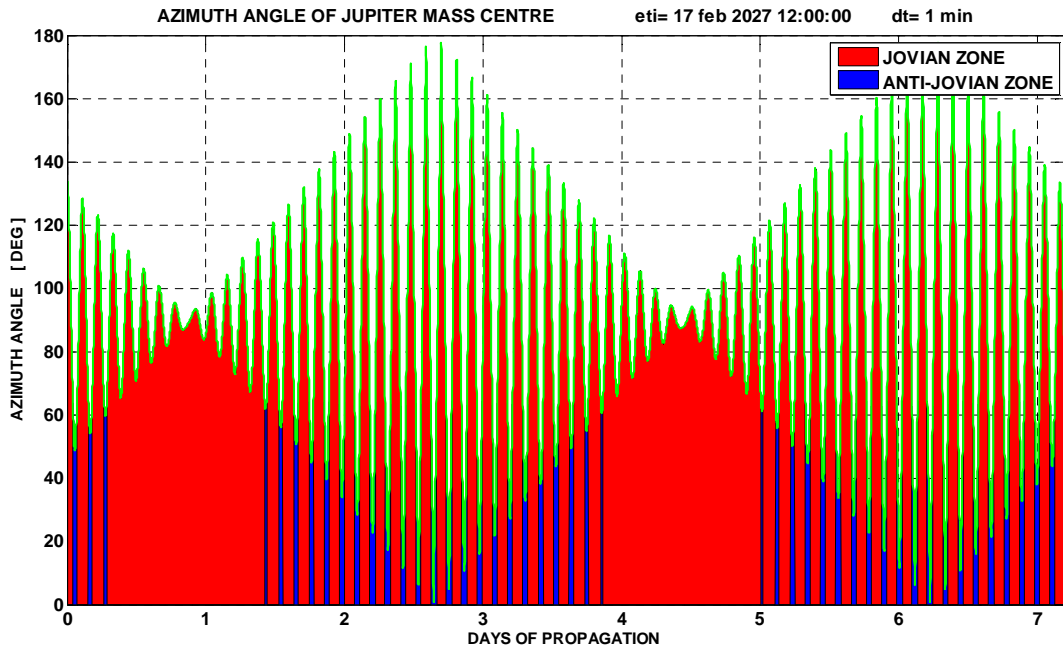


Figure 3.45: Distinction for jovian (red) and anti-jovian (blue) zone in 7 day of propagation

In figure 3.46 is showed the eclipse duration of eclipse periods presented in figure 3.45. it is possible to note that around 7 days of propagation we have 46 Jupiter eclipse phases with a maximum duration value of 56 min.

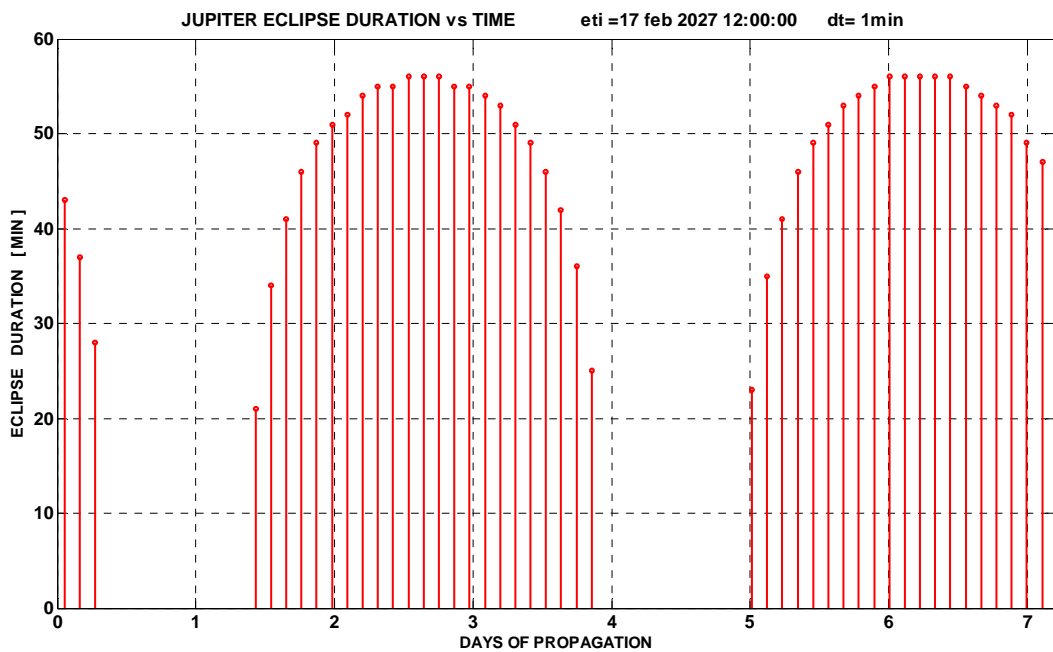


Figure 3.46: Jupiter eclipse duration vs time of propagation.

3.3 Graph results for Sun eclipse

Condition for Sun eclipse is necessary for a correct data capture by LaserAltimetry.

The LA has a protrusive telescope and we have imposed the eclipse condition on the it as reference direction, as for the RS antenna.

All the graphs we have showed from Jupiter eclipse are now reported for Sun eclipse, for about 180 days of orbit propagation (time duration for Ganymede science phase) and then , for a more detailed visual perception , around 7 days (i.e one ganymedian revolution period).

3.3.1 Graph results for 180 terrestrial days of propagation.

The Figure 3.47 shows the curve progress of the semi-angle α for Sun eclipse .

The light oscillations that graph presents are due to the Ganymede's rotation period.

It is possible to note that the graph contains around 25 oscillations since in 180 days we have around 25 ganymedian revolutions (1 ganymedian revolution is around 7 terrestrial days).

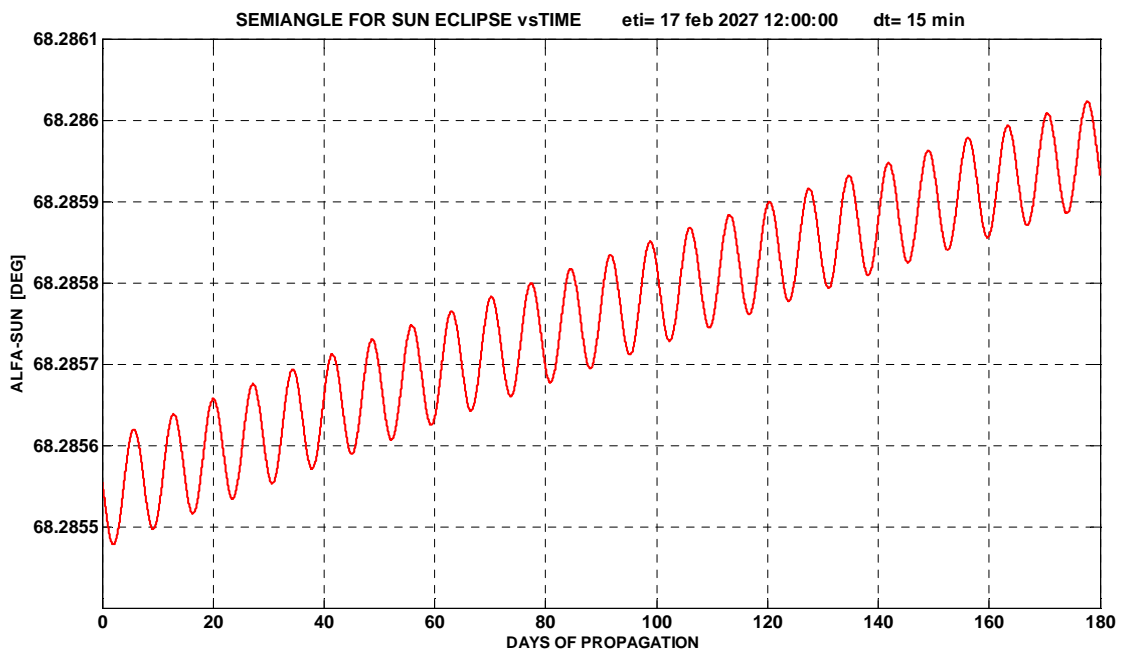


Figure 3.47 : Semi-angle for Sun eclipse.

In figure 3.48 azimuth angle of Sun mass centre respect telescope direction is showed.

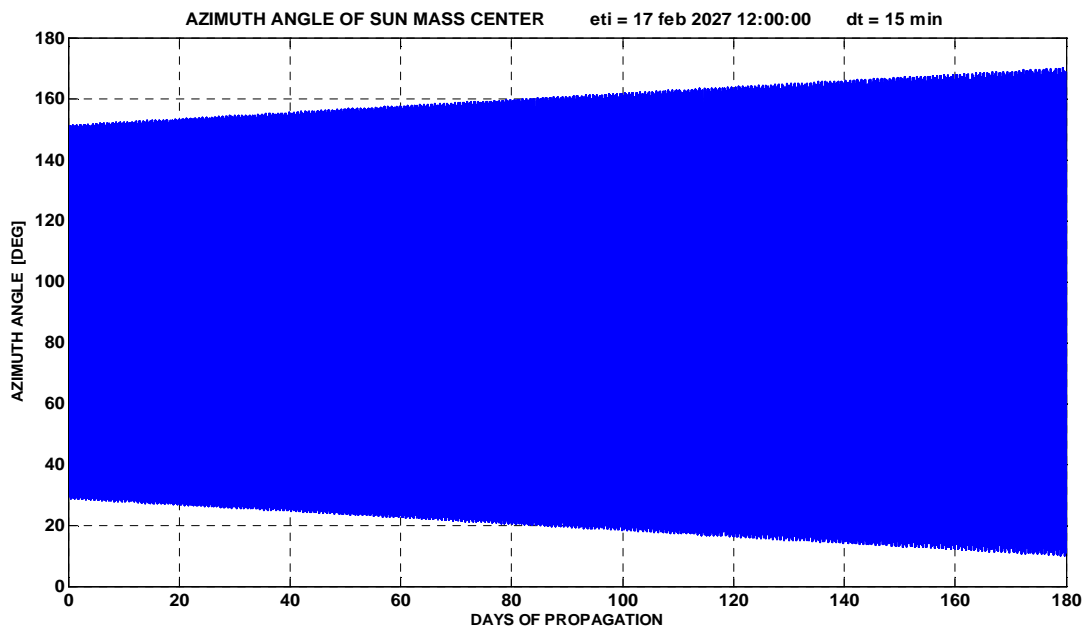


Figure 3.48: Azimuth angle of Sun mass centre respect to antenna direction

In successive figure 3.49(a) the distinction for Sun no-eclipse (red) and eclipse condition (blue) is represented (for a more visual perception see particular in figure 3.49(b)).

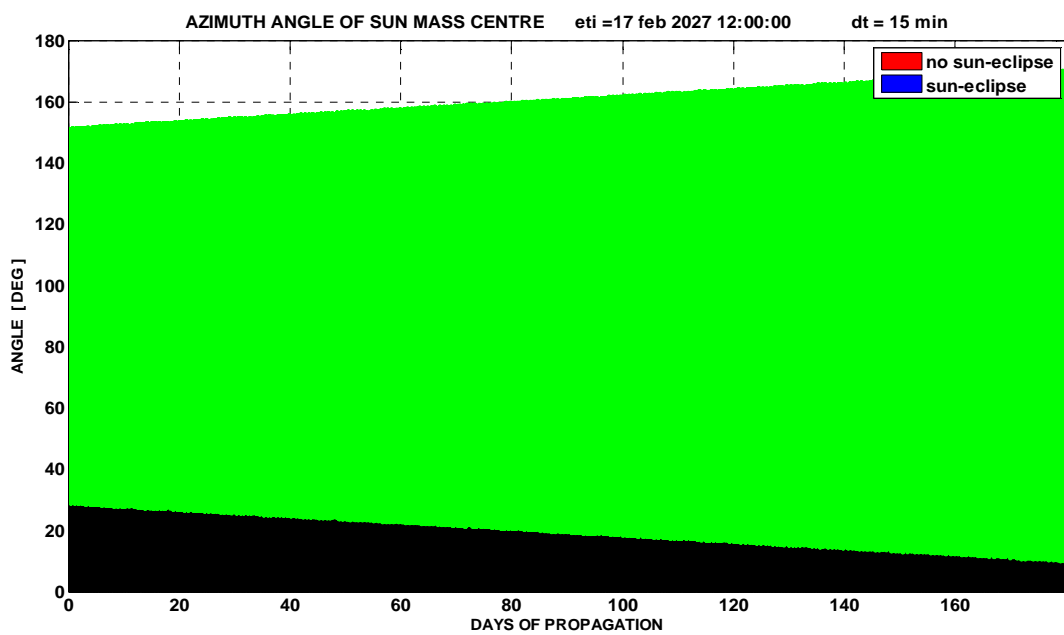


Figure 3.49(a)



Figure 3.49(b)

Figure 3.49: (a): Azimuth angle of Sun mass centre with distinction for Sun no-eclipse (red) and Sun eclipse (blue) condition; (b): Particular eclipse (blue) and not-eclipse condition (red).

The graph for Sun eclipse for 180 days is omitted since it is not well readable. To illustrate its progress in figure 3.50 the curve of Sun eclipse is presented around 75 days of propagation.

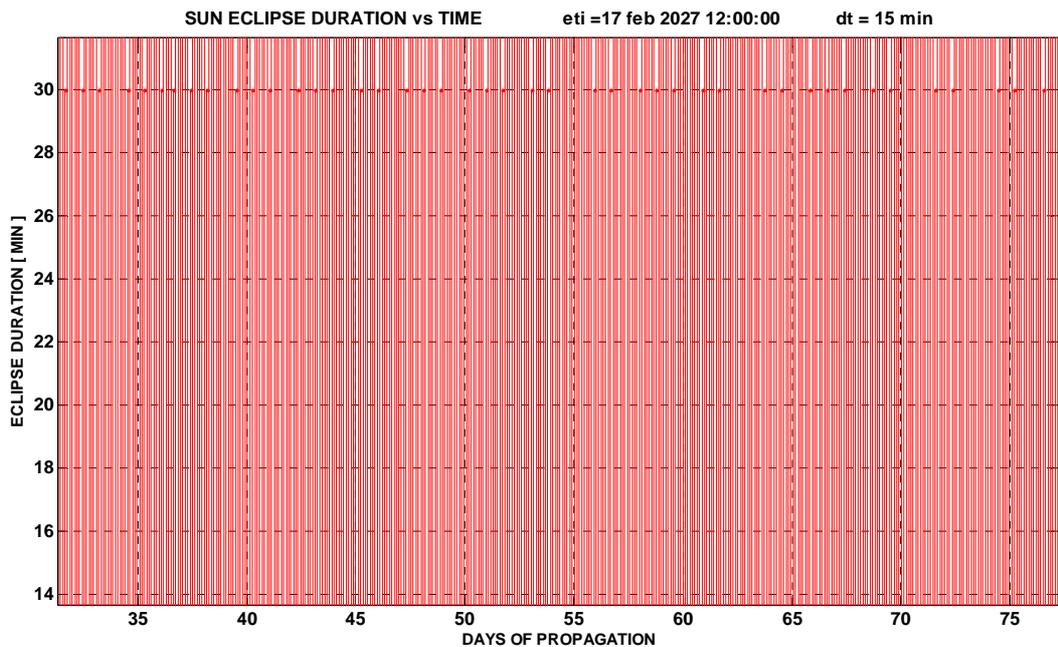


Figure 3.50 : Sun eclipse duration vs time.

3.3.2 Graph results for one ganymedian revolution period

The Figure 3.51 illustrates the curve-progress of semi-angle for Sun eclipse condition in ganymedian inertial frame. Also in this case the apparent motion of Sun around Ganymede presents almost a periodicity (since the combined motion of Ganymede with Jupiter , together around Sun) around 7 days (one revolution period)

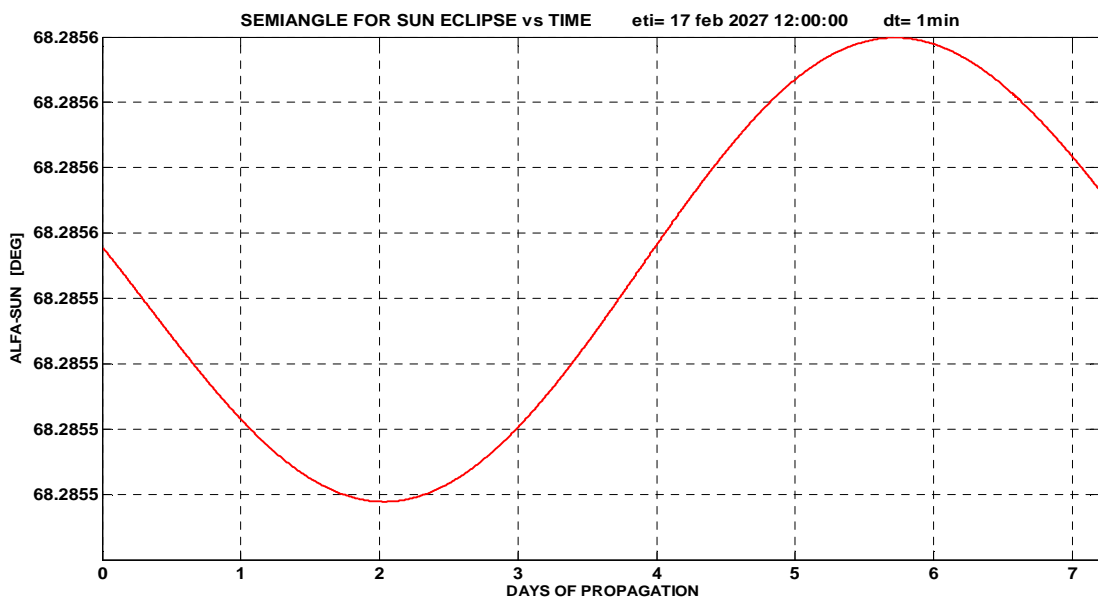


Figure 3.51: Semi-angle of sun eclipse about 7 days of propagation

Figure 3.52 shows azimuth angle of Sun mass centre respect to telescope direction.

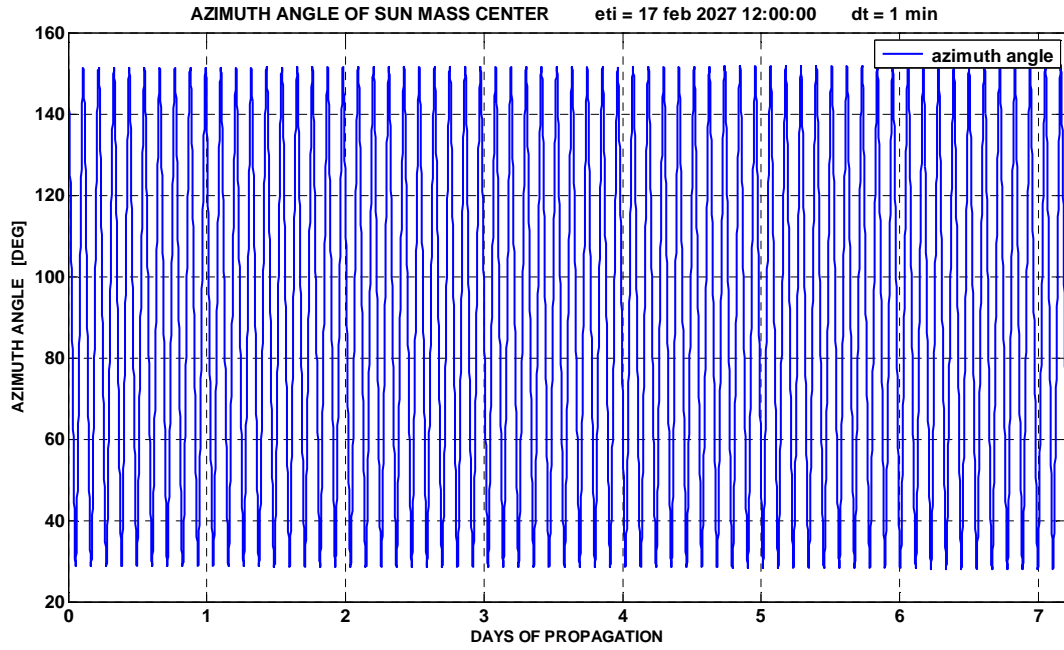


Figure 3.52: Azimuth angle of Sun mass centre respect to antenna direction.

A distinction of Sun no-eclipse and Sun eclipse zones is reported in figure 3.53.



Figure 3.53: Azimuth angle of Sun mass centre for sun no-eclipse and sun eclipse conditions.

In figure 3.54 the durations of Sun eclipse periods are presented. The maximum eclipse period have a value of 57 min.

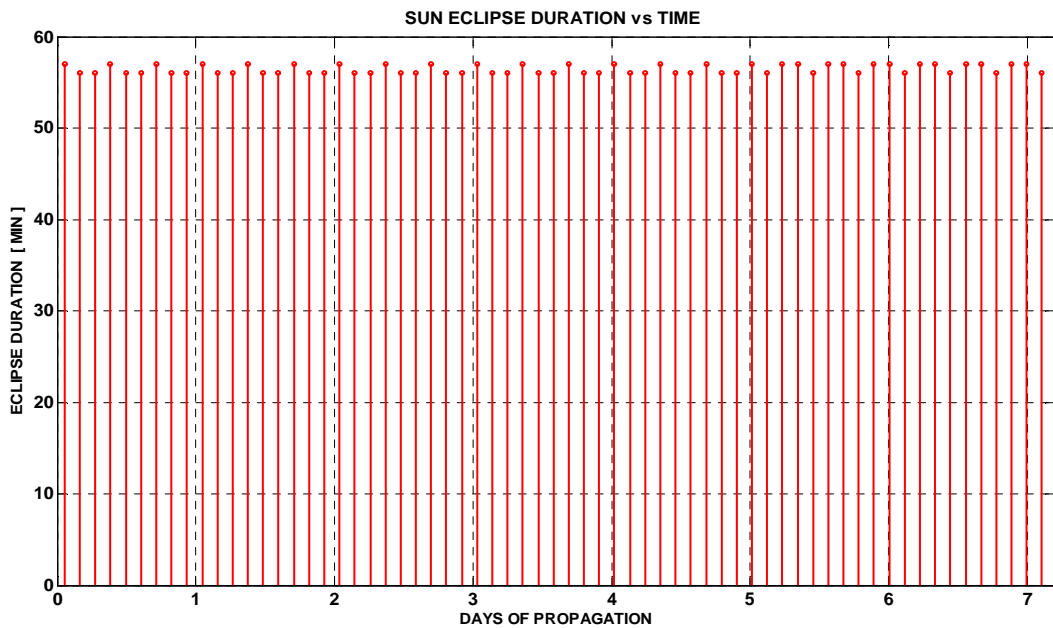


Figure 3.54: Sun eclipse duration vs time of propagation.

3.4 Useful graphs

It is useful to represent the curve-progress about the semi-angle α for Sun eclipse in a propagation period of around 12 terrestrial years , that is to say the period of revolution of Jupiter around Sun, to note its periodicity (figure 3.55).

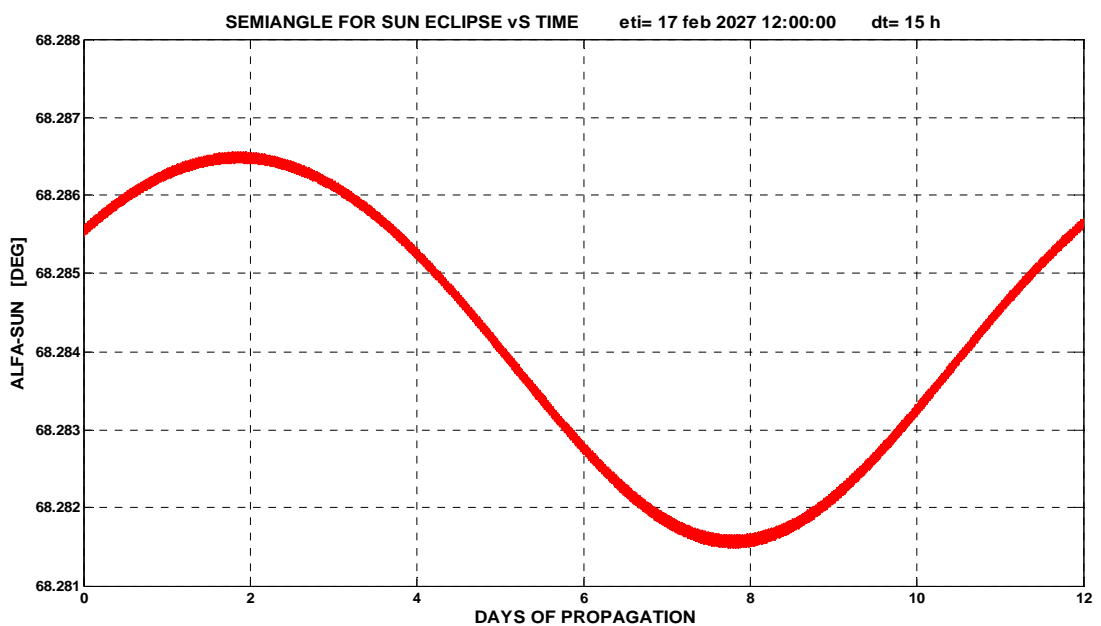


Figure 3.55 : Semi-angle of Sun eclipse for 12 years of propagation.

In Figure 3.56 a zoom of figure 3.55 is showed. It is possible to note some oscillation due to revolution period of Ganymede around Jupiter .

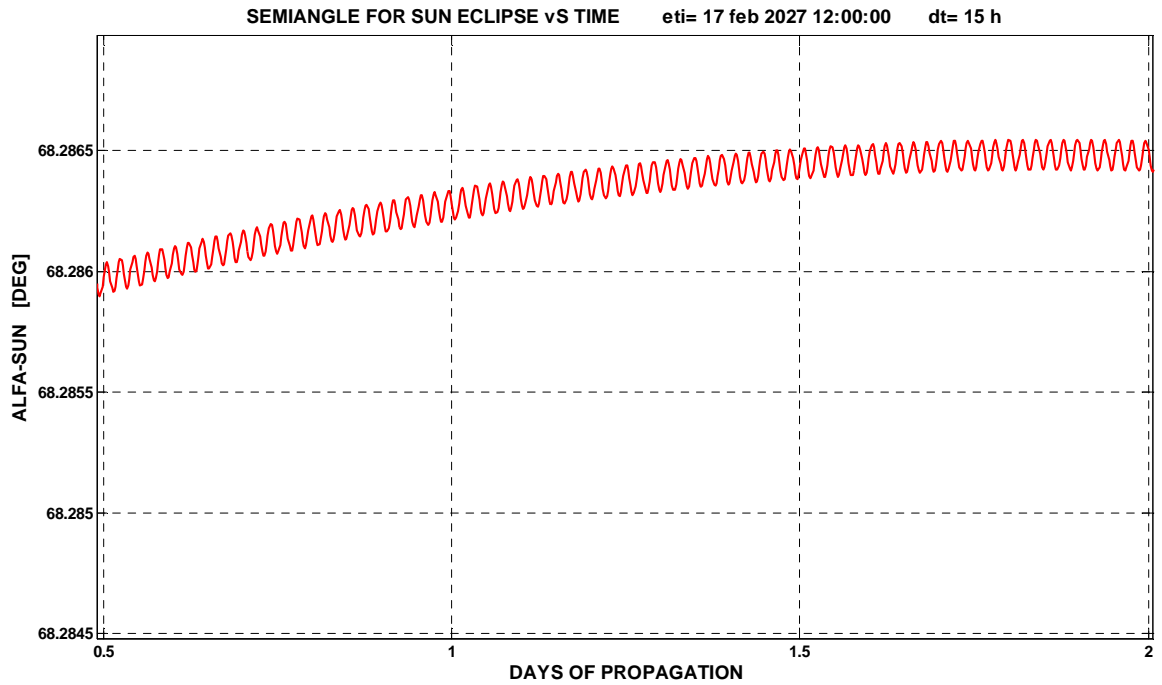


Figure 3.56: Oscillations due to revolution period of Ganymede around Jupiter.

ANNEX : Orbital Propagator Code

```
%service operation

addpath('C:\(current directory)\mice\mice\lib')
addpath('C:\(current directory)\mice\mice\src\mice')
clc
clear all
close all
cspice_kclear

cspice_furnsh('C:\(current directory)\naif0009.tls');
cspice_furnsh('C:\(current directory)\jup230.bsp');
cspice_furnsh('C:\(current directory)\pck00008.tpc');

%input data

H=200;      % altitude [Km]
dt=60;      % step time [s]

Nd=7;      % days of propagation

% starting propagation time
Ti='17 feb 2027 12:00:00';

%covert UTC to ET time
eti=cspice_str2et(Ti);

% time array iteration
ti=0:dt:Nd*86400;

% number of iteration points
npunti=(length(ti)-1);

%gravitational parameter [Km^3/s^2]
mi=9887.834 ;

% second zonal armonic
J2=126.9e-6;

%mean ganymede equatorial radius [km]
```

```

Req= 2631.2050;

%eccentricity ;
eC=0;

%major semi-axis [km]
aC=Req+H;

%minor semi-axis [km]
bC=aC*sqrt(1-eC^2);

% semilatus rectum
p=aC*(1-eC^2);

%mean motion [rad/sec]
n=sqrt(mi/(aC^3));

%starting inclination [deg ]
inc=87.5;
inc=inc*cspice_rpd;      % from [deg] to [rad]

%starting right ascension of ascending node [rad]
ra_i=0;
ra_i=ra_i*cspice_rpd;    % from [deg] to [rad]

%starting argument of the periapsis [rad]
pa_i=0;
pa_i=pa_i*cspice_rpd;    % from [deg] to [rad]

%perturbed mean motion
Mpunto= n*(1+((3/2)*J2*(Req^2/p^2))*(sqrt(1-eC^2))*(1-
((3/2)*(sin(inc))^2)));

% mean orbital period [s];
T = 2*pi/n ;

%Keplerian period [s]
perkeps=(2*pi)/n;

%Ganymede's angular speed [rad/s]
omegaganyme= 1.019227316914976e-005 ;

Rjup=69882;      % Jupiter mean radius
Rsun=694460;     % Sun mean radius

%Initial values for eccentric and mean anomaly and starting true anomaly
%true anomaly [deg] (automatic conversion to [rad])

```

```

niC(1)=0; % initial true anomaly
niC(1)=niC(1)*cspice_rpd; % conversion from [deg] to [rad]
niC(1)=niC(1);
sinEC0=sqrt(1-eC^2)*sin(niC(1))/(1+eC*cos(niC(1)));
cosEC0=(eC+cos(niC(1)))/(1+eC*cos(niC(1)));
EC(1)=atan2(sinEC0,cosEC0);
MC(1)=EC(1)-eC*sin(EC(1));

%compute mean an eccentric anomaly an time dates (numerical results)

time(1)=eti; % initial ephemeris second form J2000 epoch
for it=2:npunti
    MC(it)=MC(it-1)+n*dt;
    %Newton_ beginning
    dEC=1;
    iter=1;
    ECtry(iter)=MC(it);
    while dEC>10^-6 && iter<10
        iter=iter+1;
        ECtry(iter)=ECtry(iter-1)-(ECtry(iter-1)-
eC*sin(ECtry(iter-1))-MC(it))/(1-eC*cos(ECtry(iter-1)));
        dEC=(ECtry(iter)-ECtry(iter-1))/ECtry(iter-1);
    end
    EC(it)=ECtry(iter);
    sinniC=sin(EC(it))*sqrt(1-eC^2)/(1-eC*cos(EC(it)));
    cosniC=(cos(EC(it))-eC)/(1-eC*cos(EC(it)));
    niC(it)=atan2(sinniC,cosniC);

    time(it)=eti+(it-1)*dt; %ET seconds elapsed at i-esimo istant
from J2000 epoch

end
for it=1:npunti
    time_prop(it)=(it-1)*dt;
end

% cartesian coordinates in perifocal frame .
for it =1:npunti
    Xper(it)=aC*(cos(EC(it))-eC);
    Yper(it)=aC*(sqrt(1-(eC)^2))*sin(EC(it));
    Zper(it)=0;
end

% conversion from GANYMEDE FIXED FRAME to GANYMEDE INERTIAL FRAME
taking in count ascending node righth ascension and periapsis argument
variations

ra(1)=ra_i; % starting value of right ascension of ascending node
pa(1)=pa_i ; % starting value of periapsis argument
for it=2:npunti

```

```

% ascending node variation due to J2 effect
ra(it)=(ra_i-[3/2*J2*(Req^2/p^2)*Mpunto*cos(inc)]*time_prop(it));

% argument of periapsis variation
pa(it)=(pa_i+([(3/2)*J2*(Req^2/p^2)*Mpunto*(2*((5/2)*(sin(inc)^2)))]*time_prop(it)));
end

for it=1:npunti
% coordinates with right ascension of ascending node and periapsis argument variations in inertial frame

XIgan(it)=[[[cos(ra(it))*cos(pa(it))]-
[sin(ra(it))*sin(pa(it))*cos(inc)]]*Xper(it)]+[[[-
cos(ra(it))*sin(pa(it))]-
[sin(ra(it))*cos(pa(it))*cos(inc)]]*Yper(it)]+[[sin(ra(it))*sin(inc)]*Zper(it)];

YIgan(it)=[[[sin(ra(it))*cos(pa(it))]+[cos(ra(it))*sin(pa(it))*cos(inc)]]*Xper(it)]+[[[-
sin(ra(it))*sin(pa(it))]+[cos(ra(it))*cos(pa(it))*cos(inc)]]*Yper(it)]+[[
-cos(ra(it))*sin(inc)]*Zper(it)];

ZIgan(it)=[[[sin(pa(it))*sin(inc)]*Xper(it)]+[[cos(pa(it))*sin(inc)]*Yper(it)]+[[cos(inc)]*Zper(it)];
end

%conversion from Ganymede's inertial frame to Ganymede's body fixed frame( IAU-GANYMEDE)

pmJ2000 = 44.064*pi/180 ; % starting position of prime meridian

pm_rate = 50.3176081*pi/180; % Ganymede's angular speed

for it=1:npunti

d(it)=time(it)/86400; % days passed from epoch J2000
T(it)=d(it)/36525; % julian century = 36525 days(from J2000 epoch)
J4(it)=355.80*cspice_rpd+(1191.3*cspice_rpd)*T(it);
J5(it)=119.9*cspice_rpd+(262.1*cspice_rpd)*T(it);
J6(it)=229.8*cspice_rpd+(64.3*cspice_rpd)*T(it);

theta(it)=pmJ2000+pm_rate*d(it)+0.033*sin(J4(it))-0.389*sin(J5(it))-0.082*sin(J6(it)); %position of prime meridian at i-istant

```

```

% rotation matrix for elementary rotation around Z axis

Xrotgan(it)=[cos(theta(it))*XIgan(it)]+[sin(theta(it))*YIgan(it)]+0;
Yrotgan(it)=[-sin(theta(it))*XIgan(it)]+[cos(theta(it))*YIgan(it) ]+0;
Zrotgan(it)=0+0+ZIgan(it);

end

%Coefficients for velocity computation

for it=1:npunti
    radiusC(it)=aC*(1-eC*cos(EC(it)));
    l_1(it)=cos(ra(it))*cos(pa(it))-sin(ra(it))*sin(pa(it))*cos(inc);
    m_1(it)=sin(ra(it))*cos(pa(it))+cos(ra(it))*sin(pa(it))*cos(inc);
    n_1(it)=sin(pa(it))*sin(inc);
    l_2(it)=-cos(ra(it))*sin(pa(it))-sin(ra(it))*cos(pa(it))*cos(inc);
    m_2(it)=-sin(ra(it))*sin(pa(it))+cos(ra(it))*cos(pa(it))*cos(inc);
    n_2(it)=cos(pa(it))*sin(inc);

%Satellite velocity in ganymede's inertial frame [km/s]

Vx_Igan(it)=n*aC/radiusC(it)*(bC*l_2(it)*cos(EC(it))-
aC*l_1(it)*sin(EC(it)));
Vy_Igan(it)=n*aC/radiusC(it)*(bC*m_2(it)*cos(EC(it))-
aC*m_1(it)*sin(EC(it)));
Vz_Igan(it)=n*aC/radiusC(it)*(bC*n_2(it)*cos(EC(it))-
aC*n_1(it)*sin(EC(it)));

%Satellite velocity in ganymede's body-fixed frame [km/s]
VXrotgan(it)=[cos(theta(it))*Vx_Igan(it)]+[sin(theta(it))*Vy_Igan(it)]+0;
VYrotgan(it)=[-sin(theta(it))*Vx_Igan(it)]+[cos(theta(it))*Vy_Igan(it)
]+0;
VZrotgan(it)=0+0+Vz_Igan(it);

End

% ephemeris-data on file .txt

eph=fopen('ephemerisdata.txt','wt');
ephemeris=[time;Xrotgan;Yrotgan;Zrotgan;VXrotgan;VYrotgan;VZrotgan];
for ii=1:npunti
    for kk=1:7
        fprintf(eph,'%12.6f\t',ephemeris(kk,ii));
    end
    fprintf(eph,'\n');
end
fclose(eph);
type ephemerisdata.txt;

```

CONCLUSIONS

In this thesis the development and the performance analysis of an orbital propagator for the Jupiter Ganymede Orbiter (JGO) spacecraft, led by European Space Agency, foreseen for the joint mission ESA/NASA “*Europa Jupiter System Mission*” (EJSM) is described.

EJSM try to give an answer to the following fundamental theme: “*The emergence of habitable worlds around gas giant*”, for which Jupiter, together with its main moons (Callisto, Io, Ganymede and Europa), represents the archetype.

To satisfy the EJSM mission objectives, JGO, mounted on board also a Radar Sounder and a Laser Altimetry. The analysis of the Ganymede subsurface by means the **Radar Sounder** instrument can bring new detailed data of this icy body that, matched with the Europa sounder, will provide evidence an clues on the genesis and behavior of this exotic type of planetary body. The **Laser Altimetry** will contribute to the characterization of the mission target in the areas of geodesy and geophysics, and will also be crucial for studies of the spacecraft orbit in the gravity field of satellite by providing accurate range data.

Co.R.i.S.T.A (*Consortium of Research on Advanced Remote Sensing System*), the research centre in Naples, where this thesis has been developed, is involved in the studies of these two instruments.

Data capture by Radar Sounder, working at low frequency (20-50 MHz) could be falsified in a compromising manner by harsh Jupiter radiation environment at this range of frequency: in order to plan Radar Sounder data acquisition it is fundamental to know when JGO is in condition of Jupiter eclipse.

At the same manner data collection by Laser Altimeter would be essentially compromised in term of noise by Sun radiation, for this reason, also Sun eclipse condition for JGO has been studied.

The thesis has obtained different results: computation of JGO ephemeris by means the developed orbital propagator, analysis of Jupiter and Sun eclipse in order to optimize the Radar Sounder and Laser Altimeter performance.

According to results JGO, during one ganymedian revolution period will have 46 Jupiter eclipse phases for a total duration of 36,61 h ,i.e 21,19% of total time of propagation with a maximum value around 56 min.

Also, for one ganymedian revolution period, JGO will have 65 Sun eclipse phases for a total duration of 61,13 h ,i.e 35,37% of total time of propagation with a maximum value around 57 min.

Orbital propagator and study of Jupiter and Sun eclipse phase has been developed using SPICE routines of NASA's NAIF (*Navigation Ancillary Information Facility*) node and MICE interface with software MATLAB[®].

The analysis performed during this thesis can be of great importance for the subsequent phases of EJSM mission: our study of Jupiter and Sun eclipse for JGO will permit to optimize Radar Sounder and Laser Altimetry data acquisition, increasing the our knowledge about the jovian system.

ACRONYMS

AIT	<i>Assembly Integration an Testing</i>
AOCS	<i>Attitude and Orbit Control Subsystem</i>
AU	<i>Astronomical Unit</i>
BOL	<i>Beginning of Life</i>
CDF	<i>Concurrent Design Facility</i>
CGG	<i>Callisto Ganymede Ganymede</i>
Co.Ri.S.T.A.	<i>Consortium of Research on Advanced Remote Sensing System</i>
DoF	<i>Degree of Freedom</i>
EAM	<i>European Apogeo Motor</i>
EJSM	<i>Europa Jupiter System Mission</i>
EK	<i>Event Kernel</i>
EOL	<i>Ending of Life</i>
ESA	<i>European Space Agency</i>
ESOC	<i>European Science Operation Centre</i>
ET	<i>Ephemeris Time</i>
FK	<i>Frame Kernel</i>
GA	<i>Gravity Assits</i>
HGA	<i>High Gain Antenna</i>
IAU	<i>International Astronomical Union</i>
IK	<i>Instrument Kernel</i>
Isp	<i>Specific Impulse</i>
JEO	<i>Jupiter Europa Orbiter</i>

JGO	<i>Jupiter Ganymede Orbiter</i>
JOI	<i>Jupiter Orbit Insertion</i>
JSDT	<i>Joint Science Definition Team</i>
JSDT	<i>Joint Science Definition Team</i>
LA	<i>Laser Altimetry</i>
LEOP	<i>Launch and Early Operations Phase</i>
LGA	<i>Low Gain Antenna</i>
LILT	<i>Low intensity Low Temperature</i>
MLI	<i>Multi Layer Insulation</i>
MMH	<i>Monomethylhydrazine</i>
MON	<i>Mixed Oxides of Nitrogen</i>
NAIF	<i>Navigation and Ancillary Information Facilities</i>
NASA	<i>National Aeronautic and Space Administration</i>
OSR	<i>Optical Solar Reflector</i>
PCDU	<i>Power Control and Distribution Unit</i>
PCK	<i>Planet Constant Kernel</i>
PDF	<i>Planetary Data Definition</i>
PDS	<i>Planetary Data System</i>
PM	<i>Prime Meridian</i>
PRF	<i>Pulse Repetition Frequency</i>
PRM	<i>Perijove Raising Manoeuvre</i>
RADAR	<i>Radio Detection and Ranging</i>
RS	<i>Radar Sounder</i>
S/C	<i>Spacecraft</i>
SA	<i>Solar Array</i>
SCLK	<i>Spacecraft Clock Kernel</i>

SNR	<i>Signal to Noise Ratio</i>
SPK	<i>Spacecraft Kernel</i>
TAI	<i>International Atomic Time</i>
TC/TM	<i>Tele-communications/Telemetry</i>
TDB	<i>Barycentric Dynamical Time</i>
TDT	<i>Terrestrial Dynamical Time</i>
TRL	<i>Technology Readiness Level</i>
TRL	<i>Technology Readiness Level</i>
TT&C	<i>Tracking Telemetry and Command</i>
TWTA	<i>Travelling Wave Tube Amplifier</i>
UTC	<i>Universal Coordinated Time</i>
UV	<i>Ultra Violet</i>
VEEGA	<i>Venus Earth Earth Gravity Assist</i>

BIBLIOGRAPHY

Chapter 1

- [1] <http://opfm.jpl.nasa.gov/europajupitersystemmissionejsm/> , last visit September 2009.
- [2] "*Europa Jupiter System Mission*" .
<http://opfm.jpl.nasa.gov/library/> , last visit September 2009.
- [3] "*Jupiter's Moons*". *The Planetary Society*.
http://www.planetary.org/explore/topics/our_solar_system/jupiter/moons.html ,
last visit September 2009.
- [4] "*Ganymede*". nineplanets.org. October 31, 1997.
<http://www.nineplanets.org/ganymede.html> . , last visit September 2009
- [5] "*Solar System's largest moon likely has a hidden ocean*". *Jet Propulsion Laboratory*. NASA.
<http://www.jpl.nasa.gov/releases/2000/aguganymederoundup.html> , last visit
September 2009.
- [6] [http://en.wikipedia.org/wiki/Ganymede_\(moon\)](http://en.wikipedia.org/wiki/Ganymede_(moon)) , last visit October 2009.
- [7] Showman, Adam P.; Malhotra, Renu (1999). "*The Galilean satellites*".
- [8] Kivelson, M.G.; Khurana, K.K.; Coroniti, F.V. et al. (2002). "*The Permanent and Inductive Magnetic Moments of Ganymede*".
- [9] Hall, D.T.; Feldman, P.D.; McGrath, M.A. et al. (1998). "*The Far-Ultraviolet Oxygen Airglow of Europa and Ganymede*".

- [10] Eviatar, Aharon; Vasyliunas, Vytenis M.; Gurnett, Donald A. et al. (2001). *"The ionosphere of Ganymede"*.
- [11] *"Sidereus Nuncius"*. Eastern Michigan University. <http://www.physics.emich.edu/jwooley/chapter9/Chapter9.html>. last visit September 2009.
- [12] *"Satellites of Jupiter"*. The Galileo Project. http://galileo.rice.edu/sci/observations/jupiter_satellites.html. last visit September 2009
- [13] *"Pioneer 11"*. Solar System Exploration. http://sse.jpl.nasa.gov/missions/profile.cfm?Sort=Advanced&MCode=Pioneer_1_1. last visit September 2009.
- [14] William K. Hartmann (May 2005). *"The Grand Tour: A Traveler's Guide to the Solar System"* .
- [15] Musotto, Susanna; Varadi, Ferenc; Moore, William; Schubert, Gerald (2002). *"Numerical Simulations of the Orbits of the Galilean Satellites"*.
- [16] Bills, Bruce G. (2005). *"Free and forced obliquities of the Galilean satellites of Jupiter"*.
- [17] *"High Tide on Europa"*. SPACE.com. http://www.space.com/searchforlife/seti_tidal_europa_021003.html. last visit October 2009 .
- [18] Showman, Adam P.; Malhotra, Renu (1997). *"Tidal Evolution into the Laplace Resonance and the Resurfacing of Ganymede"*.

- [19] Peale, S.J.; Lee, Man Hoi (2002). *"A Primordial Origin of the Laplace Relation Among the Galilean Satellites"*.
- [20] Kuskov, O.L.; Kronrod, V.A. (2005). *"Internal structure of Europa and Callisto"*.
- [21] Spohn, T.; Schubert, G. (2003). *"Oceans in the icy Galilean satellites of Jupiter?"*
- [22] Calvin, Wendy M.; Clark, Roger N. Brown, Robert H.; and Spencer John R. (1995). *"Spectra of the ice Galilean satellites from 0.2 to 5 μm : A compilation, new observations, and a recent summary"*.
- [23] *"Ganymede: the Giant Moon"*. Wayne RESA.
<http://www.resa.net/nasa/ganymede.htm> ,last visit September 2009
- [24] McCord, T.B.; Hansen, G.V.; Clark, R.N. et al. (1998). *"Non-water-ice constituents in the surface material of the icy Galilean satellites from Galileo near-infrared mapping spectrometer investigation"*.
- [25] McCord, Thomas B.; Hansen, Gary B.; Hibbitts, Charles A. (2001). *"Hydrated Salt Minerals on Ganymede's Surface: Evidence of an Ocean Below"*.
- [26] Domingue, Deborah; Lane, Arthur; Moth, Pimol (1996). *"Evidence from IUE for Spatial and Temporal Variations in the Surface Composition of the Icy Galilean Satellites"*.
- [27] Domingue, Deborah L.; Lane, Arthur L.; Beyer, Ross A. (1998). *"IEU's detection of tenuous SO₂ frost on Ganymede and its rapid time variability"*.
- [28] Hibbitts, C.A.; Pappalardo, R.; Hansen, G.V.; McCord, T.B. (2003). *"Carbon dioxide on Ganymede"*.

- [29] Kivelson, M.G.; Warnecke, J.; Bennett, L. et al. (1998). *"Ganymede's magnetosphere: magnetometer overview"*.
- [30] Paranicas, C.; Paterson, W.R.; Cheng, A.F. et al. (1999). *"Energetic particles observations near Ganymede"*.
- [31] Feldman, Paul D.; McGrath, Melissa A.; Strobell, Darrell F. et al. (2000). *"HST/STIS Ultraviolet Imaging of Polar Aurora on Ganymede"*.
- [32] Hauk, Steven A.; Aurnou, Jonathan M.; Dombard, Andrew J. (2006). *"Sulfur's impact on core evolution and magnetic field generation on Ganymede"*.
- [33] Kuskov, O.L.; Kronrod, V.A.; Zhidicova, A.P. (2005). *"Internal Structure of Icy Satellites of Jupiter"*.
- [34] Bland; Showman, A.P.; Tobie, G. (March 2007). *"Ganymede's orbital and thermal evolution and its effect on magnetic field generation"*.
- [35] EJSM-JGO ESA_Assessment_Report
<http://opfm.jpl.nasa.gov/europajupitersystemmissionejsm/ejsmpresentations> ,
 last visit September 2009.
- [36] Jupiter Ganymede Orbiter Concurrent Design Facility: summary study results
 (15 July 2008).
- [37] Image from <http://www.arianespace.com/index/index.asp> last visit October 2009.
- [38] D. Senske: *Summary of the 2007 Jupiter System Observer Study*. May, 21st 2008.
- [39] Payload Definition Document for the Jupiter Ganymede Orbiter of the Europa Jupiter System Mission, Issue 2, 27 March 2009 .

[40] *"Laser Altimeter for the Jupiter Ganymede Orbiter"* ,Co.Ri.S.T.A

[41] *"Radar Sounder instruments for the EJSM / Laplace Mission "*,Co.Ri.S.T.A.

Chapter 2

[42] Image available at http://naif.jpl.nasa.gov/naif/solar_system_geometry.pdf , last visit September 2009.

[43] <http://naif.jpl.nasa.gov/naif/data.html> last visit September 2009.

[44] <http://naif.jpl.nasa.gov/naif/spiceconcept.html> last visit September 2009.

[45] <http://naif.jpl.nasa.gov/naif/tutorials.html> last visit September 2009.

[46] Salvatore Tuosto ,*"NAIF and SPICE library :an application in scenario of Post-EPS Mission"* , thesis degree 2009.

[47] Spice file data available at:

<ftp://naif.jpl.nasa.gov/pub/naif/GLL/kernels/pck/pck00007.tpc> , last visit September 2009

[48] Report of the IAU/IAG Working Group on cartographic coordinates and rotational elements: 2006.

[49] http://naif.jpl.nasa.gov/pub/naif/toolkit_docs/MATLAB/info/mice_idx.html , last visit september 2009.

[50] Carlo Cauli , *"Performance Evaluation and Simulation of the Laser Altimeter for Topographic Analysis of Ganymede during Europa Jupiter System Mission"*, thesis degree 2008.

[51]Giovanni Mengali , " *Meccanica del volo spaziale* ".

ACKNOWLEDGEMENTS

Sin da bambino, tra i vari argomenti trattati dai libri di storia leggevo di uomini che avevano tentato di volare, di cose, animali ed uomini inviati sulla Luna , mentre io continuavo a pormi domande come queste: Perché fanno questo? E' lontana la Luna? E come ci si arriva? ma nessuno che io conoscessi riusciva a darmi risposte esaurienti.

Crescendo le domande erano sempre di più e sempre più strane, allora, arrivato ad un certo punto capii che l'unico modo per "*capirci qualcosina in più*" era entrare nel vivo delle cose, intraprendere studi sull'argomento che potessero in un certo qual modo soddisfare la mia curiosità. Da qui la mia scelta di frequentare il corso di laurea in ingegneria aerospaziale. Gli anni sono passati, molte delle mie domande hanno trovato quelle risposte mai avute prima, altre una risposta l'attendono ancora, ma forse mai nessuno sarà in grado di darle; io intanto ho svolto la buona parte del mio lavoro ma manca ancora qualcosa, la tesi di laurea. La passione per lo Spazio è ancora viva e decido di scegliere come argomento della tesi qualcosa che avesse a che fare con esso, ma non so ancora cosa. Il mio relatore mi dà la possibilità di sviluppare la tesi al Co.Ri.S.T.A , un centro di ricerca per lo sviluppo di satelliti di telerilevamento; la cosa mi entusiasma molto e accetto molto volentieri.

Ricordo il mio primo giorno lì, quando la mia relatrice mi affida il compito, che poi sarebbe stato l'oggetto della mia tesi, di determinare la durata di eclissi per un satellite che avrebbe dovuto orbitare attorno ad una luna di Giove, Ganymede, per una missione spaziale organizzata in collaborazione tra la NASA e l'Agenzia spaziale Europea, il cui lancio è previsto per il 2020 e il cui obiettivo è quello di scoprire nuovi potenziali mondi abitabili. Io, che di Giove, NASA ed ESA fino a quel momento avevo letto solo sui libri o appreso da internet, mi trovo a ricoprire, anche se piccolo, un ruolo in prima persona per la realizzazione di una missione spaziale.

La gioia è grandissima e immediatamente mi metto a lavoro, ricerca dopo ricerca, simulazione su simulazione per cercare di ottenere risultati accettabili.

Ora sono giunto alla fine ed è con grande entusiasmo che , dopo diversi giorni trascorsi a cercare di svolgere questo lavoro nel modo migliore possibile, mi trovo a

scrivere le ultime righe di questa tesi, forse le righe più difficili da *buttar giù*, in cui, con immenso piacere sento il dovere di ringraziare tutte le persone che mi hanno aiutato sia materialmente ma soprattutto moralmente a superare questo ultimo (almeno per ora) e attesissimo gradino. Per tale motivo quindi in primo luogo rivolgo la mia gratitudine al Prof. *Marco D'Errico*, il quale, dal primo giorno di lezione del corso di Astrodinamica, giorno in cui disegnò sulla lavagna una circonferenza chiamandola "*orbita*", fino all'ultimo giorno di lezione del corso di Impianti Aerospaziali in cui pronunciò la sua ben nota frase: "*Un domani sarete ingegneri con la "i" maiuscola!*", ha saputo suscitare in me grande interesse verso il settore spaziale, grazie al suo metodo di insegnamento, rendendo la lezione al contempo molto interessante e poco pesante.

Un grazie di cuore va al mio tutore la Dott.ssa Maria Rosaria Santovito con la quale ho avuto l'immenso piacere di portare al termine il mio lavoro, per la sua disponibilità ad ascoltare le mie proposte, per la sua disponibilità ad apportare correzioni laddove ce ne fosse stato bisogno (spesso!) ma soprattutto la ringrazio per il modo in cui mi ha ospitato negli uffici del Co.Ri.S.T.A facendomi sentire sin dall'inizio a mio agio come se quegli uffici fossero lo studio di casa mia.

Ringrazio il mio tutore "adottivo" l' Ing. *Gianni Alberti*, e la Dott.ssa *Giulia Pica* per l'ospitalità riservatami.

Grande gratitudine è rivolta ai miei due amici *Tommaso Borrelli* e *Carminè D'Errico* i quali non solo mi hanno fornito parte degli strumenti informatici che mi erano necessari, ma soprattutto per le critiche da loro ricevute quando sottoponevo alla loro attenzione quelle che erano le mie idee su come impostare il lavoro da svolgere.

Un forte ringraziamento va ai miei *genitori* e a mio fratello *Michele* non solo per il loro supporto economico ma in particolare per il loro supporto morale, incitandomi giorno dopo giorno, esame dopo esame a fare sempre meglio e interessandosi in maniera profonda a quello che era e sarà l'oggetto dei miei studi.

Un grazie di cuore va a mia nonna *Veneranda* con la quale ho vissuto per tutta la durata della mia carriera universitaria e la quale si è occupata di me nonostante la sua non più giovane età. Con tutto il cuore rivolgo la mia gratitudine al mio amore *Maria*, la quale ha sopportato con grande pazienza i miei momenti di nervosismo dovuto agli studi e agli esami da affrontare, con la quale ho condiviso il mio stato di

ansia per lo svolgimento della tesi aiutandomi a fare in modo che tutto andasse per il meglio. Infine ringrazio i suoi genitori che sono stati un po' anche i miei genitori e tutti i docenti del corso di laurea in Ingegneria Aerospaziale della SUN per aver inculcato in me le loro conoscenze.

Aversa , 16 Dicembre 2009